INFORMATION TO USERS

This manuscript has been reproduced from the microfilm master. UMI films the text directly from the original or copy submitted. Thus, some thesis and dissertation copies are in typewriter face, while others may be from any type of computer printer.

The quality of this reproduction is dependent upon the quality of the copy submitted. Broken or indistinct print, colored or poor quality illustrations and photographs, print bleedthrough, substandard margins, and improper alignment can adversely affect reproduction.

In the unlikely event that the author did not send UMI a complete manuscript and there are missing pages, these will be noted. Also, if unauthorized copyright material had to be removed, a note will indicate the deletion.

Oversize materials (e.g., maps, drawings, charts) are reproduced by sectioning the original, beginning at the upper left-hand corner and continuing from left to right in equal sections with small overlaps.

ProQuest Information and Learning
300 North Zeeb Road, Ann Arbor, MI 48106-1346 USA
800-521-0600

UMI®

Reproduced with permission of the copyright owner. Further reproduction prohibited without permission.

Reproduced with permission of the copyright owner. Further reproduction prohibited without permission.

NOTE TO USERS

This reproduction is the best copy available.

UMI®

Reproduced with permission of the copyright owner. Further reproduction prohibited without permission.

Reproduced with permission of the copyright owner. Further reproduction prohibited without permission.

A

DELINEATION OF THE COASTAL AQUIFER OF ISRAEL BASED ON THE ANALYSIS OF CARBON-14 AND TRITIUM ISOTOPES

by

Deborah Lynn Bruce

A dissertation submitted to the Graduate Faculty in Earth and Environmental Sciences in partial fulfillment of the requirements for the degree of Doctor of Philosophy, The City University of New York

2003

Reproduced with permission of the copyright owner. Further reproduction prohibited without permission.

UMI Number: 3103090

Copyright 2003 by
Bruce, Deborah Lynn

All rights reserved.

UMI®

UMI Microform 3103090
Copyright 2003 by ProQuest Information and Learning Company.
All rights reserved. This microform edition is protected against
unauthorized copying under Title 17, United States Code.

ProQuest Information and Learning Company
300 North Zeeb Road
P.O. Box 1346
Ann Arbor, MI 48106-1346

Reproduced with permission of the copyright owner. Further reproduction prohibited without permission.

©2003

DEBORAH LYNN BRUCE

All Rights Reserved

Reproduced with permission of the copyright owner. Further reproduction prohibited without permission.

This manuscript has been read and accepted for the Graduate Faculty in Earth and Environmental Sciences in satisfaction of the dissertation requirement for the degree of Doctor of Philosophy.

7/30/03
Date

Gerald M. Friedman
Chair of Examining Committee

PROF. GERALD M. FRIEDMAN

8/26/03
Date

Executive Officer

Prof. David Locke

Prof. C. Nehru

Dr. Yoseph Yechieli
Supervisory Committee

THE CITY UNIVERSITY OF NEW YORK

Reproduced with permission of the copyright owner. Further reproduction prohibited without permission.

Abstract

DELINEATION OF THE COASTAL AQUIFER OF ISRAEL BASED ON THE ANALYSIS OF CARBON-14 AND TRITIUM ISOTOPES

by

Deborah Lynn Bruce

PhD. Program in Earth and Environmental Sciences

The City University of New York

Advisor: Distinguished Professor Gerald M. Friedman

Twenty-nine wells were sampled along the Coastal Aquifer of Israel for major ions, ^{14}C, tritium, and ^{13}C in the 1970s and again in the 1990s. It is shown that double sampling can more accurately determine the age of the groundwater and its recharge sources.

The spatial variation in radiocarbon concentration in the coastal aquifer exhibits lower concentrations in the western section of the aquifer (55-70 percent modern carbon or PMC) as compared to the eastern section (80-100 PMC). These results can be explained by the existence of two systems within the same coastal aquifer, whereby the eastern section of the aquifer is a more open system and the western section is a more closed system.

Based on the presence of detectable levels of tritium throughout most of the aquifer, the groundwater in the coastal aquifer was determined to contain a young component with a transit time of less than forty years. The ^{14}C results of most groundwater were found to be lower than 100 PMC, probably due to water-rock interactions rather than decay due to old age. However, it is possible that some older waters exist in the lower sub-aquifers of the deeper wells (120-140m) where both lower ^{14}C values and low levels of tritium were

Reproduced with permission of the copyright owner. Further reproduction prohibited without permission.

found. It is also possible that in some parts of the aquifer there is a mixture of several sources of water, some of which are young (containing tritium), and others which are older (having a relatively low ^{14}C concentration).

Analysis of the tritium values from the two sampling periods using the tritium bomb spike curve allowed a better age estimation, overcoming the complication of tritium data in which the same value could yield two ages. Therefore, repetition of sampling over an extended time interval was determined to be effective in assisting in calculating groundwater ages through both the use of the tritium curve and analysis of the chemical and isotopic data over the twenty-year period. The correct age could be used to determine the real dilution factor (Q) in the aquifer and thus be utilized for age determination of older samples in the aquifer.

Reproduced with permission of the copyright owner. Further reproduction prohibited without permission.

ACKNOWLEDGMENTS

I would like to express my sincere thanks and heartfelt gratitude to Professor Gerald M. Friedman for seeing the potential in me and for constantly providing the needed incentive, influence and advice to advance me through this program. To Dr. Yossi Yechieli for his patience, perseverance, and continuous guidance in mentoring me throughout this project to a level above and beyond the call of duty. I would also like to thank Professors Nehru and Locke for serving on my committee, and to Ms. Lina McClain who keeps all the wheels turning.

I would like to thank Dr. Aaron Kaufman for providing the sampling data of the 1970s, which enabled me to conduct the comparative analysis study. Thanks to I. Carmi for assisting with the tritium analysis and for providing information of tritium concentration in rain. Thanks to A. Zelinger and S. Tzuk from the Mekorot Water Company for the valuable discussion and information about the coastal aquifer. Field work could not have been completed without the help of Haim Hemo of the Geological Survey of Israel. I would also like to thank B. Cohen and N. Shragai for their help in preparing some of the figures, and D. Stiber, S. Ehrlich, B. Schilman and A. Ayalon from the geochemical department of the Geological Survey of Israel for their continuous assistance and scholarly advice.

Finally, I would like to thank my parents who have always had faith in me, as well as my husband, Gary, whose encouragement and support helped in bringing me to the completion of this work.

Reproduced with permission of the copyright owner. Further reproduction prohibited without permission.

TABLE OF CONTENTS

Reproduced with permission of the copyright owner. Further reproduction prohibited without permission.

Chapter Page

Appendix

Reproduced with permission of the copyright owner. Further reproduction prohibited without permission.

LIST OF TABLES

Reproduced with permission of the copyright owner. Further reproduction prohibited without permission.

LIST OF FIGURES

Reproduced with permission of the copyright owner. Further reproduction prohibited without permission.

LIST OF FIGURES

Figure Page

Reproduced with permission of the copyright owner. Further reproduction prohibited without permission.

LIST OF FIGURES

Reproduced with permission of the copyright owner. Further reproduction prohibited without permission.

1. INTRODUCTION

Carbon-14 (^{14}C) is the most commonly used environmental radioisotope for dating groundwater since its first application by Munnich and Vogel in dating groundwater in the eastern Sahara in 1962. Complications involving the ^{14}C method occur in the various water-rock interactions in the unsaturated and saturated zones. Tritium has a short half-life, relative to ^{14}C, and is thereby a useful indicator of groundwater ages, which have been more recently recharged. Anthropogenic influences within the past 50 years have affected both ^{14}C and tritium levels.

^{14}C and tritium are used in this research to determine transport time of groundwater in a Coastal Aquifer of Israel. ^{14}C and tritium ages determined for the coastal aquifer will assist in defining local and regional groundwater movement and principal recharge points, which can vary within the different sub-aquifer units. Determining ages and recharge rates can be applied to identification and flow rate of possible pollution sources.

The Coastal Aquifer of Israel is an ideal study site for this research due to the amount of information currently available on its physical characteristics and chemical make-up, as well as its accessibility in terms of sampling locations. There has been very little published on the application of the ^{14}C method in Israel. However, between 1974 and 1976, A. Kaufman, of the Weizmann Institute, collected ^{14}C, carbon-13, and tritium isotopic data from 26 wells along the coastal aquifer (unpublished work). Kaufman, along with the professional staff of Israel's two main water companies, Tahal and Mekorot, chose these specific wells based on their current data and the geographical grid of Israel.

Reproduced with permission of the copyright owner. Further reproduction prohibited without permission.

This information was then utilized to derive a sampling plan, which would provide a representative sampling of the groundwater along the coastal aquifer. These data, which was never published, was the basis of this research.

Twenty of these wells, or their closest current substitute were re-sampled in the period between 1993-1998. The purpose of this re-sampling was to more accurately determine the age of the groundwater and its recharge sources through the analysis of the sample results over this 20-year interval. The aquifer was examined as a whole unit in order to study its large-scale variations in ^{14}C and to gain a better understanding of the spatial variations of these ^{14}C values in the coastal aquifer by evaluating the factors that affect its initial ^{14}C value. In addition, the significance of using ^{14}C as a tracer for chemical and isotopic processes was also studied.

Carbon-14

^{14}C is an environmental radioisotope produced by nuclear reactions between cosmic rays and the stable atoms of the atmosphere. The following nuclear reaction between cosmic rays and nitrogen nuclei form ^{14}C:

$$^{14}N + \text{neutron} \Rightarrow {}^{14}C + \text{proton}$$

The ^{14}C atoms oxidize to form $^{14}CO_2$ molecules, which then mix with the inactive carbon dioxide in the atmosphere. In this form, the ^{14}C can enter the biosphere and hydrosphere as part of the natural carbon cycle. This cycle provides a continuous source of ^{14}C in naturally formed carbon compounds, such as tropospheric carbon dioxide, oceanic bicarbonate, and living terrestrial plants and animals (Mook, 1980).

Reproduced with permission of the copyright owner. Further reproduction prohibited without permission.

^{14}C concentrations are usually given as specific activities (the radioactivity of ^{14}C, in disintegrations per minute per gram of carbon). The natural specific activity of atmospheric CO_2, oceanic bicarbonate, and living plants and animals is approximately, $A_0 \cong 14$ disintegrations per minute/g C (Mook, 1980). The specific activities are then compared with a standard activity, and the measured activity of a sample is given as a percentage of this standard activity in units of percentage of modern carbon (PMC). Deviations of a measured natural value from the standard activity are also expressed as delta (Δ) values.

As the carbon moves from one reservoir to the next, isotope fractionation occurs. The extent of the fractionation is measured by the stable carbon isotope ratio $^{13}C/^{12}C$.

Where $$\delta^{13}C = \frac{^{13}C/^{12}C_{(sample)} - {}^{13}C/^{12}C_{(standard)}}{^{13}C/^{12}C_{(standard)}} \times 10^3 ‰$$

The standard for carbon is the calcite of a belemnite from the Peedee Formation in South Carolina known as PDB. Although fractionation of $^{14}C/^{12}C$ also occurs, it is not a major factor since the ^{14}C is given in concentration units and not δ values. Measurement of the $\delta^{13}C$ value can correct the original ^{14}C content of the material for fractionation (Mook, 1980). By convention, the ^{14}C activities are corrected to a $\delta^{13}C$ value of –25 per mil vs. PDB (Mook, 1980).

The natural ^{14}C content of the atmosphere has been anthropogenically influenced since the start of the industrial revolution. The combustion of fossil fuels, which does not contain ^{14}C, has reduced the relative tropospheric ^{14}C level by approximately 10% (Mook, 1980). However, nuclear test explosions into the atmosphere between 1952 and

Reproduced with permission of the copyright owner. Further reproduction prohibited without permission.

1969 have outweighed the industrial effect and increased the natural levels of atmospheric ^{14}C to a temporary value of a factor of 2 above normal (Mook, 1980).). Gradual exchange with the ocean causes a decrease in ^{14}C levels toward natural ^{14}C conditions (Levin et al, 1980) (Fig. 1).

The decay of ^{14}C takes place by β^- *emission to stable* ^{14}N:

$$^{14}C \Rightarrow {}^{14}N + \beta^-$$

The disintegration follows the Law of Radioactivity, which states that the rate of decay of a radioactive nuclide is proportional to the number of atoms of that nuclide remaining at any time:

$$A = A_0 e^{-\lambda t}$$

A = measured specific radioactivity of the material

A_0 = original specific radioactivity of the material

t = time

λ = the decay constant of ^{14}C (0.1209×10^{-3}) (Faure, 1991)

This is related to the half-life ($T_{1/2}$) by:

$$T_{1/2} = \frac{\ln 2}{\lambda}$$

The half-life used in hydrology for ^{14}C, is 5730 (±40) years (Mook, 1980).

Reproduced with permission of the copyright owner. Further reproduction prohibited without permission.

Reproduced with permission of the copyright owner. Further reproduction prohibited without permission.

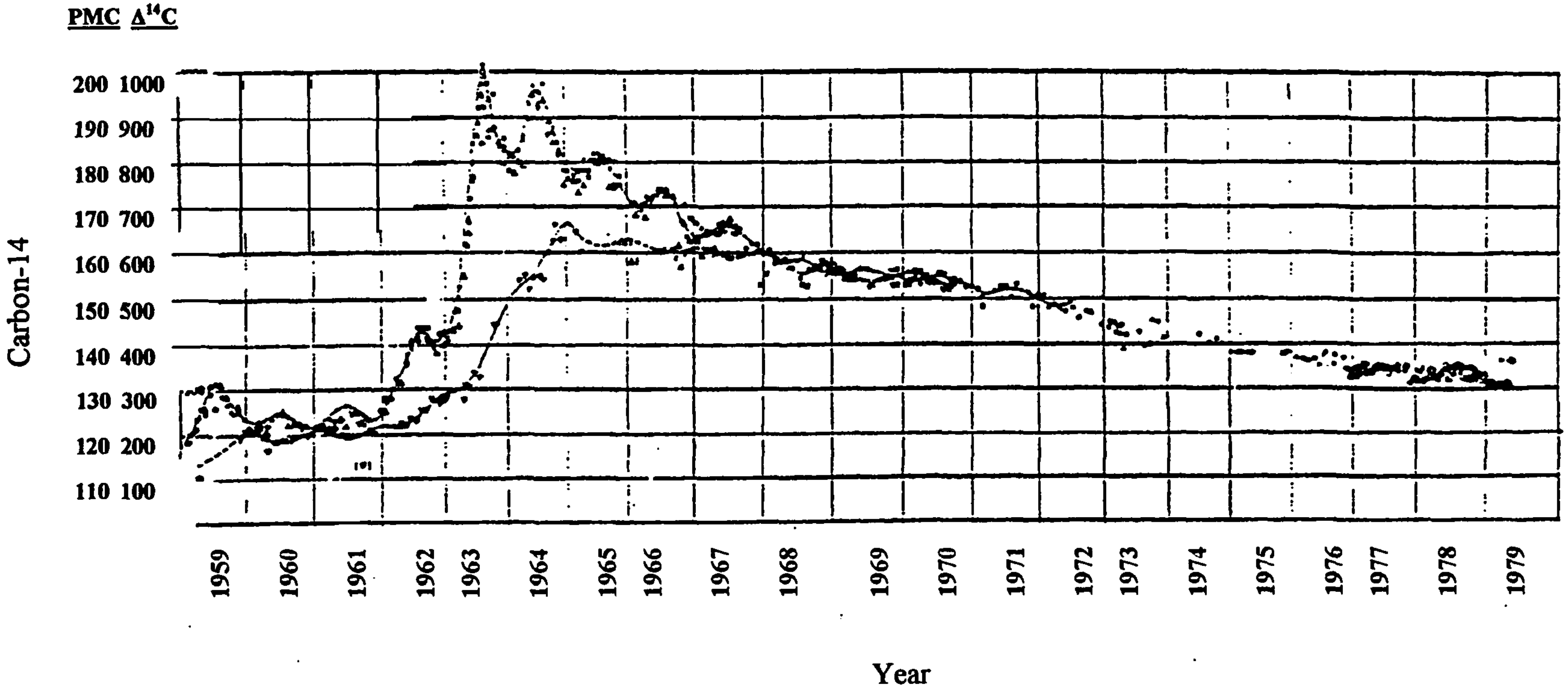

Fig. 1. Ranges for radiocarbon in tropospheric CO_2. The lower curve depicts the ^{14}C concentration in the southern hemisphere and the upper one depicts the variations in the upper hemisphere (Levin et al., 1980).

In hydrogeological dating, the A_o is not as easily obtained as in plant or animal carbon. In these instances, the origin of the carbon in the water must be assumed from the stable carbon isotopic composition and the hydro-chemical data (Mook, 1980).

As water infiltrates through the soil atmosphere into the groundwater, dissolved inorganic carbon (DIC) is gained by dissolution of CO_2 and is altered by the weathering of carbonate and silicate parent material. When gaseous carbon dioxide or $CO_{2\,(g)}$ diffuses into water, it forms four main species of DIC.

	$CO_{2\,(aq)}$	Dissolved or aqueous CO_2
	H_2CO_3	Carbonic acid or hydrated CO_2
	HCO_3^-	Bicarbonate or dissociated carbonic acid
+	CO_3^{2-}	Carbonate or the second dissociation species of carbonic acid
	ΣDIC	

Their distribution is a function of pH. The pH will increase and the distribution of DIC species will shift toward bicarbonate (HCO_3^-) and carbonate (CO_3^{2-}) according to the reactions:

$$CO_{2\,(g)} \leftrightarrow CO_{2\,(aq)}$$

$$CO_{2\,(aq)} + H_2O \leftrightarrow H_2CO_3$$

$$H_2CO_3 \leftrightarrow H^+ + HCO_3^-$$

$$HCO_3^- \leftrightarrow H^+ + CO_3^{2-}$$

Reproduced with permission of the copyright owner. Further reproduction prohibited without permission.

Figure (2) depicts the distribution of carbonate species in pure water as a function of pH at 25°C, calculated for a total DIC content of 1.6 mmoles/L (or 100 mg/L as HCO_3^-) (Clark and Fritz, 1997). The greater the CO_2 concentration in the soil, the larger the amount of calcite will be dissolved, and the higher will be the groundwater's DIC. The groundwater will typically move toward equilibrium with calcite, whose solubility will control pH and the equilibrium of carbonate species (Clark and Fritz, 1997).

Possible sources for dissolved inorganic carbon in groundwater

A. Atmospheric CO_2, which becomes dissolved in the rainwater and transported to the groundwater. This can be an important contributor in areas of little to no vegetation. However, atmospheric CO_2 ($\delta^{13}C$ = -7‰) is a relatively small contributor in areas of heavy vegetation where soil gas CO_2 plays a more important role (Mook, 1980).

B. Production of DIC in the upper soil zones by the decomposition of the organic matter (recent) in the soil. Beginning with a natural ^{14}C content in the organics at 100 PMC, and 0 PMC in the limestone, the dissolved bicarbonate is expected to have an original ^{14}C content of 50 PMC (Mook, 1980). For temperate climatic vegetations, the $\delta^{13}C$ value of the soil CO_2 in the form of dissolved bicarbonate would be -25‰, and -15‰ for semi-arid regions (Mook, 1980). In soil limestone, the $\delta^{13}C$ value is believed to be +1‰. The value in dissolved bicarbonate is therefore, -12 or -7‰ (Mook, 1980). Mixing of the two end members is expected to give an intermediate value.

C. Some of the H^+ ions in the acid soil water are believed to originate from humic acids (Vogel and Ehhalt, 1963).

Reproduced with permission of the copyright owner. Further reproduction prohibited without permission.

Reproduced with permission of the copyright owner. Further reproduction prohibited without permission.

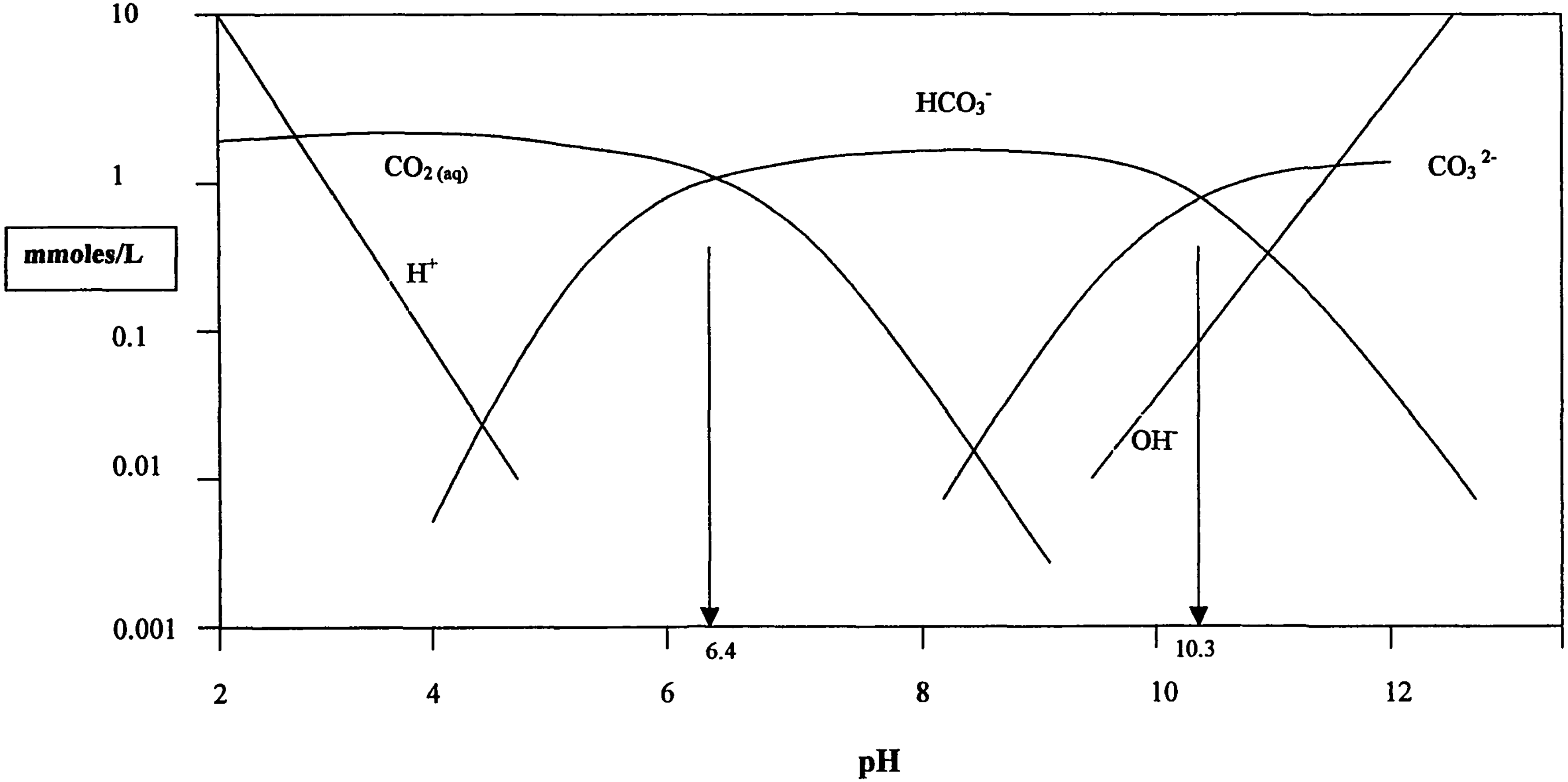

Fig. 2. Distribution of carbonate species in pure water as a function of pH at 25° C, calculated for a total dissolved inorganic carbon content of 1.6 mmoles/L. (Clark and Fritz, 1997)

$$2CaCO_3 + 2H(Hum) \Rightarrow Ca(Hum)_2 + Ca^{+2} + 2HCO_3^-$$

The carbonate is assumed to have ^{14}C values of 0 PMC and $\delta^{13}C$ of +1‰. This, however, is usually a minor process.

D. Change in the ^{14}C and C-13 content of the ground water due to underground generation of CO_2 in the aquifer (Mook, 1980). Carbon can be added through oxidation of organic material (peat) during groundwater movement within the saturated zone of the aquifer.

$$6nO_2 + (C_6H_{10}O_5)_n + nH_2O \Rightarrow 6nH^+ + 6nHCO_3^-$$

This can be followed by dissolution of carbonate:

$$mH^+ + mCaCO_3 \Rightarrow mCa^{+2} + mHCO_3^-$$

This process is important only in an aquifer whose sediments are rich in organic matter (Mook, 1980; Boarretto et al, 1998).

E. Without free oxygen, sulfate reduction might occur in an aquifer, causing further oxidation of organic matter (Mook, 1980):

$$SO_4^{-2} + CH_4 \Rightarrow HS^- + H_2O + HCO_3^-$$

The ^{14}C activity in this scenario depends entirely on the age of the organic matter. The $\delta^{13}C$ values of the dissolved bicarbonate will also depend on the values of the organic matter. It will be very low in the case of CH_4, which is produced by bacterial decomposition of organic matter ($\delta^{13}C \sim -70‰$) (Mook, 1980). Reduction of other ions, such as nitrate, would also cause oxidation of organic matter (Mook, 1980).

Geyh and Kunzl (1981) performed a study using 123 representative groundwater samples throughout Germany, and including coal-mining areas, which have occurrences of natural

Reproduced with permission of the copyright owner. Further reproduction prohibited without permission.

gas. The sampling was done in order to test the effect of sulfate reduction or fermentation on the ^{14}C dating of groundwater. It was confirmed from the sampling results, that methane only effects the ^{14}C dating in exceptional cases (Geyh and Kunzl, 1981).

F. Exchange with the soil carbonate or limestone in the unsaturated zone, or in the aquifer is another source of DIC in groundwater. In this case, the ^{14}C content of the dissolved bicarbonate would decrease.

G. Dissolution could also be due to calcium-sodium exchange. This will cause additional carbonate to dissolve to maintain saturation with respect to calcite, and therefore, more dead CO_2 will be added to the system (Mook, 1980 after Pearson and Swarzenki, 1974).

There are two processes, isotope exchange and dissolution-precipitation of carbonates in the soil (Mook, 1980 from Ingerson and Pearson, 1964; Geyh, 1972; Salmons and Mook, 1976), which can change the isotopic values without affecting the DIC of the water. Isotope exchange involves a solid-state diffusion of CO_3^{-2} ions between the ground water and the calcite crystals without dissolution. Influence on the ^{14}C age of the groundwater has been found to be limited. This depends on the grain size; on the carbonate content of the aquifer relative to the dissolved carbonate concentration of the water, as well as on the pH and temperature (Mook, 1980). Dissolution- precipitation of carbonates in the soil is fairly common in regions subject to long periods of dryness and high surface temperatures. This process is mostly confined to a small soil zone, and it is not considered to be significant (Mook, 1980).

Reproduced with permission of the copyright owner. Further reproduction prohibited without permission.

Open and closed systems

In regard to CO_2-$CaCO_3$ interaction, there are two types of systems, the open system and the closed system. An open system is defined as, the system in which "the carbonate is dissolved by water in continuing contact with the CO_2 reservoir at a fixed partial pressure" (Mook, 1980). In a closed system, the carbonate is dissolved by infiltrating water without the presence of CO_2 gas.

Transfer of ^{14}C from soil CO_2 to soil water solution depends on the partial pressure of CO_2 in soil air and whether carbonate dissolution by $CO_{2\,(aq)}$ occurs in open system, and/or in closed system conditions (Figure 3). In open system conditions, the bicarbonate is expected to equilibrate with the soil CO_2 in the unsaturated zone and thereby in contact with the dominant soil CO_2 exchange reservoir. The expected ^{14}C value for these conditions would be approximately 100 PMC with a $\delta^{13}C$ of approximately -15 ‰ (expected fractionation of approximately 9 ‰; Clark and Fritz, 1997). In closed system conditions of the saturated zone the descending water is cut off from the atmosphere and isolated from the soil CO_2. Therefore, the dissolution of old carbonate is expected to change the initial values of both the ^{14}C and $\delta^{13}C$ (expected ^{14}C of 50 PMC and $\delta^{13}C$ of –10to –12‰).

A greater amount of ^{14}C transfer to the groundwater by carbonate dissolution will occur under open system conditions due to:

1. The constant replenishment of modern soil CO_2 that, in the aqueous form, is continuously consumed by dissolution of ^{14}C free soil carbonate.

Reproduced with permission of the copyright owner. Further reproduction prohibited without permission.

Fig. 3. Depiction of the movement of ^{14}C and $\delta^{13}C$ in the atmosphere, soil surface, and water table, and through open, closed, and mixed systems. This figure denotes values before the effect of the nuclear tests.

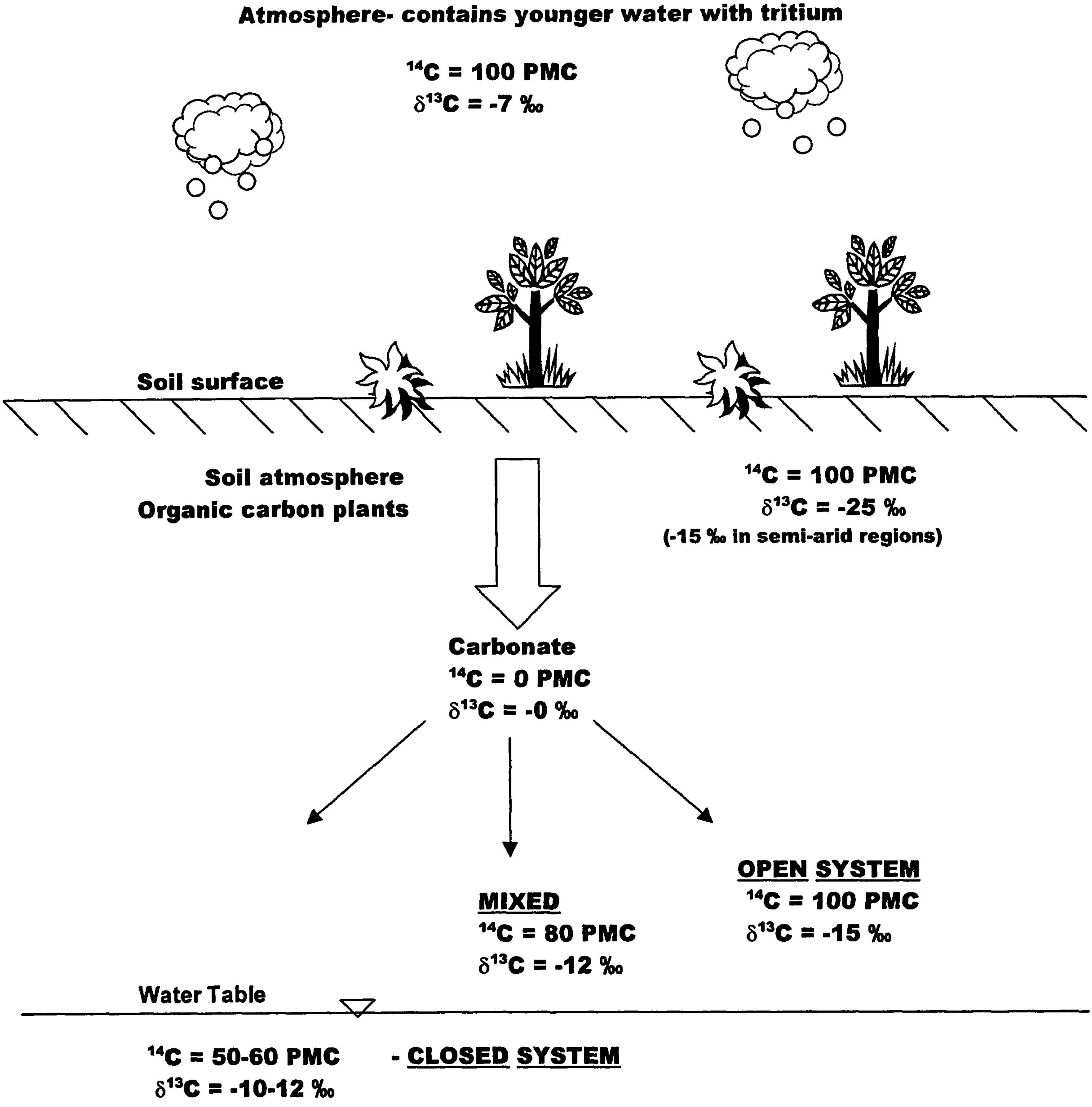

Reproduced with permission of the copyright owner. Further reproduction prohibited without permission.

2. The $^{14}C/^{12}C$ isotope ratio of DIC ($CO_{2\,(aq)} + HCO_3^- + CO_3^{-2} = DIC$) is raised to the modern ^{14}C level in soil CO_2 by carbon exchange between the dissolved carbon species (Dorr et al., 1987). Therefore, at a specific soil CO_2 content, both the carbon mass and ^{14}C transfer to the soil solution are maximal for carbonate dissolution in open system conditions (Dorr et al., 1987).

In contrast, carbonate dissolution in closed system conditions is dependent on the amount of available dissolved CO_2, which the water has accrued in the unsaturated zone (Dorr et al., 1987). Carbonate dissolution by carbonic acid in a closed system results in an approximate 50% dilution to the initial ^{14}C:

$$^{14}CO_2 + H_2O + CaCO_3 \Rightarrow Ca^{+2} + HCO_3^- + H^{14}CO_3^- \text{ (Clark and Fritz, 1997)}$$

Most systems lie between open and closed conditions, and groundwaters reach calcite saturation during this transition from open to closed conditions (Clark and Fritz, 1997). Therefore, it is believed, that in nature the carbonate dissolution will occur under mixed conditions (Mook, 1980).

As carbonate is dissolved, the $\delta^{13}C_{DIC}$ becomes increasingly enriched. In open system conditions, this is attributed to the increase in fractionation of ^{13}C between soil gas and DIC (Clark and Fritz, 1997). The effective enrichment of ^{13}C between $CO_{2\,(soil)}$ and HCO_3^-, as the pH rises, becomes significant and the $\delta^{13}C_{DIC}$ will increase (Clark and Fritz, 1997). While in closed system conditions, the increase in $\delta^{13}C_{DIC}$ is based wholly on the mixing between soil DIC and marine carbonate ($\delta^{13}C \cong 0‰$), and, therefore, the effects of carbonate dissolution are more easily detected (Clark and Fritz, 1997).

Reproduced with permission of the copyright owner. Further reproduction prohibited without permission.

The boundary between the open and closed system has most commonly been placed at the intersection of the saturated with the unsaturated zone and at the intersection of the phreatic with the confined part of an aquifer.

Calculation of ^{14}C dates

Once the ^{14}C is isolated from the atmosphere, the amount of decayed ^{14}C in the groundwater can be used to determine its age. Dilution of the initial ^{14}C activity due to dissolution of old carbonate makes it difficult to determine an "absolute age" of the groundwater. Complications involving the Carbon-14 method occur due to the various water-rock interactions in the unsaturated and saturated zones. Dilution of dead carbon lowers the ^{14}C values and therefore must be corrected to more accurately determine the data. Therefore, in order to calculate ^{14}C dates, it is first necessary to know the amount of dilution that has taken place as the water dissolves carbonate species. Following is the decay equation used for ^{14}C calculation:

$$A = QA_0 2^{-t/T} \text{ (Wigley, 1975)}$$

A = the measured ^{14}C activity

A_0 = the activity at time zero

t = age

T = the half life

Q = the adjustment factor

Reproduced with permission of the copyright owner. Further reproduction prohibited without permission.

The two methods of adjustment used to relate to Q, the adjustment for non-decay ^{14}C loss (i.e. dilution), are (1) mass balance and a model of carbonate mineral dissolution, i.e. a geochemical relationship, and (2) the stable C-13 isotope. The stable carbon isotopic composition (δ^{13}C) can be used to identify the source of DIC, and determine which part of the measured ^{14}C concentration was due to mixing, and which part was due to decay. A graph of ^{14}C concentrations in the troposphere in combination with a tritium rainwater curve is another method of adjustment that will be addressed in this research in order to provide a more accurate method for groundwater age estimation. Choosing a correction method is subjective based on an understanding of the specific system.

One of the main issues that must be addressed when dating groundwater is the estimation of the initial ^{14}C value. This topic has been examined in many different research studies (e.g. Dorr et al., 1987; Leany and Allison, 1986; Geyh and Wirth, 1980), which were unsuccessful in determining a universal solution. Various initial values are applied to different parts of the world and for different locations. The accepted values of initial ^{14}C in recent groundwater are between 60-100 PMC, however, these values are not well constrained. The limit of the ^{14}C method is 35,000 years, but use of the accelerator mass spectrometry (AMS) technique can somewhat increase this limit. The AMS technique, also allows for the ^{14}C analysis to be done on samples of a much smaller size. The distinction between open and closed systems within the groundwater network is one of the main factors in evaluating the initial ^{14}C value of the groundwater.

In open systems, the isotopic composition is determined based on fractionation (Wigley, 1975). In closed systems, assuming there is no isotopic exchange between water and the surrounding rock, the isotopic composition can be determined by mass balance

Reproduced with permission of the copyright owner. Further reproduction prohibited without permission.

computations (Wigley, 1975). Pearson and Henshaw (1970) introduced correction factors for cases where carbon content has increased during the course of the water in the aquifer, with a linear mixing between carbon derived from soil $CO_{2(g)}$ and carbon from soil carbonates (dead CO_2). The ^{14}C of modern carbon is then described by the use of the "$\delta^{13}C$ reduction factor". This correction model, however, does not take into account open system process, and will therefore underestimate the initial ^{14}C content of the groundwater (Dorr, et al., 1987). Models by Mook (1976) and Fontes and Garnier (1979), which include carbon mass and isotope balance equations with isotope fractionation between the dissolved carbon species, give better estimates of the initial ^{14}C content (Dorr, et al., 1987). Any model, however, of the geochemical evolution of groundwater and its isotopic composition will not be accurate if DIC is affected by carbonate dissolution and precipitation processes further within the groundwater system. This dissolution could be caused by magmatic CO_2, thermal waters, and "dead" biogenic CO_2 produced by microbial oxidation of fossil organic carbon in the groundwater matrix (Dorr et al., 1987). For any model of the geochemical evolution and dating of groundwater and its isotopic composition the initial ^{14}C values are of extreme importance.

Two studies, which took into consideration the effects of open and closed system conditions on ^{14}C dating of groundwater, were Taylor (1994) and Leaney and Allison (1986). In Taylor (1994), the application of chemical and isotopic evidence of river and groundwater properties was used to identify the recharge mechanisms, chemical evolution, and age of the ground water in the aquifer. The study area was the Poverty Bay Flats on a coastal alluvial plain in New Zealand's North Island. Open and closed system aquifers were identified, as well as evidence for chemical reactions that have an affect on

Reproduced with permission of the copyright owner. Further reproduction prohibited without permission.

the carbon isotopic composition of the ground water. An ion-exchange process involving the aquifer material is believed to replace calcium ions with sodium and magnesium. As a result, the following reaction:

$$(x + y)CO_2 + xCaCO_3 + (x+ y)H_2O \Rightarrow xCa^{+2} + 2xHCO_3^- + yH_2CO_3$$

can go to completion even after there is saturation of calcite (Taylor, 1994).

Closed system behavior was found to be associated with an increase in total DIC content, believed to be from decay of recent organic material (Taylor, 1994). Open system behavior involved the addition of soil CO_2 and CO_2 from organic decay (Taylor, 1994). The estimated error in this study, of ages since recharge, is about 4300 years. However, it was noted that this number could be up to 1300 years greater due to uncertainty in the initial (pre-humic acid influence) ^{14}C concentration of the water (Taylor, 1994).

Leaney and Allison (1986) measured thirty-three boreholes in a saline unconfined aquifer in southern Australia for ^{14}C concentration. Local recharge under natural conditions in this area has been interpreted to be at a low value of 0.1 and 0.2 mm/yr. To estimate the effect of dissolution and precipitation reactions on modification of the ^{14}C content, Leaney and Allison (1986) used an approach that takes into consideration both the initial open system conditions, as well as the closed system conditions which the ground water would later follow. It was found in the study, that "the estimate of local recharge (0.25 mm/yr) made using the ^{14}C may be considered an upper estimate due to the possibility of

Reproduced with permission of the copyright owner. Further reproduction prohibited without permission.

some diffusional input of $^{14}CO_2$ to the water table" (Leaney and Allison, 1986). This phenomenon is significant only in areas of low recharge.

Tritium

The tritium (^3H) isotope is produced naturally in the atmosphere, and its analysis is an essential part of the ^{14}C sampling process. Since tritium is part of the water molecule, it is unaffected by chemical processes in the groundwater. It has a short half-life (12.3 years) relative to Carbon-14 (5730 years), and is thereby a useful tool for dating younger groundwater. ^3H is measured in tritium units (TU) where each tritium unit equals one ^3H molecule in 10^{18} atoms of hydrogen. The tritium concentration in the atmosphere increased several fold during the peak of the atomic testing period (Fig. 4). At the height of nuclear testing in the 1960's, the levels of tritium in precipitation in Israel were detected at concentrations of 600 TU (Carmi and Gat, 1973). Tritium can therefore assist in distinguishing between waters that entered the groundwater before nuclear weapons testing (1952-1969). In 1994, the tritium concentration in precipitation was measured at 10 T.U. or less (Yechieli et al., 1994). The groundwater should retain the tritium concentration of the rain at the time of recharge and the concentration should decrease only as a result of the half-life decay process. Flow and mixing patterns, however, can also affect tritium losses and additions to the aquifer system. The absence of tritium would indicate a long travel time in the unsaturated zone, and/or the saturated zone, with transport times greater than 40 years. However, due to the possibility of obtaining two ages for the same tritium values, a single tritium measurement does not usually allow for greater accuracy, which can be better accomplished by repetitive analysis.

Reproduced with permission of the copyright owner. Further reproduction prohibited without permission.

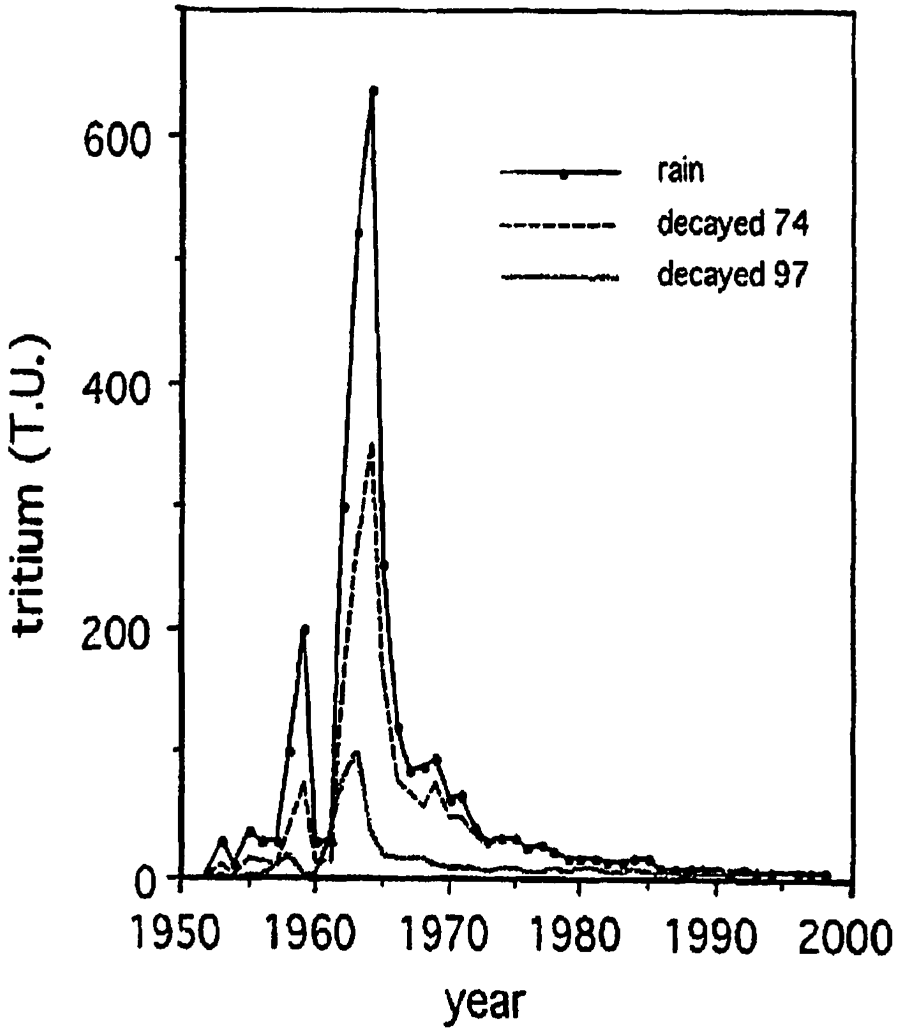

Fig. 4. Tritium concentration of rainwater in Israel, with expected decay values for both 1974 and 1997 (modified after Yechieli et al., 1994).

Reproduced with permission of the copyright owner. Further reproduction prohibited without permission.

2. PREVIOUS RESEARCH USING ^{14}C

Many case studies are reported in the scientific literature. Those given here are mainly from Israel. Kroitoru et al. (1989) performed a study on the chemical evolution of groundwater composition in the Judean aquifer recharge area of the Judean Mountains of Israel. A computer simulated geochemical-isotopic-mass-transfer program was used to select flow paths in agreement with the chemical composition of the groundwater. This study concluded that infiltration to the recharge and unsaturated zone is karstic (i.e. rapid and conduit controlled), and calcite dissolution is said to dominate in the unsaturated zone, while incongruent dolomite dissolution dominates in the saturated zone (Kroitoru et al., 1989). The Q factor, for this study, used to adjust the decrease of ^{14}C concentrations due to water-rock interactions, was found to be 62% of the ^{14}C in the soil CO_2. Variations in the ^{14}C concentrations were attributed to pre-and post bomb age water, and not due to decay processes (Kroitoru et al., 1989).

Nativ and Weisbrod (1994) address the problem of whether the coastal aquifer should be treated as a homogeneous water unit. From their analysis of two representative strips that extended through both the western and eastern sections of the aquifer, it was concluded that the clay lenses form a distinct hydraulic boundary between the sand layers. This conclusion was based on the distinct water-level fluctuations, different residence times, and the different chemical and isotopic compositions found within the groundwater of the various clay layers. ^{14}C concentrations measured in the shallower wells were found to contain modern water (^{14}C >100 PMC with measurable tritium), while samples taken from the deeper well separated by a clay layer contained $^{14}C = 35$ PMC with no measurable tritium (Nativ and Weisbrod, 1994; Yechieli et al., 2001). Waters in the upper layers were found to circulate faster than those in the lower layers, and its quality was projected to be inferior to that of the lower layer (Nativ and Weisbrod, 1994). It should be noted, however, that groundwaters sampled in previous studies were taken from distinct layers in observation wells which may only represent small lenses of water, while samples from this study were taken mainly from pumping wells, and are, therefore, better representative of the aquifer as a whole.

Yechieli et al (1996) performed a preliminary ^{14}C study on the fresh-saline water interface of the coastal aquifer. ^{14}C and tritium were used to estimate the residence time of saline waters in the aquifer and the mechanisms of their inland penetration. The distinct isotopic compositions of the groundwater on a vertical scale demonstrated variable rates of groundwater recharge in the different sub-aquifers.

Bruce et al. (2001) explained the distinctive variations in ^{14}C values between the eastern and western sections of the coastal aquifer as a result of different hydrological conditions. The lithology of the eastern section of the aquifer, which includes fewer clay layers, was determined to consist of a more open system than the western section (Bruce et al., 2001). The results of this study will be discussed further in the results and discussion sections of this thesis.

Geyh and Wirth (1980) constructed hydroisochrons (lines of equal age) from the distribution of ^{14}C ages in samples of a confined aquifer in northern Nigeria. The hydroisochrons were found, primarily, to follow the isopotential lines, and from these, the velocity and direction of flow of the groundwater were determined. ^{14}C ages were found

Reproduced with permission of the copyright owner. Further reproduction prohibited without permission.

to be lower near the area of recharge, and increased with the direction of flow (Geyh and Wirth, 1980).

Thirteen water production wells were tested for major ions, in 1976 and 1988, by Fritz et al (1991) in Ontario, Canada for movement of bomb-spike tritium and ^{14}C through the aquifer. The reliability of a hydro-geochemical evaluation of an aquifer based on a single sampling episode was also assessed. Results showed that twelve out of the thirteen wells sampled observed a decrease in tritium relative to the 1976 sampling, while ^{14}C activity for the wells had not changed by more than 6 PMC since the first sampling (Fritz et al., 1991). The thermonuclear input of bomb-spike ^{14}C into the atmosphere was much less concentrated than that of tritium; therefore, ^{14}C is less detectable than tritium in its flow through the aquifer system. The smaller variance in ^{14}C was also attributed to dissolution kinetics between calcite and dolomite, which caused precipitation of ^{14}C-bearing calcite in the saturated zone (Fritz et al., 1991). Samples collected in 1976 were not able to detect how fast the tritium spike was moving, while 1988 samples were able to indicate movement which could give qualitative information related to permeable zones in the aquifer and direction of water flow (Fritz et al., 1991). It was concluded that the chemistry of the aquifer could be adequately depicted with one sampling; however, recharge rates and groundwater flow paths are best determined by multiple sampling using a specific isotope tracer (Fritz et al., 1991).

An isotopic study of DIC in the catchment of the Waimakariri River and deep groundwater in New Zealand was done by Taylor and Fox (1996). Using ^{14}C evidence, mean residence time was found to be 800 years just outside the confined zone, and 2000-

Reproduced with permission of the copyright owner. Further reproduction prohibited without permission.

3000 years within the confined zone itself (Taylor and Fox, 1996). Taylor and Fox (1996) also utilized ^{13}C data to assess the total DIC input to each sample by the river and biogenic components at the time of recharge. Their results were found to be consistent with the ^{14}C residence times when pre-industrial ^{14}C values were given to the two components.

Both ^{14}C and tritium were used as tracers of groundwater recharge by Izbicki et al. (1992) for aquifers underlying the Oxnard Plain in California. The aquifers contain both an upper system, and a thicker lower system close to the coast of the Pacific Ocean. Tritium was detected in the groundwater throughout most of the upper system but not in the lower system more than 3 miles down gradient from the river spreading grounds. The tritium data was also found to be within the parameters of estimated groundwater data calculated from the hydraulic properties of the aquifer (Izbicki et al., 1992). ^{14}C was measured in both the upper and lower systems with values of 73 PMC for the upper to a range of 64 PMC to less than detection limits for the lower system (Izbicki et al., 1992). It was determined from this study based on the data collected, that most water in the upper system was recharged after the early 1950's, however surface spreading to the lower system is impeded by the clay layers of the aquifer system (Izbicki et al., 1992). This case study is not much unlike the Coastal Aquifer of Israel, which contains both, unconfined and confined layers.

Reproduced with permission of the copyright owner. Further reproduction prohibited without permission.

3. THE COASTAL PLAIN AQUIFER OF ISRAEL

The Coastal Aquifer of Israel, which has a large storage capacity and serves as the source for 25% of Israel's drinking water supply, is considered a very important natural resource for the country. Therefore, it is essential to know the direction and rate of groundwater flow in the aquifer. This knowledge will assist in understanding potential pollution mechanisms, and in the assessment of yet untapped potable groundwater sources. The climate in the aquifer region is Mediterranean with an average precipitation of 500 mm/yr.

Geology

The Coastal Plain Aquifer of Israel extends along the coast of the Mediterranean Sea in the west to the Samarian and Judean Mountains in the east. The length of the coastal aquifer, from Mt. Carmel to the Gaza Strip, is 140 km, with a varying width of 8 km in the north, to around 30-km in the south (Fig. 5). The aquifer is located above the mountain and foothill formations of Cretaceous and Paleogene age in the east, and the Neogene formations in the west (Issar, 1968). Only small amounts of calcium carbonate are found in the fine-grained sands (<7%) of the coast (Emery and Neev, 1960). Although most of the coastal sands are non-carbonate, recent Pleistocene and Neogene carbonate sediments are exposed along the extent of the coast (Gavish and Friedman, 1969).

The oldest layers of stratum from the Cretaceous to Miocene System are exposed along the extent of the coastal aquifer. Miocene appears in the northeast section of the coastal aquifer in the form of pebble conglomerates or as limestone facies (strongly distinguished as Coral and *Millipora*-reef) (Picard and Avnimelech, 1937). The Pliocene

Reproduced with permission of the copyright owner. Further reproduction prohibited without permission.

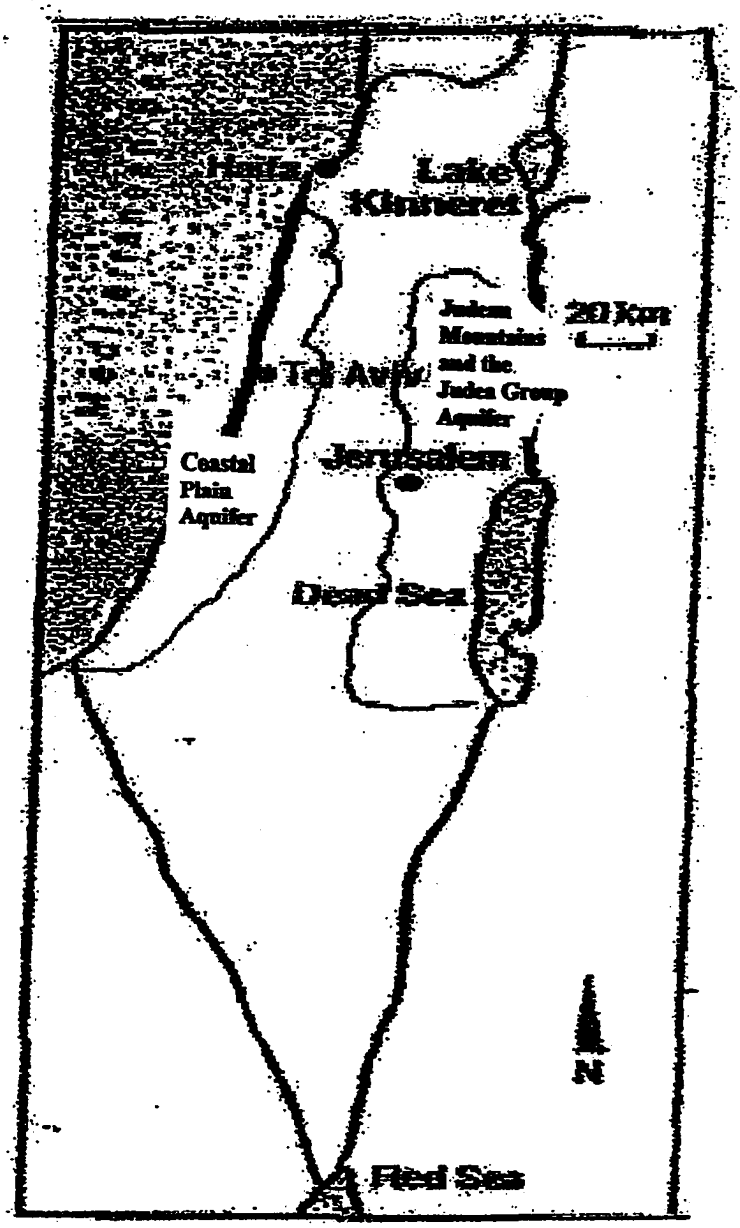

Fig. 5. Location map of Israel with both the Coastal Plain Aquifer and Judea Group Aquifer detailed.

Reproduced with permission of the copyright owner. Further reproduction prohibited without permission.

occurs mainly along the coast as marl, limestone, chalk, sandstone, and conglomerates. The facies are variable and characterize the filling of a sea basin very far from the coast, which formed the subsoil of the coastal plain, rising in thickness in the direction of the current coast (Picard and Avnimelech, 1937).

The Plio-Pleistocene sand and calcareous sandstone of the aquifer are mainly lithified carbonate rocks known as "kurkar" (Gavish and Friedman, 1969). Kurkar defined by Picard (1943) is "calcareous sandstone derived from littoral as well as coastal dune-sand and later diagenetically hardened by calcareous solutions." Gavish and Friedman (1969) subdivided the carbonate rocks located along the coast into four categories:

1. Recent beach rocks (mainly whole shells and skeletal fragments of mollusks, corals, coralline algae, echinoids, and foraminifers).
2. Recent carbonate sands (unconsolidated sands consisting mostly of carbonate grains).
3. Pleistocene carbonate rocks (consolidated sedimentary rocks that were deposited by wind, or eolianite).
4. Neogene carbonate rocks (variable in nature).

The stratigraphy and depositional setting of the Pleistocene sequence located on the Mediterranean coastal plain of Israel has been studied at length (Picard, 1937; Picard and Avnimelech, 1937; Itzhaki, 1961; Avnimelech, 1962; Issar, 1968; Gavish and Friedman, 1969; Issar, 1980). Based on these studies it was determined that the complete Pleistocene sequence was formed by a series of four transgressive and regressive cycles from the Quaternary glacial and interglacial periods. The oldest transgression was the

Reproduced with permission of the copyright owner. Further reproduction prohibited without permission.

most widespread (most penetrating inland), while each successive transgression infiltrated to a lesser degree inland (Buchbinder and Friedman, 1980).

The Plio-Pleistocene sand and calcareous sandstone of the aquifer (the Kurkar Group) is interbedded with marine and continental clay, silt, and shale lenses which represent the different periods of sea water transgressions and regressions of the Pleistocene (Issar, 1968). Beneath the Kurkar group is the Yafo Formation of the Saqiye group (Fig. 6), which is composed of impermeable marine clays and shales of the Pliocene and Miocene Series (Fig. 6). The Yafo Formation forms an aquiclude that separates the Kukar Group from the underlying rock units. In the western section, the aquifer is composed of silt, loam, and clay interbedded with calcareous sandstone, sand, and reddish sand known locally as Hamra (Fig. 6). Its thickness along the coast reaches up to 200 meters, and thins towards the eastern sections (Fig. 6).

Hydrogeology

Due to the clay lenses, mainly near the coast, the aquifer can be divided into four, or possibly more, sub-aquifers (Fig. 6). The divisions of the various sub-aquifer levels were determined in accordance with the geological cross sections of Tolmach (1977); and Acker (1999). In some places, the lenses can reach as far as 10 km from the shoreline. These lenses, which form the hydraulic barriers between the sub-aquifers, cause variant chemical and isotopic compositions for the waters found between them, as well as different recharge mechanisms (Nativ and Weisbrod, 1994).

The upper units of the aquifer are unconfined, while areas of the lower units are confined and their recharge sources are indirect (Nativ and Weisbrod, 1994). In the southern area

Reproduced with permission of the copyright owner. Further reproduction prohibited without permission.

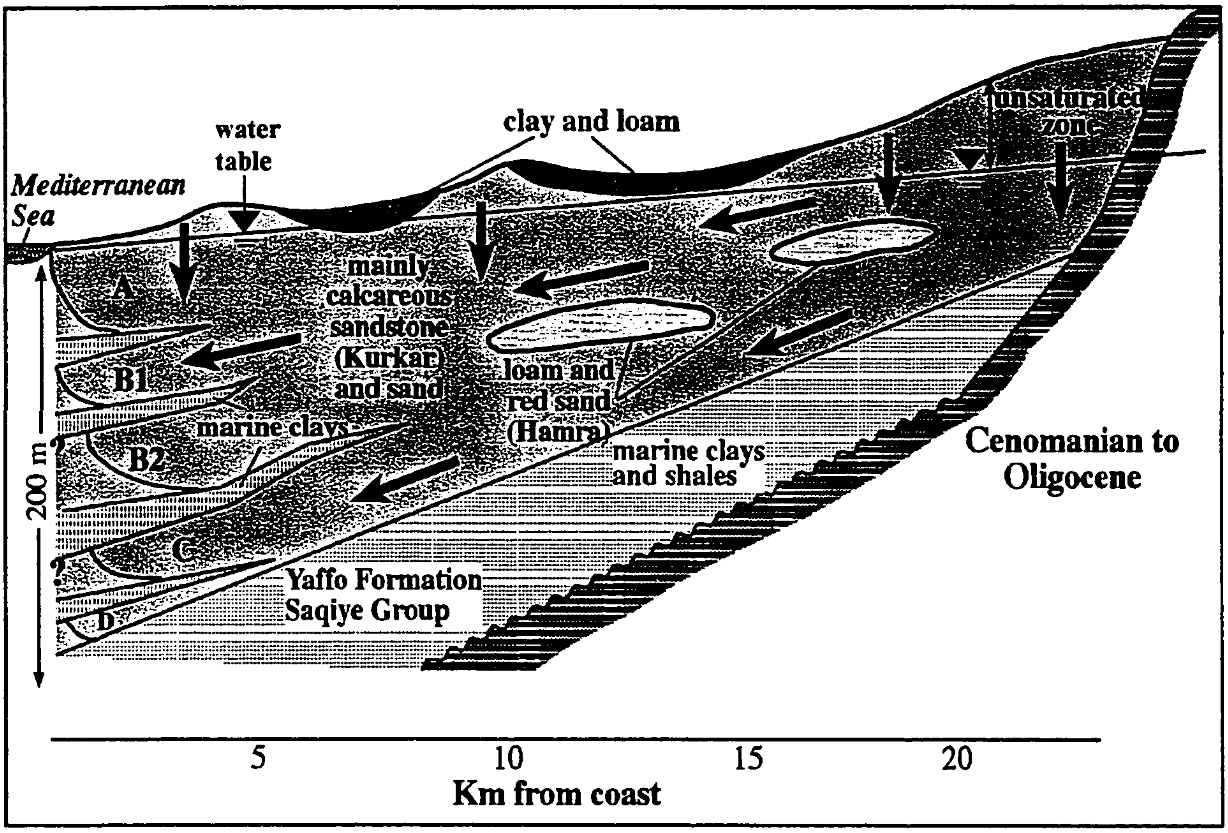

Coastal Plain Aquifer

Fig. 6. Schematic hydrogeological cross-section of the coastal aquifer of Israel. Arrows denote main directions of water flow.

Reproduced with permission of the copyright owner. Further reproduction prohibited without permission.

of the aquifer, saline groundwater has been found in its deepest parts (Vengosh and Rosenthal, 1994). The natural flow of groundwater is from the Judean Mountains in the east to the Mediterranean Sea in the west (Fig. 5). However, this flow path has been distorted in some places due to extensive pumping. Rainwater, irrigation return-flow, and artificial recharge from the Kinneret Lake (Fig. 5) in several generally known locations near the coast recharge the aquifer. The average transport time of water in the aquifer was calculated, using the hydraulic parameters of the aquifer and of the unsaturated zone, to be approximately 30 years, although in some specific regions the transport time was calculated to be more than 500 years (Mercado et al. 1975). The water recharging the eastern part of the aquifer flows west where it then mixes in some locations with waters recharging directly in the west (Mercado, personal communication, 1998). Different mixing mechanisms between several groundwater bodies can occur artificially in some wells due to pumping from wells whose screen lengths are tens of meters long and thus draw water from several sub-aquifers.

Due to the expansion in agriculture in Israel over the past two decades, there came an increased need for irrigation in the Coastal Plain area. Water was therefore imported to the aquifer from the Kinneret Lake and the Judea Group Aquifer, which had a significant effect on the salinity levels of the coastal aquifer. Changes in the chemistry and isotopic composition of the aquifer can also be attributed to agricultural works, seawater intrusion or an isolated salt plume (Vengosh et al., 1999).

Reproduced with permission of the copyright owner. Further reproduction prohibited without permission.

Salinization trends in the Coastal Aquifer

Many different causes have been attributed to salinization of the coastal aquifer. Some maintain that saline waters entering the aquifer along the eastern margin are caused by dissolution of salts lining fissures and faults, which cut through the Hashepela aquitard that is in direct hydraulic contact with the Coastal Aquifer (Rosenthal et al., 1992). In the past half-century, increased agricultural activity, as well as lowering of the water table due to increased pumping, has caused the movement of solutes from the rock surfaces into the fissures and faults to the subsurface.

Golts and Kolton (1994), discuss the effect of tectonics on the salinization of the Coastal Aquifer. Numerous fault zones, which slice up the lower Cretaceous-Neogene succession, have been revealed as well as vertical displacements, which effect the upper Plio-Pleistocene formation. These authors believe that the structural displacements produce the passageway through which saline water from below can rise as a result of new pressure gradients formed by increased pumping of groundwater (Golts and Kolton, 1994).

Vengosh et al. (1994) describe the salinization along the western coast to partly be a result of seawater encroachment. The chemical composition of the water in the interface zone was found by Vengosh et al. (1994) to be a mixture of both seawater and fresh water. However, different groups of saline water occur at various depths, which cannot be explained simply by seawater encroachment. These saline water samples were found to have a chemical composition distinctly different from that of seawater, as well as a Cl and Ca content much higher than that of modern seawater (Vengosh et al., 1994).

Reproduced with permission of the copyright owner. Further reproduction prohibited without permission.

Samples of saline water determined not to originate from seawater are believed to either be from water-rock interactions (Mercado, 1985) or contact with subsurface evaporated brines (Vengosh et al., 1991). Today, seawater intrusion is regulated by a system of “coastal collectors”, recharge barriers, and inland exploitation (Mercado, 1985).

The concentration of nitrates in the coastal aquifer has increased since the agricultural cultivation of the land approximately 60 years ago. During the initial development of the coastal region, mineralization of soil organic matter caused the release of nitrogen. In an analysis of nitrate trends in the coastal aquifer by Kanfi et al. (1983), samples were taken from pumping wells in 1973, and again in 1981, in an attempt to determine the rate of increase of the nitrate levels. From an original nitrate concentration of 52 mg/l in 1973, the rate of increase for 1981 was determined to be 0.13 mg/l/yr (Kanfi et al., 1983). It was also observed, based on the history of nitrate trends along the coastal aquifer, that the rate of nitrate increase has been decreasing steadily and could be reaching a steady state (Kanfi et al., 1983). This observation was attributed to either a change in the hydrological regime, and/or a change in the amount of nitrogen being put into the system (Kanfi et al., 1983). However, constant pollution from fertilizers, manure, sewage, and irrigation water continue to effect the nitrate concentrations.

Reproduced with permission of the copyright owner. Further reproduction prohibited without permission.

4. METHODS

Sampling locations and procedure

Samples were collected from pumping wells along the majority of the Coastal Aquifer area (Fig. 7). Most samples were collected from sub-aquifers A and B, which are connected in most areas of the aquifer at an approximate depth of 50-100m (Fig. 6). Only a small number of wells (Nitzanim, Bitania 1, and Ayanot b') with access to the lower sub-aquifers (B and C) were available for sampling. Therefore, additional wells with better accessibility to the lower sub-aquifers were also sampled during the 1990 re-sampling period (See Appendix 1 for a detailed description of the well logs).

Twenty-six wells were sampled along the coast of Israel for ^{14}C, $\delta^{13}C$, tritium and major ions between 1974-1976. Chemical analyses of the sampled wells from the 1970s were also gathered from the Hydrological Service of Israel (Table 1). Twenty of these wells were again re-sampled in the period between 1993-1998 or their closest current substitute where the original well was no longer in existence for ^{14}C, $\delta^{13}C$, tritium, and major and trace ions (Tables 1, 2 and 7- Appendix 2). The additional wells sampled in the 1990s were also tested for the same variables (Tables 3 and 4).

In the field, the sampled wells were tested for pH (Sentron pH-System 1001), electrical conductivity with a HI 933100 portable microprocessor conductivity meter (Series-IP67), dissolved oxygen (Oxi 325 meter), and temperature (Table 5).

A $BaCl_2$ solution was added to the samples, collected in 1974, together with NaOH in order to precipitate the carbonates for ^{14}C and $\delta^{13}C$ analysis. A total of approximately 90-

Reproduced with permission of the copyright owner. Further reproduction prohibited without permission.

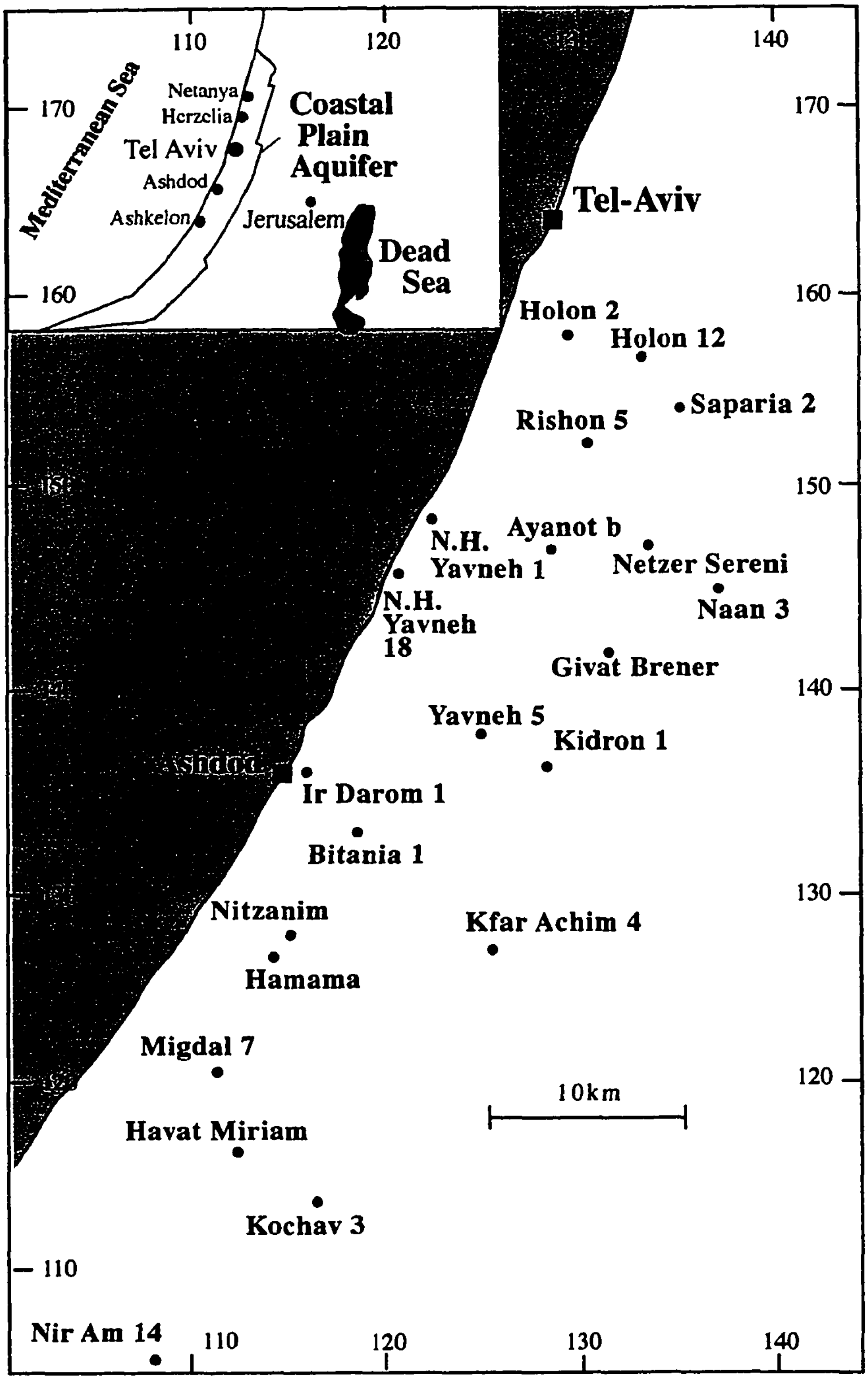

Fig. 7. Location map of Israel (inset) and of sampled wells in the 1970s in the Coastal Plain Aquifer (excluded are the northernmost wells and those from the Gaza Strip).

Reproduced with permission of the copyright owner. Further reproduction prohibited without permission.

100 liters of sample, which was to be used for the extraction of CO_2 for ^{14}C and $\delta^{13}C$ analysis of samples taken in the 1990's, were collected from the wells using 20-liter jerry cans. The samples taken in the 1990's were placed in sealed containers for isotopic analysis. One liter of sample was collected in a plastic bottle for tritium analysis, and thirty-ml samples were also collected in plastic bottles for analysis of $\delta^{18}O$.

Samples for major ion analyses were taken in 250 ml plastic bottles. Samples for trace ions were prepared in 250 ml. plastic bottles by first being completely filled with 1:2 HNO_3 solution for 24 hours, rinsed three times with deionized water, and then filled with 10 ml. of 1:5 HNO_3. At the sampling site, the water was then filtered into the prepared sample bottles using argon and a Millipore filter.

For comparison purposes, separate sets of 125 ml. or 500 ml. samples were collected in dark glass bottles, with or without mercury chloride poison (to eliminate biological activity) or filtered for $\delta^{13}C$ analysis at the Geological Survey of Israel. These samples were taken at nine different wells.

Analytical Procedure

The Ba-carbonate of the samples obtained in the 1970s was treated with acid to obtain the CO_2 for the ^{14}C and $\delta^{13}C$ analyses. The ^{14}C concentration was measured by means of proportional counters on ethane produced from the extracted CO_2 with a counting error of 1 PMC.

Reproduced with permission of the copyright owner. Further reproduction prohibited without permission.

The water from the jerry cans of the 1990's samples was transferred, through the use of a water pump, to a 100-liter sealed container designed to extract and trap the CO_2 gas as a precipitate in a sodium hydroxide solution. 32% hydrochloric acid was added to the 100-liter container through a separatory funnel. A gas circulating pump was then used to facilitate the reaction through a double trap system where the first trap (T_1) contained the sodium hydroxide and the second trap (T_2) was used to capture liquid (Fig. 8). Any excess liquid trapped in T_2 after the extraction procedure was then added to the contents of T_1. This extraction was done within 48 hours of sampling. The samples were then analyzed for ^{14}C at the Weizmann Institute using a LKB 1220 Quantulus scintillation counter with a maximal error of 0.5 PMC.

These same samples were also analyzed for $\delta^{13}C$ using a mass spectrometer with a maximal error of 0.1 ‰. The results are expressed in δ per mil vs. the PDB standard. In addition, tritium analyses were conducted at the Weizmann Institute, using a Quantulus scintillation counter with a maximal error of 1 T.U. in the 1970s and 0.3 T.U. (after enrichment) in the 1990s.

^{18}O was analyzed on a mass spectrometer with a precision of 0.1 ‰ at the GSI. The results are expressed in δ per mil vs. the standard mean ocean water or SMOW standard.

Major and trace ions were analyzed at the GSI on a Perkin-Elmer Optima 3300 ICP Atomic Emission Spectroscope and ICP-MS. Anion concentrations were measured at the GSI using a Dionex Series 4000I Gradient Ion Chromatograph and High Performance

Reproduced with permission of the copyright owner. Further reproduction prohibited without permission.

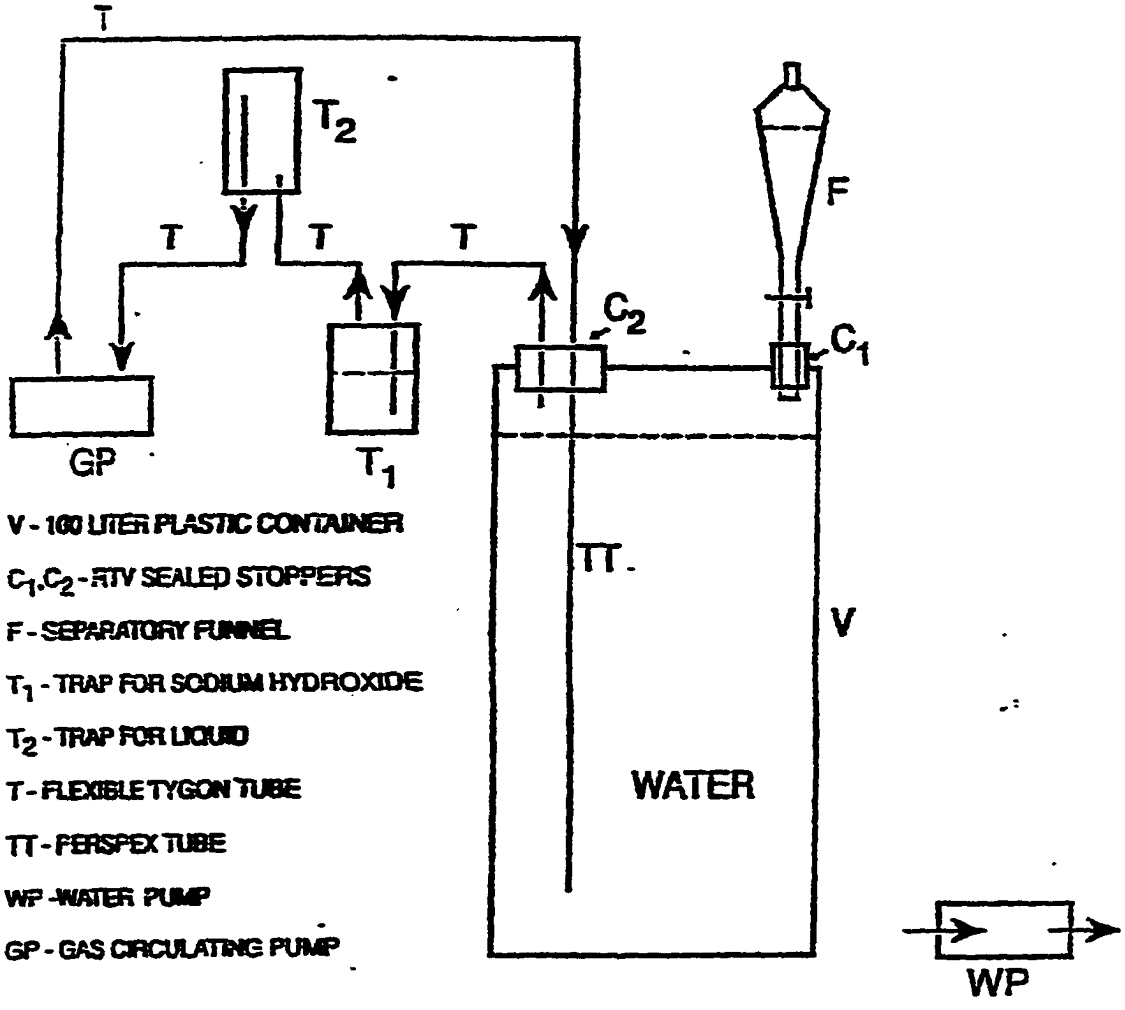

Fig. 8. System built for the extraction of CO_2 from water (from Yechieli, 1997).

Reproduced with permission of the copyright owner. Further reproduction prohibited without permission.

Liquid Chromatography (HPLC). HCO_3^- was analyzed through titration in the laboratory using a 1:50 N hydrochloric acid solution, indicator, and 50 ml. of sample.

The samples analyzed for $\delta^{13}C$ at the GSI used a vacuum extraction, which first involved preparation of the CO_2 line or creating the vacuum, sample bottle preparation, and finally running the sample into an ampoule to get a total CO_2 (ΣCO_2) concentration in mmol/kg. The ampoule was then analyzed on a SIRA-II (VG) mass spectrometer. Results are given in Table 6.

Sediment samples of four select wells from both the eastern and western sections of the aquifer were analyzed at the Geological Survey of Israel (GSI) using XRD. The purpose of this experiment was to identify the main constituents of the sediments at varying depths in both sections of the aquifer.

Samples of variant depths from four wells, Naan, and Kfar Achim 4 from the east, and Nitzanim and Ben Zachai 8 from the west, were prepared for mineralogical analysis by first grinding the material in a mechanical mortar for 3-5 minutes. The samples were then sieved through a 200- mesh sieve. The final powder was approximately 63 μm in size as per the "standard preparation technique" described by Gavish and Friedman (1973). The analyses were made on an X-ray diffraction unit with a Cu tube, crystal monochromator and a proportional counter. The machine was operated at 40 KV and 30 milliamperes.

A Scanning Electron Microscope (SEM) was used at the GSI for analysis of sediment samples for the purpose of examination of the different generations of calcite

Reproduced with permission of the copyright owner. Further reproduction prohibited without permission.

cementation. Two different wells were studied, Sapiria 2 from the eastern section of the aquifer and Holon 2 from the western section. Two samples from the Sapiria 2 well were taken from the unsaturated zone and one was taken from the saturated zone. One sample was taken from the Holon 2 well at a depth of 44.3 meters from the saturated zone. This sample was initially analyzed using an optical microscope.

Reproduced with permission of the copyright owner. Further reproduction prohibited without permission.

5. RESULTS

Chemical and isotopic analyses

Results of the chemical and isotopic analyses are given in Tables 1- 4 and 7. ^{14}C values for both the 1970s and the 1990s showed a clustering of values ranging mainly from 60 to 70 PMC and 90 to 100 PMC (Table 2; Fig. 9). ^{14}C values were, with few exceptions, relatively similar for both sampling periods (Table 2). The lower ^{14}C concentrations were found to be located primarily in the western section of the aquifer, while the higher concentrations were associated with the eastern section of the aquifer (Fig. 10). In the 1990s, there are an increased number of ^{14}C values between 70-90 PMC relative to the 1970s. These values were determined to be located in both the central and eastern sections of the aquifer. Tritium values measured in the 1970s are quite variable, while values taken in the 1990's have a tighter range between 0 and 7 TU relative to the 1970 values (Table 2; Fig. 11).

Most of the $\delta^{13}C$ values are similar throughout the aquifer with no significant differences between the two sampling periods having values ranging from –13 to –9 ‰ relative to PDB (Table 2). The $\delta^{13}C$ values of the 1970s are depicted in Figure 12. Results of $\delta^{13}C$ values measured at the GSI were slightly more positive, with or without the added poison, than those from Weizmann (Table 6). The sample from the Nitzanim well that was left open for 6 days had a noticeably lower ΣCO_2 and more positive $\delta^{13}C$ than the other two samples from the same well (Table 6). This would indicate a loss of ΣCO_2 from the well water sampled and the enrichment of $\delta^{13}C$ as it mixes with the CO_2 of the atmosphere. The $\delta^{13}C$ results from the Weizmann Institute are referred to in this study as the ^{14}C analysis was done on these samples at the Institute as well.

Reproduced with permission of the copyright owner. Further reproduction prohibited without permission.

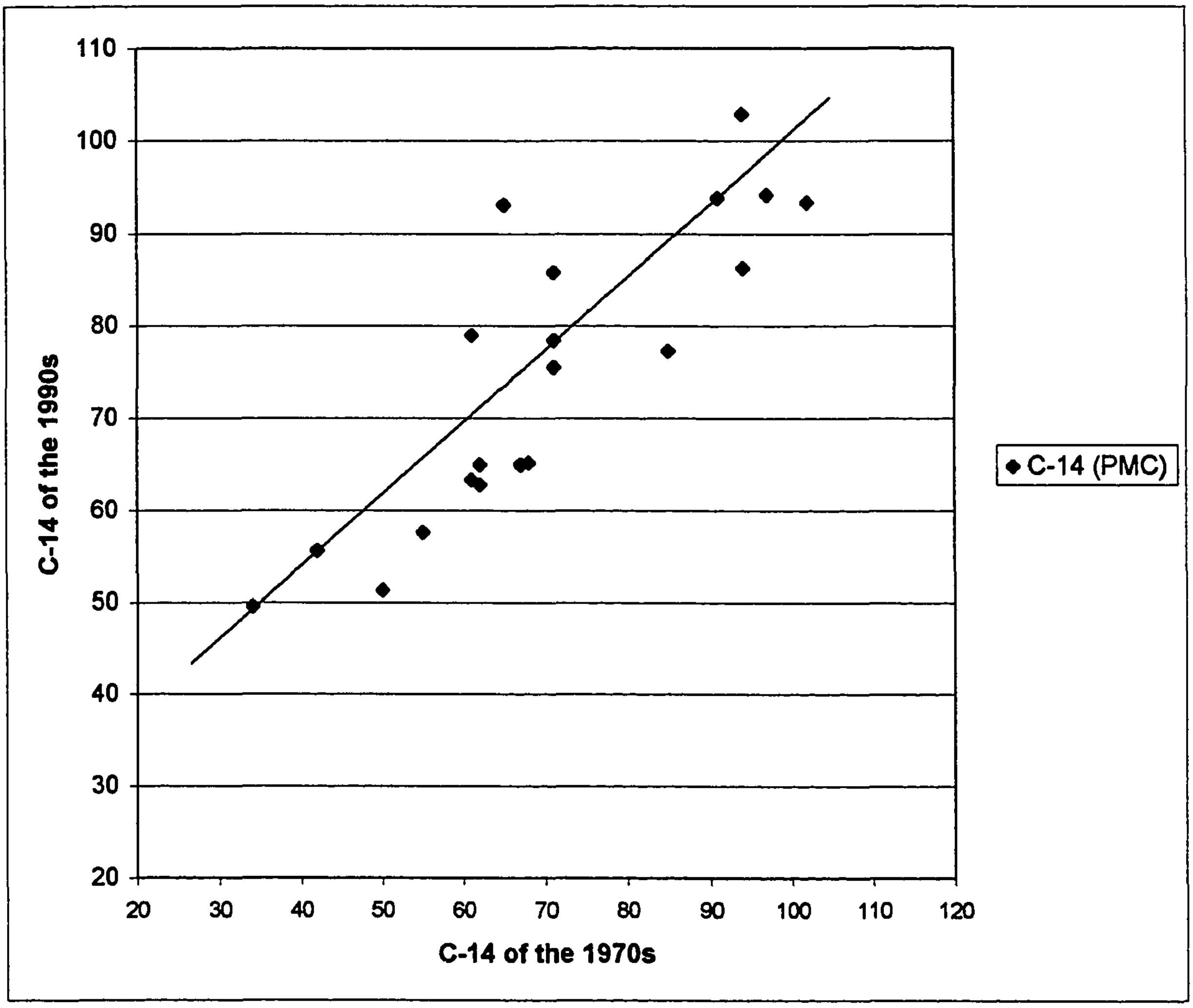

Figure 9. ^{14}C of the 1970s vs. ^{14}C of the 1990s.

Reproduced with permission of the copyright owner. Further reproduction prohibited without permission.

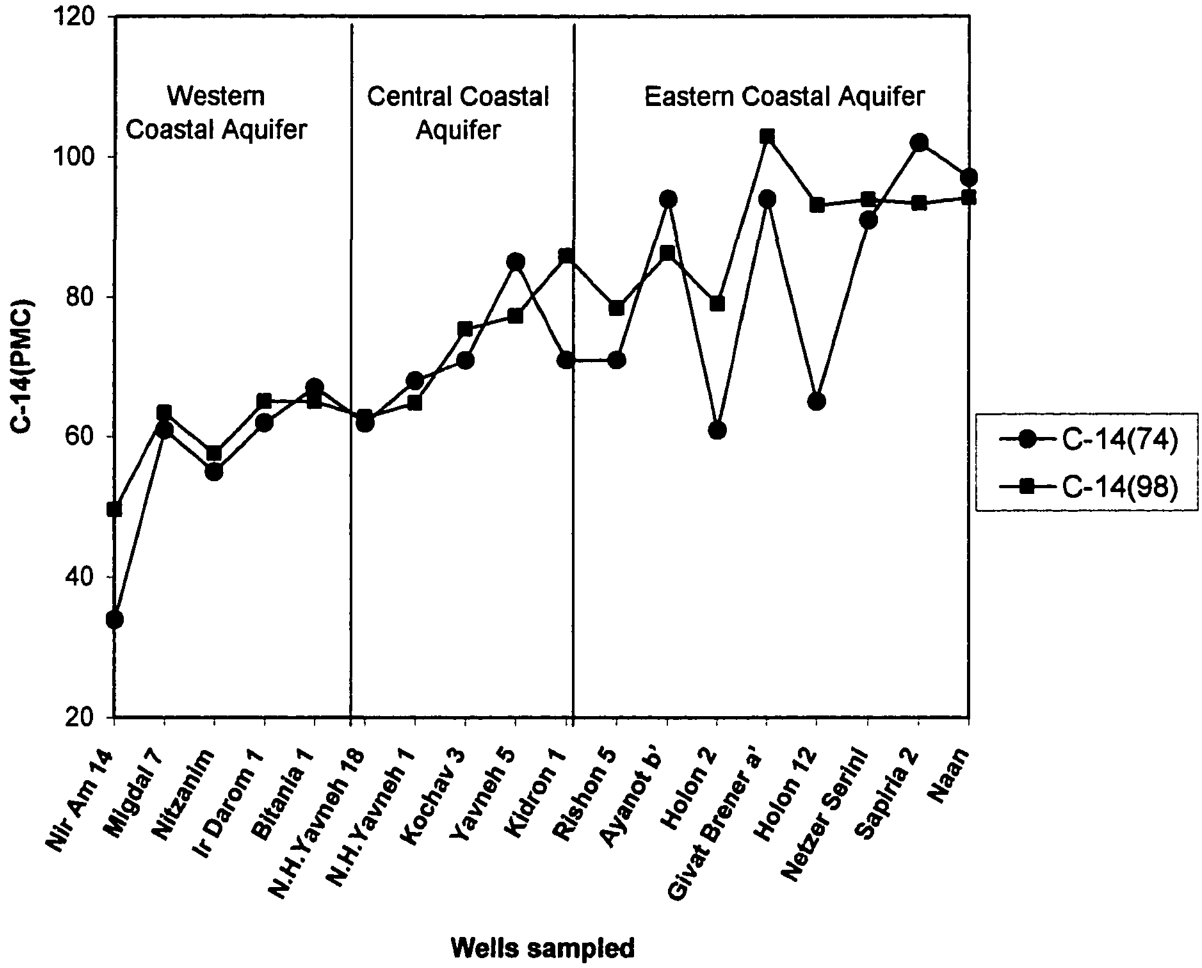

Fig 10. ^{14}C of the 1970s and the 1990s relative to its location within the aquifer. Note: The northernmost wells are not depicted here.

Reproduced with permission of the copyright owner. Further reproduction prohibited without permission.

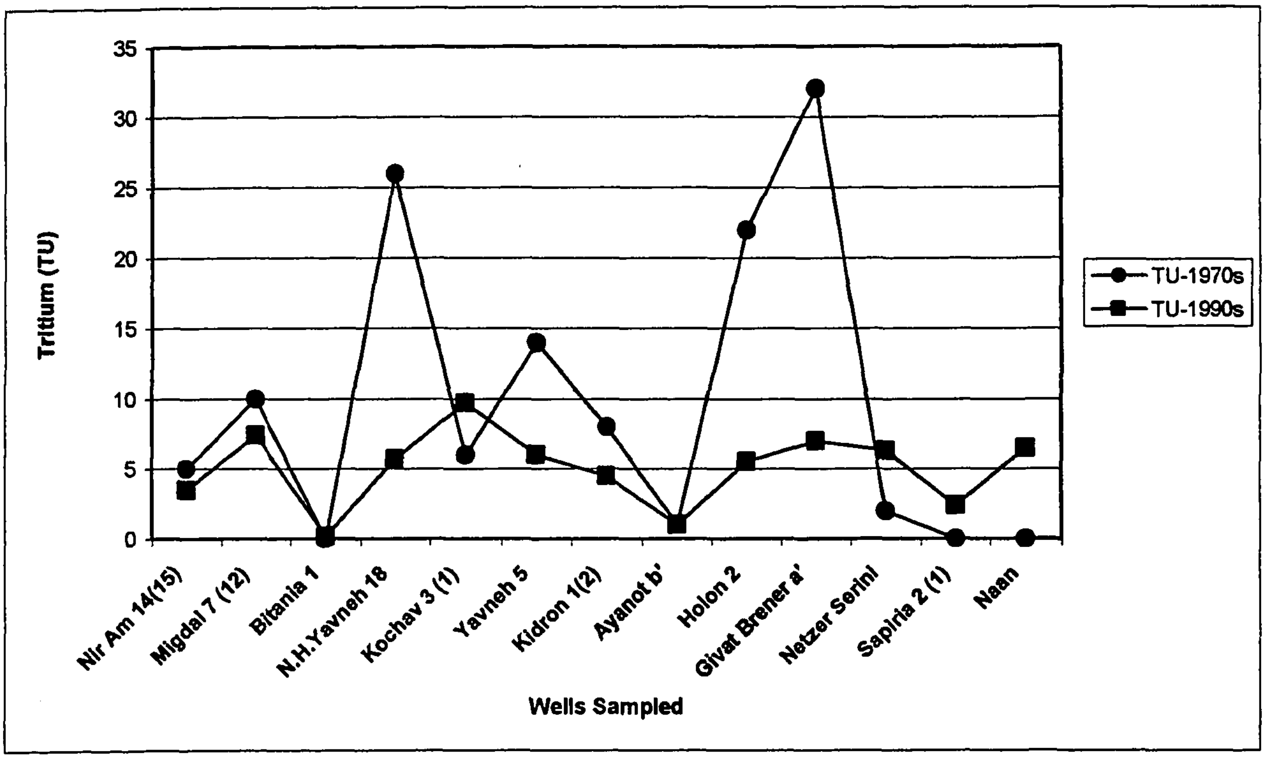

Fig. 11. Tritium of the 1970s versus tritium of the 1990s. (Numbers in parenthesis indicate substitute wells sampled in the 1990s.)

Reproduced with permission of the copyright owner. Further reproduction prohibited without permission.

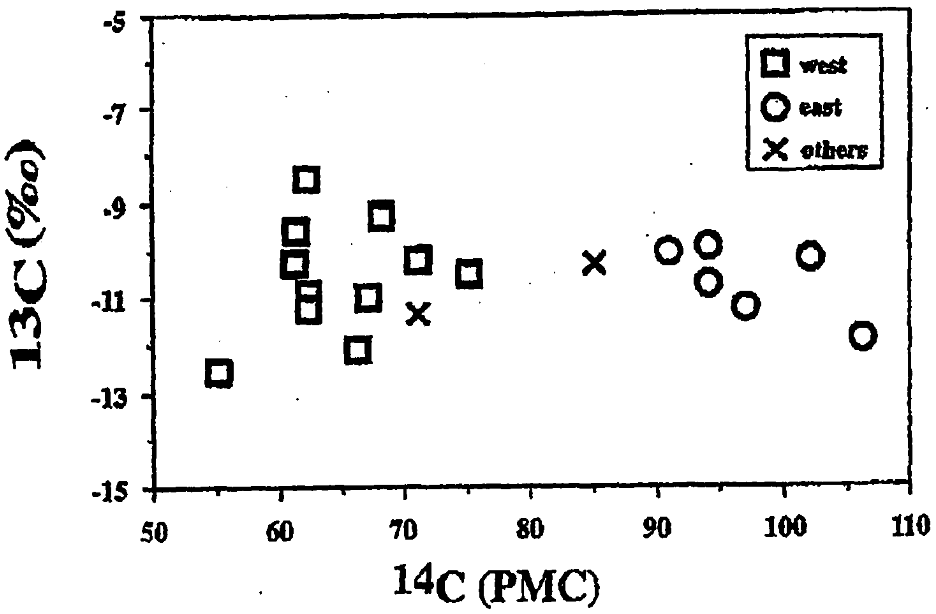

Fig. 12. ^{14}C (PMC) versus δ^{13}C (‰) for the 1970s.

Reproduced with permission of the copyright owner. Further reproduction prohibited without permission.

$\delta^{18}O$ values of most of the samples were relatively uniform, with values ranging from -4 to –5 ‰, with a few exceptions (Table 2, Fig.13). The $\delta^{18}O$ values were above –4 ‰ in only a small number of the wells, which would imply that the majority of the sampled wells were unaffected by wastewater or Lake Kinneret waters.

Field measurements

The groundwater temperatures ranged from 19-25°C reflecting the mean annual temperature for this area (Table 5). The majority of groundwater samples can be typified with having low salinity, with electrical conductivity values ranging from 0.6-2.5 ms (Table 5). The groundwater samples are characterized by medium to high pH values ranging from 6.8-8.3 (Table 5), with a mean value of 7.4. The majority of wells tested were close to saturation in dissolved oxygen (Table 5).

The reaction errors (RE), where RE = | cations – anions | / (cations + anions) * 100, for the majority of the sampled wells are within normal parameters (0-2) (Tables 1 and 3). Exceptions can be attributed to possible inaccuracies of the older data or exclusion of data.

The Cl content of the wells varied greatly not only throughout the aquifer, but between the sampling periods (Tables 1 and 2). Figure 14 depicts the changes in Cl concentrations of Lake Kinneret and four wells.

Reproduced with permission of the copyright owner. Further reproduction prohibited without permission.

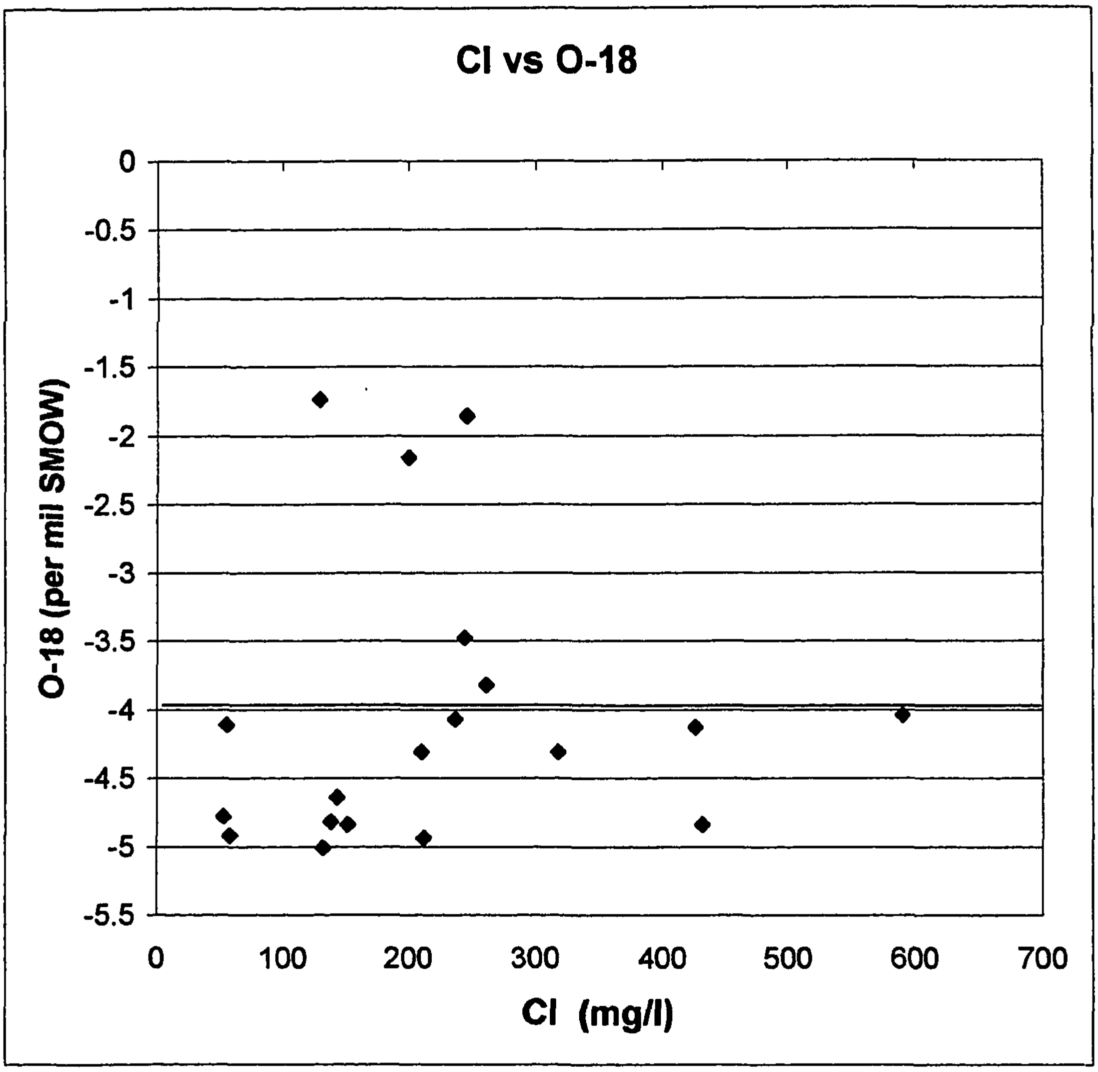

Fig. 13. Cl (mg/l) versus δ^{18}O (‰). δ^{18}O values below the bold line (<-4 ‰) represent the groundwater unaffected by wastewater or the Kinneret Lake.

Reproduced with permission of the copyright owner. Further reproduction prohibited without permission.

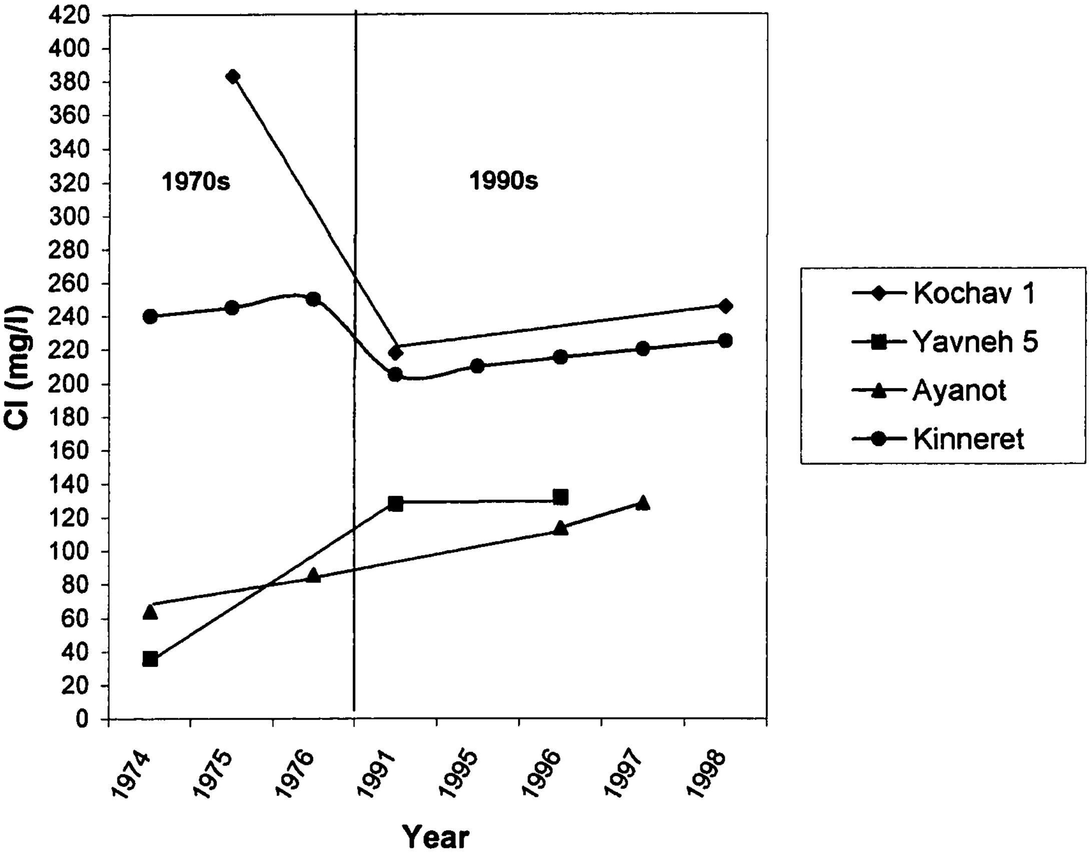

Fig. 14. Variation of Cl concentration between 1974-1998 in selected wells and the Kinneret Lake.

Reproduced with permission of the copyright owner. Further reproduction prohibited without permission.

Reproduced with permission of the copyright owner. Further reproduction prohibited without permission.

Table 1: Major ion analyses (mg/l) of well waters sampled from 1972-1998

NAME	X	Y	Sampling Date	Ca	Mg	Na	K	Cl	SO_4	HCO_3	NO_3	RE%	Na/Cl	SO_4/Cl	Well Depth (m)	Screen Depth (m)
Nir Am 14	10849	10269	05/08/74	29.2	26.6	298	2.30	269	78.6	418	30.4	0.24	1.70	0.11	143	121-143
Nir Am 14	10849	10269	20/07/81	27.0		280	5.00	263	78.0		34.0	[ ]	1.64	0.11		
^Nir Am 15	10929	10366	05/08/74	37.2	27.2	234	2.30	241	60.5	360	15.4	0.39	1.50	0.09	133	101-128
Nir Am 15	10929	10366	28/4/98	38.7	29.9	197	3.09	262	52.4	293	7.2	1.0	1.16	0.07		
Kochav 3	11667	11280	27/10/75	48.0	54.7	278	4.80	425	65.8	335	17.0	0.03	1.01	0.06	136	124-136
Kochav 3	11667	11280	23/06/91	43.2	39.2	267	4.30	325	62.0	335	10.0	3.00	1.27	0.07		
^Kochav 1	11649	11175	31/10/75	51.0	54.0	266	5.00	383	72.0	*305	15.0	3.17	1.07	0.07	123	104-115
Kochav 1	11649	11175	28/4/98	25.8	26.7	203	2.87	246	52.3	265	5.5	0.0	1.27	0.08		
Havat Miriam c'	11591	11562	30/07/73	38.1	49.9	209	2.74	280	81.7	342	28.8	1.58	1.15	0.11	94.5	
Havat Miriam c'	11591	11562	16/07/92	32.2	51.0	228	3.00	409	50.0	127	29.0	2.19	0.86	0.05		
Migdal 7	11271	11856	03/09/74	41.0	42.0	234	3.00	282	63.0	342	42.0	0.68	1.28	0.08	109	72.7-107
Migdal 7	11271	11856	19/07/90	68.0	68.0	367	6.00	605	80.0	*342	55.0	0.22	0.94	0.05		
^Migdal 12	11326	11773	24/08/72	42.0	50.0	211	3.00	262	68.0	336	60.0	0.62	1.24	0.10	103	87.7-102
Migdal 12	11326	11773	27/11/97	57.2	66.0	275	3.76	432	69.5	337	89.8	0.60	0.98	0.06		
Hamama	11580	12470	1975	40	39	111										
Nitzanim	11630	12610	24/05/74					173							87	57.1-87.0
Nitzanim	11630	12610	27/11/97	78.4	44.7	104	2.55	210	45.1	261	84.7	1.14	0.77	0.08		
Kfar Achim 4	12610	12700	12/09/75					241							73	57.6-68.4
Kfar Achim 4	12610	12700	12/10/97	141	67.3	185	2.9	427	27	410	39	1.88	0.67	0.02		
Bitania 1	11966	13172	19/06/74	90.0	47.0	185	4.00	314	58.0	*375	31.0	0.60	0.91	0.07	98	55.1-93.4
Bitania 1	11966	13172	17/12/96	73.0	38.6	165	4.70	244	59.2	323	18.6	1.45	1.04	0.09		
Ir Darom 1	11638	13485	11/5/76	49.0	13.0	40.0	2.0	53.0	14.0	*216	10.0	1.68	1.16	0.10	65	56.4-64.1
Ir Darom 1	11640	13478	12/10/97	76.3	16.4	55.8	2.01	138	30	216	22	[5.31]	.62	0.09		
Kidron 1	12888	13664	22/08/73	110	29.2	110	44.6	216	33.6	366	101	2.04	0.79	0.06	73	64.1-70.6

Table 1: continued

NAME	X	Y	Sampling Date	Ca	Mg	Na	K	Cl	SO_4	HCO_3	NO_3	RE%	Na/Cl	SO_4/Cl	Well Depth (m)	Screen Depth (m)
^Kidron 2	12903	13838	25/05/76	90.0	41.0	138	7.00	222	43.0	*354	40.0	1.62	0.96	0.07	64.3	38.6-64.3
Kidron 2	12903	13838	12/10/97	173	78.7	196	9.56	590	70.0	354	55.0	1.86	0.51	0.04		
Yavneh 5	12520	13760	28/08/74	59.0	7.00	24.0	1.00	36.0	10.0		17.0	[ ]	1.03	0.10	101	88.8-101
Yavneh 5	12520	13760	17/12/96	79.7	29.2	76.6	3.80	132	28.9	276	46.5	1.05	0.89	0.08		
Givat Brenner a'	13110	14177	15/11/63	90.6	22.3	64.2	1.50	104	21.0	323	32.7	0.05	0.96	0.08	90	82-90
Givat Brenner a'	13110	14177	12/10/97	156	48.7	101	6.52	318	68.0	300	85.0	0.93	0.49	0.08		
N.H. Yavneh 18	12044	14512	23/11/72	63.0	10.0	29.0	2.0	41.0	15.0	*201	17.0	2.33	1.09	0.14	35	
N.H. Yavneh 18	12062	14556	3/6/98	77.9	16.3	76.3	1.63	177	24.7	200	14.0	2.4	0.66	0.05		
Naan	13696	14530	17/07/74	106	73.0	200	2.74	461	81.7	330	31.5	1.30	0.67	0.07	80.3	73.3-78.3
Naan	13696	14530	23/12/97	308	199	816	5.62	2000	303	268	49.0	0.36	0.63	0.06		
Ayanot b'	12798	14696	30/06/76					86								68-90
Ayanot b'	12798	14696	23/12/97	118	15.5	50.4	1.26	129	45.4	239	51.3	0.25	0.60	0.13		
Netzer Sereni	13212	14806	29/08/73	106	4.86	39.1	0.78	78.0	43.2	195	80.1	1.10	0.77	0.20	92.4	
Netzer Sereni	13212	14806	27/11/97	144	25.3	65.8	1.29	151	76.3	249	160	1.36	0.67	0.19		
N.H. Yavneh 1	12232	14877	16/5/76	68.0	6.0	26.0	1.0	38.0	16.0	*227	17.0	3.4	1.06	0.16	41	27.7-39.0
N.H. Yavneh 1	12232	14877	3/6/98	73.6	7.9	31.2	1.33	55.9	14.3	227	23.7	2.3	0.86	0.09		
Rishon 5	12970	15230	27/11/97	63.8	12.7	31.2	1.26	53.5	9.5	195	29.1	2.22	0.90	0.07	134	110-132
Sapiria 2	13486	15436	30/06/75	122	29.0	69.0	2.00	161	42.0	247	80.0	3.50	0.66	0.10	110	88.8- 103
^Sapiria 1	13400	15568	17/12/96	74.7	36.5	133	5.60	237	68.3	256	3.60	1.19	0.87	0.11		
Holon 12	13210	15718	26/07/72	60.2	25.5	50.6	2.35	95.7	43.2	256	34.6	[6.31]	0.81	0.17	101	82.8-93.2
Holon 12	13210	15718	23/12/97	83.0	29.5	94.6	3.64	201	50.6	171	17.3	4.83	0.73	0.09		
Holon 2	12855	15823	02/06/74	58.0	9.00	18.0	1.00	30.0	13.0	180	26.0	0.47	0.92	0.16	52.1	46.9-52.1
Holon 2	12855	15823	3/6/98	68.9	10.6	25.5	1.15	58.5	21.8	198	33.1	3.8	0.67	0.14		

Reproduced with permission of the copyright owner. Further reproduction prohibited without permission.

Reproduced with permission of the copyright owner. Further reproduction prohibited without permission.

Table 1: continued

NAME	X	Y	Sampling Date	Ca	Mg	Na	K	Cl	SO_4	HCO_3	NO_3	RE%	Na/Cl	SO_4/Cl	Well Depth (m)	Screen Depth (m)
Petach Tikvah 3	13745	16666	22/07/74	154	26.8	62.1	2.74	113	91.3	317	91.8	3.68	0.84	0.30	39	36.4-39.8
Tel Mond 8	14102	18386	09/09/75	72.0	15.0	36.0	2.00	82.0	19.0	200	23.0	0.69	0.68	0.09	95	80.3-95.0
Tel Mond 8	14102	18386	01/09/90	110	16.0	52.0	2.00	123.0	44.0	214	67.0	0.83	0.65	0.13		
^Tel Mond 13	14266	18364	18/06/73	68.1	17.0	46.0	1.17	85.1	19.2	225	28.0	0.87	0.83	0.08	72	
Tel Mond 13	14266	18364	23/12/97	61.8	14.2	51.9	1.67	73.8	17	212	27.2	1.55	1.08	0.09		
Givat Haim b'	14389	20060	17/07/74	134	36.5	117	2.35	269	24.0	391	25.2	0.15	0.67	0.03	94	75-89
Givat Haim b'	14389	20060	13/04/92	52.6	30.2	103	2.40	200	29.0	174	22.0	1.06	0.79	0.05		
^Givat Haim c'	14389	20060	23/12/97	64.1	19.5	102	2.78	143	18	249	26.7	2.25	1.10	0.05	90	

* = estimated value RE= reaction error [ ] = Reaction Error is large due to possible inaccuracies or exclusion of data.
^ = Alternative well sampled closest in location to an original well which was no longer in service.

Table 2: Isotopic analyses of wells sampled in the 1970's and 1990's, including Cl.

Name	^{14}C (PMC) 1974-1976	^{14}C (PMC) 1993-1998	$\delta^{13}C$ (‰) 1974-1976	$\delta^{13}C$ (‰) 1993-1998	Tritium (TU) 1974-1976	Tritium (TU) 1993-1998	Cl (mg/l) 1974-1976	Cl (mg/l) 1993-1998	$\delta^{18}O$ (‰) 1998
Nir Am 14	34		-17.2		5		269		
Nir Am 15		49.6		-12.2		3.5	241	262	-3.82
Migdal 7	61		-10.3		10		282		
Migdal 12		63.3		-12.9		7.4	270	432	-4.84
Havat Miriam c	75		-10.5		4		280		
Hamama	62		-11		3.5				
Nitzanim	55	57.6	-12.5	-12.3		2.8	173	210	-4.31
Ir Darom 1	62	65.0	-11.2	-11.1		7.8	44.0	138	-4.82
Kochav 3	71		-10.2		6		425		
Kochav 1		75.5		-10.4		9.7	383	246	-1.86
Bitania 1	67	65	-11	-11.1	0	0.2	314	244	-3.48
N.H.Yavneh 18	62	62.8	-8.5	-9.4	26	5.7	222		-4.96
N.H.Yavneh 1	68	65.2	-9.3			6.3	38.0	55.9	-4.11
Yavneh 5	85	77.3	-10.3	-11.5	14	6	36	132	-5.01
Kfar Achim 4	163	84.4	-13.6	-11.3		4.8	241	427	-4.13
Ayanot b'	94	86.3	-10.7	-13.6	1	1.0	64	129	-1.74
Holon 2 (1993) (1998)	61	90.6 79.0	-9.6	-9.9 -11.1	22	7 5.5	30	58.5	-4.92
Kidron 1	71		-11.3		8		216		
Kidron 2		85.8		-14.4		4.5	222	590	-4.04
Rishon 5	71	78.4	-9.1	-11.1		6.2		53.5	-4.78
Givat Brenner a'	94	102.9	-9.9	-13.5	32	7.0	103	318	-4.31
Holon 12	65	93.1	-10.2	-12.6		2.9	44	200	-2.16
Netzer Serini	91	93.9	-10	-13.1	2	6.3	80	151	-4.84
Sapiria 2	102		-10.2		0		161		-4.07
Sapiria 1		93.4		-12.1		2.4		237	
Naan	97	94.2	-11.2	-13.2	0	6.5	460	2000	-3.80
Petach Tikva 3	83		-11.3		1		113		
Tel Mond 8	50		-9.7				82		
Tel Mond 13		51.3		-13.1		0.2		212	-4.94
Givat Haim b'	42						269		
Givat Haim c'		55.6		-14.7		7.6		143	-4.64

Reproduced with permission of the copyright owner. Further reproduction prohibited without permission.

Reproduced with permission of the copyright owner. Further reproduction prohibited without permission.

Table 3: Chemical data of groundwater (mg/l) from additional wells sampled in the 1990s (unless otherwise noted).

NAME	X	Y	Sampling Date	pH	Ca	Mg	Na	K	Cl	SO_4	HCO_3	NO_3	RE %	Na/Cl	SO_4/Cl
Lahat 3	11132	11528	7/9/97	7.43	56.7	55.9	233	2.86	334	76.9	342	28.7	1.5	1.07	0.08
Yad Mordecai 2	10725	11029	7/9/97	7.42	32.0	32.1	93.9	1.74	95.7	23.3	266	24.5	2.6	1.51	0.09
Yad Mordecai 6	10707	11094	7/9/97	7.0	52.9	29.2	57.8	2.00	85.5	22.8	220	48.0	2.4	1.04	0. 10
Beit Yehoshua 9	13743	18500	19/8/98	7.50	108	11.4	50.5	1.3	112	39.8	217	70.7	0.70	0.69	0.13
42/1	13660	18638	19/8/98	8.30	82	7.2	39	1.3	69.5	15.8	251	13.9	1.6	0.86	0.08
Herzalia a'	13536	17436	19/8/98	7.96	130	17.8	82	1.6	244	22.7	215	33.1	0.65	0.51	0.03
Bnei Dror c'	14071	18513	19/8/98	7.70	94.5	15	48	1.7	89	47.1	203	89.9	0.92	0.83	0.19
R-161	9840	10470	1976												
E-11A	10210	10400	1976												
G2 Q-12	10520	10190	1976												

*Due to the location of wells R-161, E-11A, and G2 Q-12 in the Gaza Strip further data was unavailable.

Reproduced with permission of the copyright owner. Further reproduction prohibited without permission.

Table 4: Isotopic data of groundwater from additional wells sampled in the 1990s (unless otherwise noted).

Well	**C-14 (PMC)**	**$\delta^{13}C$ (‰)**	**Tritium (T.U.)**	**$\delta^{18}O$ (‰)**	**Well Depth (m)**	**Screen depth (m)**	**Sub-aquifer**
Lahat 3	63.1±0.4	-11.2	0.1±0.1	-4.67	122	87.62-121.60	C
Yad Mordecai 2	60.1±0.4	-12.2	3.7±0.2	-5.22		87.20-115.50	
Yad Mordecai 6	65.2±0.4	-11.6	4.1±0.2	-4.88		56.64-68.80	
Bet Yehoshua 9	75.5±0.4	-12.4	3.6	-5.03			
42/1	69.5±0.4	-11.4	0.7	-5.00	142	48-?	B and C
Herzalia a	67.8±0.4	-12.4	0.8	-4.88	131.3	109.6-126.50	C
Bnei Dror c	76.3±0.4	-12.4	7.4	-5.15		72.50-82.40	
R-161 (1976)	59	-9.4					
E-11A (1976)	53	-10.3					
G2 Q-12 (1976)	58	-13.1					

Table 5: Field measurements of pH, temperature, electrical conductivity (EC), and dissolved oxygen (DO).

NAME	X	Y	Sampling Date	pH	Temp. °C	EC (ms)	DO (mg/l) and/or % saturation
Nir Am 15	10929	10366	28/4/98	7.24	25.0	1.44	3.30
Kochav 1	11649	11175	28/4/98	7.30	25.1	1.26	6.65
Migdal 12	11326	11773	27/11/97	7.65	23.7	N/A	7.91 (94.2%)
Nitzanim	11630	12610	27/11/97	7.5	22.6	N/A	7.55
Kfar Achim 4	12610	12700	12/10/97	6.79	25.6	2.15	6.02 (85.5%)
Bitania 1	11966	13172	17/12/96	7.42	22.2	1.4	4.7 (55%)
Ir Darom 1	11640	13478	12/10/97	7.20	25.6	.861	5.60 (76.0%)
Kidron 2	12903	13838	12/10/97	6.79	24.6	2.48	6.50 (84%)
Yavneh 5	12520	13760	17/12/96	7.27	22.7	0.99	5.72 (65%)
Givat Brenner a'	13110	14177	12/10/97	6.96	25.0	1.82	N/A
N.H. Yavneh 18	12062	14556	3/6/98	7.28	22.4	.926	8.38
Naan	13696	14530	23/12/97	7.01	24.0	N/A	7.43 (85.4%)
Ayanot b'	12798	14696	23/12/97	7.25	22.2	N/A	7.46 (83.2%)
Netzer Sereni	13212	14806	27/11/97	7.42	22.6	N/A	7.86 (90.5%)
N.H. Yavneh 1	12232	14877	3/6/98	6.87	22.3	.598	4.98
Rishon 5	12970	15230	27/11/97	7.73	23.2	N/A	8.05 (92.6%)
Sapiria 1	13400	15568	17/12/96	7.00	18.6	1.27	12.5 (100%)
Holon 12	13210	15718	23/12/97	7.36	21.8	N/A	7.84 (84.4%)
Holon 2	12855	15823	3/6/98	7.60	22.6	.612	7.46
Tel Mond 13	14266	18364	23/12/97	7.53	22.4	N/A	7.16 (81.3%)
Givat Haim c'	14389	20060	23/12/97	7.9	21.4	N/A	4.42 (48.8%)
Lahat 3	11132	11528	7/9/97	7.43	24.0	1.91	85.4%
Yad Mordecai 2	10725	11029	7/9/97	7.42	23.0	.806	74%
Yad Mordecai 6	10707	11094	7/9/97	7.0	22.7	.730	79.5%
Beit Yehoshua 9	13743	18500	19/8/98	7.50	22.7	.908	6.70 (78.2%)
42/1	13660	18638	19/8/98	8.30	22.8	.678	3.80 (44.4%)
Herzalia a'	13536	17436	19/8/98	7.96	23.3	1.27	6.76 (86.6%)
Bnei Dror c'	14071	18513	19/8/98	7.70	26.5	.905	9.31 (117%)

Reproduced with permission of the copyright owner. Further reproduction prohibited without permission.

Table 6: Results of ΣCO_2 and $\delta^{13}C$ analyses from the GSI and Weizmann Institute.

	ΣCO_2 (mmol/kg)	$\delta^{13}C$- GSI	$\delta^{13}C$- Weizmann
Lahat 3			-11.2
125 ml	3.61	-9.9	
125 ml poison	4.82	-9.77	
500 ml poison	4.13	-10.01	
Kfar Achim 4			-11.3
125 ml poison	8.02	-11.6	
Givat Brenner			-13.5
125 ml poison	3.85	-11.15	
Yad Mordecai 6			-11.6
125 ml poison	3.82	-9.74	
500 ml poison	3.59	-10.25	
500 ml	3.30	-10.49	
Ir Darom 1			-11.1
125 ml poison	2.58	-9.03	
Kidron 2			-14.4
125 ml poison	6.14	-11.23	
Yad Mordecai 2			-12.2
125 ml poison	3.04	-10.51	
Nitzanim			-12.3
125 ml poison	3.59	-9.01	
125 ml poison + filter	4.11	-9.74	
125 ml open 6 days	2.29	-5.30	
Migdal 12			-12.9
125 ml poison	4.06	-9.67	
125 ml poison + filter	5.74	-9.25	

Reproduced with permission of the copyright owner. Further reproduction prohibited without permission.

SEM analyses

Using an optical microscope, the Holon 2 sample at a depth of 44.3 meters was found to contain quartz grains coated with a carbonate matrix of authigenic origin. This is further depicted in figure 15A upon more detailed examination with the SEM, where the calcite crystals, which display rhombohedral textures, can be seen packed between quartz. C Figure 15B also depicts the calcite cement between the pore spaces of quartz grains. In figure 16A, different calcite phases can be observed with smaller (1 μm) crystals on top of the quartz grain and larger carbonate crystals to the right. In figure 16B, detrital carbonate can be observed with quartz grains on the left. In both figures 16C and 16D, etched calcite can be observed. Figure 16C shows a more detailed view of the carbonate at a stronger magnification, while figure 16D shows the etched carbonate cement on top of the quartz.

The SEM photos of the Sapiria 2 well were taken from both the saturated and unsaturated zones. In the unsaturated zone, at a depth of 23.7 m. feldspar grains can be observed in figure 17A. At this same depth, in figure 17B, as well as at 32m (also in the unsaturated zone) in figure 17C, an abundance of calcite crystals are seen on top of quartz, also in rhombohedral textures as in the Holon 2 well. In figure 17D, calcite can be seen growing below the quartz as pore filler with clay minerals growing together to the left of the calcite, at 23.7 m. In figure 18A, at 32 m., two kinds of crystals can be observed; an earlier first generation of cement of calcite or aragonite (to the left), and a younger, second generation, of calcite cement (to the right). In figure 18B, at 32 m two generations of calcite can also be observed growing on a quartz grain. Figure 18C at 32 m. depicts different sizes of calcite crystals.

Reproduced with permission of the copyright owner. Further reproduction prohibited without permission.

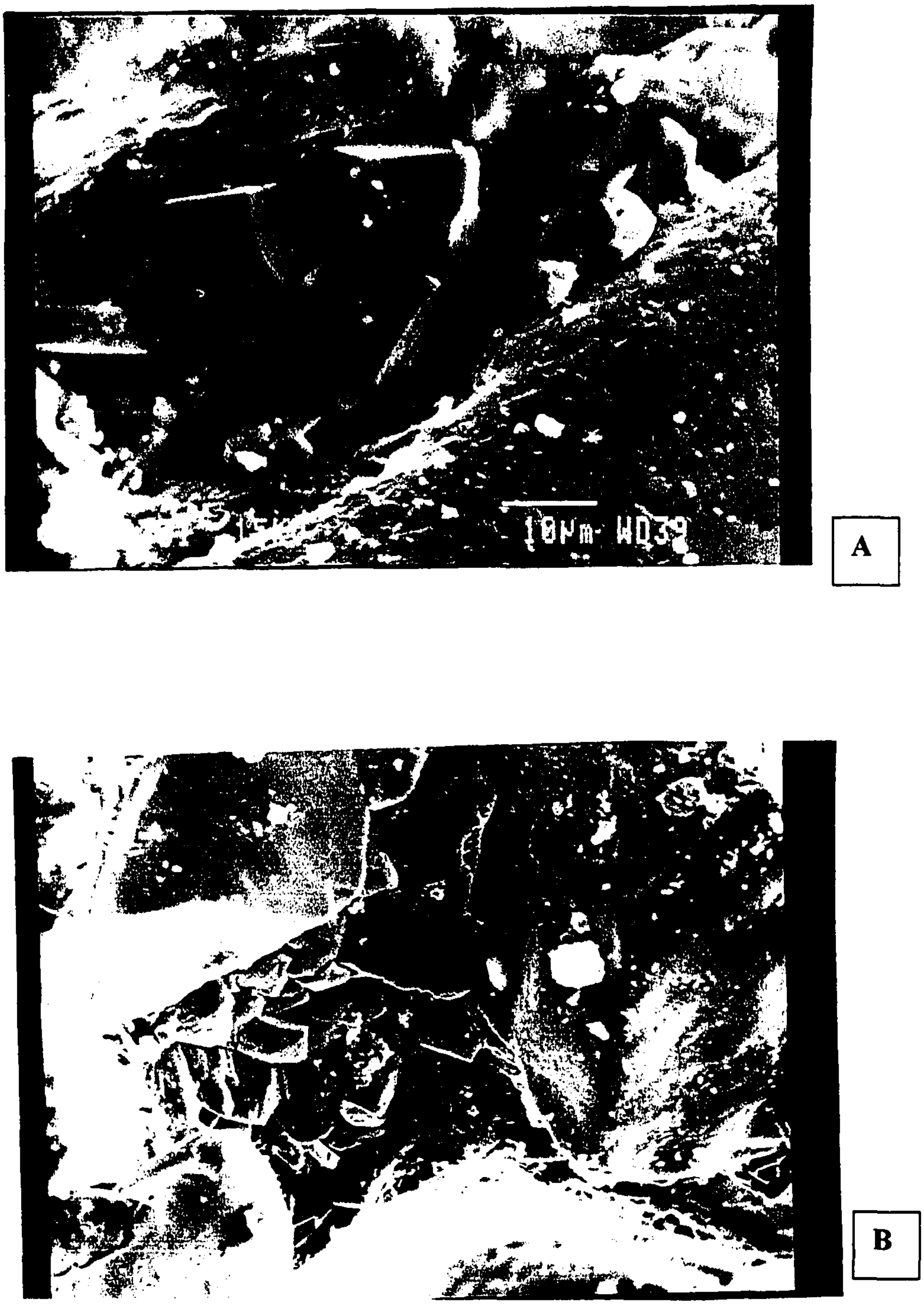

Fig. 15. SEM photographs of Holon 2 well at 44.3 m. (A) authigenic calcite crystals (center) packed between quartz and (B) calcite cement (center) between pore space of quartz grains. Scale bar 10 µm.

Reproduced with permission of the copyright owner. Further reproduction prohibited without permission.

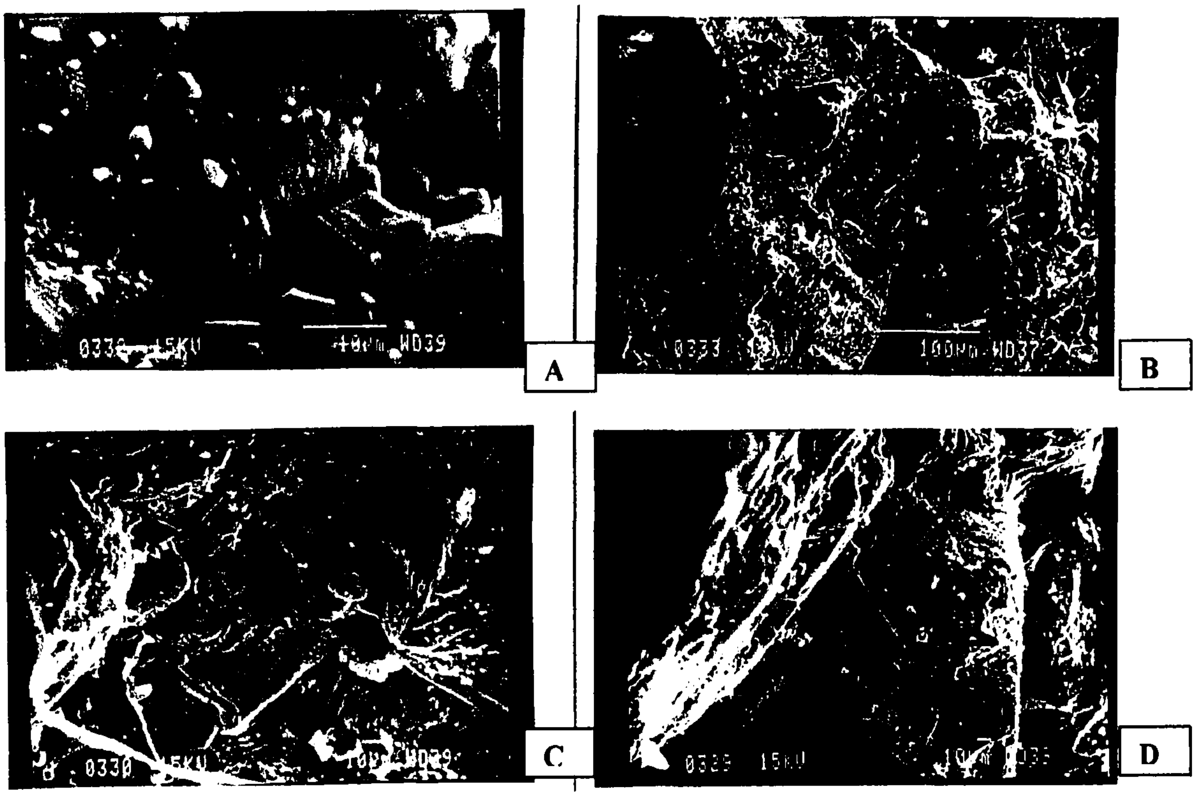

Fig. 16. SEM photographs of the Holon 2 well at 44.3 m. (A) different calcite phases-smaller crystals on top of quartz grain and larger crystals to the right. (B) Detrital carbonate with quartz grains to the left. (C) Etched authigenic calcite (magnified) and (D) etched carbonate cement on top of quartz. Scale bar 10 μm.

Reproduced with permission of the copyright owner. Further reproduction prohibited without permission.

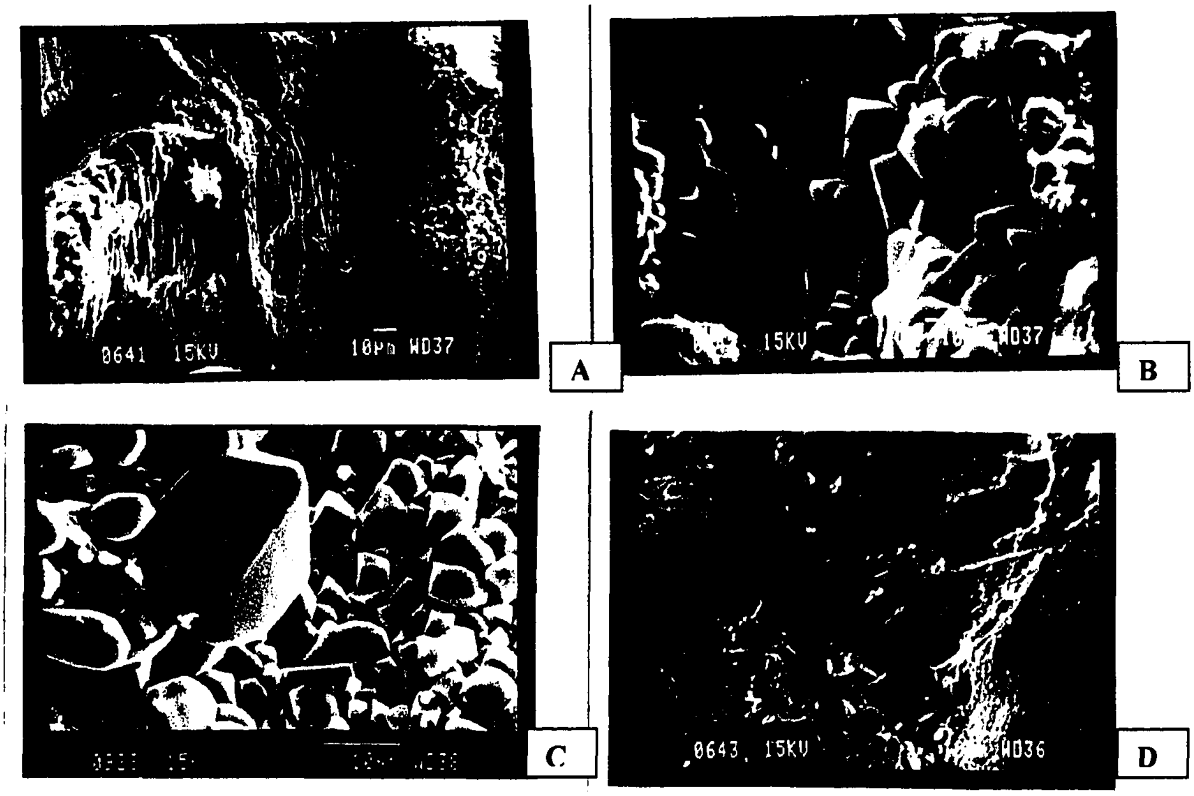

Fig. 17. SEM photographs of the Sapiria 2 well. (A) Feldspar grains at 1100 magnification at a depth of 23.7 m. (unsaturated zone). (B) Calcite crystals (rhombohedral textures) at 23.7 m. and (C) 32 m. (unsaturated zone) at 2000 magnification. (D) Calcite can be seen growing below the quartz as pore filler with clay minerals growing together to the left of the calcite (23.7 m.). Scale bar 10 μm.

Reproduced with permission of the copyright owner. Further reproduction prohibited without permission.

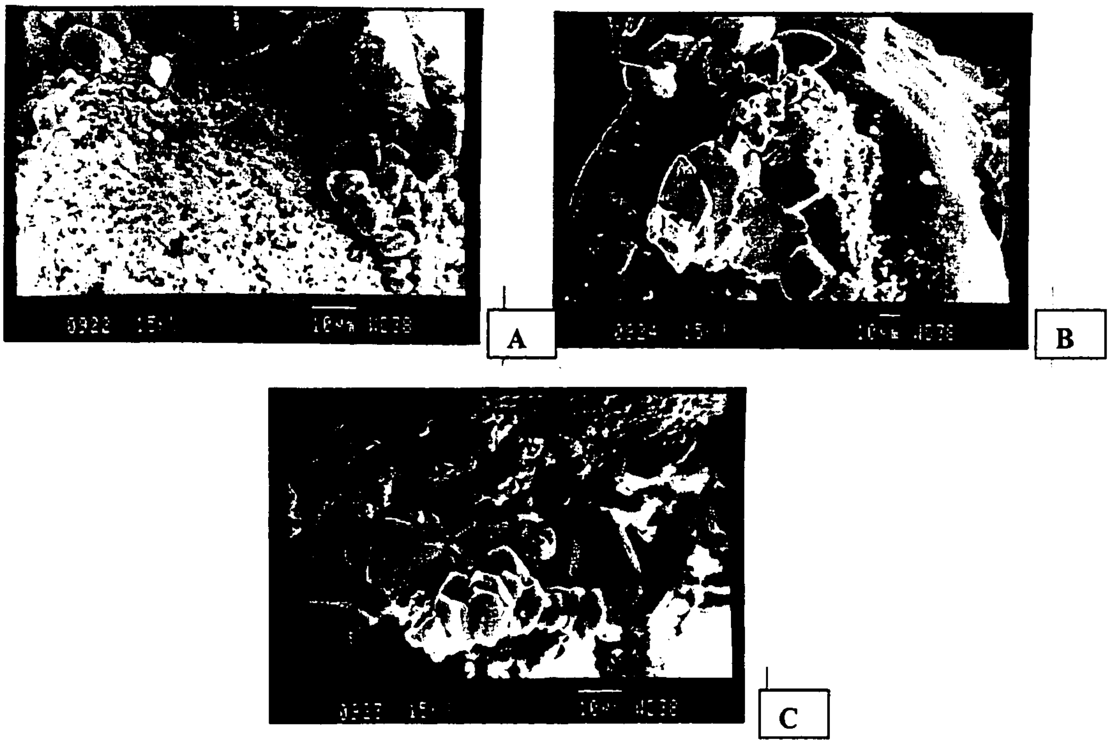

Fig. 18. SEM photographs of the Sapiria 2 well at 32 m. (A) First generation calcite (or aragonite) cement to the left and second generation calcite cement to the right (1300 magnification). (B) Two generations of calcite crystals growing on top of quartz grain (650 magnification). (C) Different sizes of calcite crystals (1500 magnification). Scale bar 10 µm.

Reproduced with permission of the copyright owner. Further reproduction prohibited without permission.

In figure 19A, in the saturated zone of the Sapiria 2 well, at 105.8 m, clays can be seen covering quartz with some calcite crystals. In figure 19B, at the same depth, a small amount of carbonate can be seen (center) with clays to the left and quartz to the right.

XRD analyses

Results of the XRD analysis were based on the relative intensity and angle of the peaks. Results showed the major constituents of the samples to be calcite, quartz, and various clay minerals, with greater peak intensities noted for calcite as opposed to quartz in the deeper sediments of the wells (see Appendix 3 for peak intensity graphs).

Reproduced with permission of the copyright owner. Further reproduction prohibited without permission.

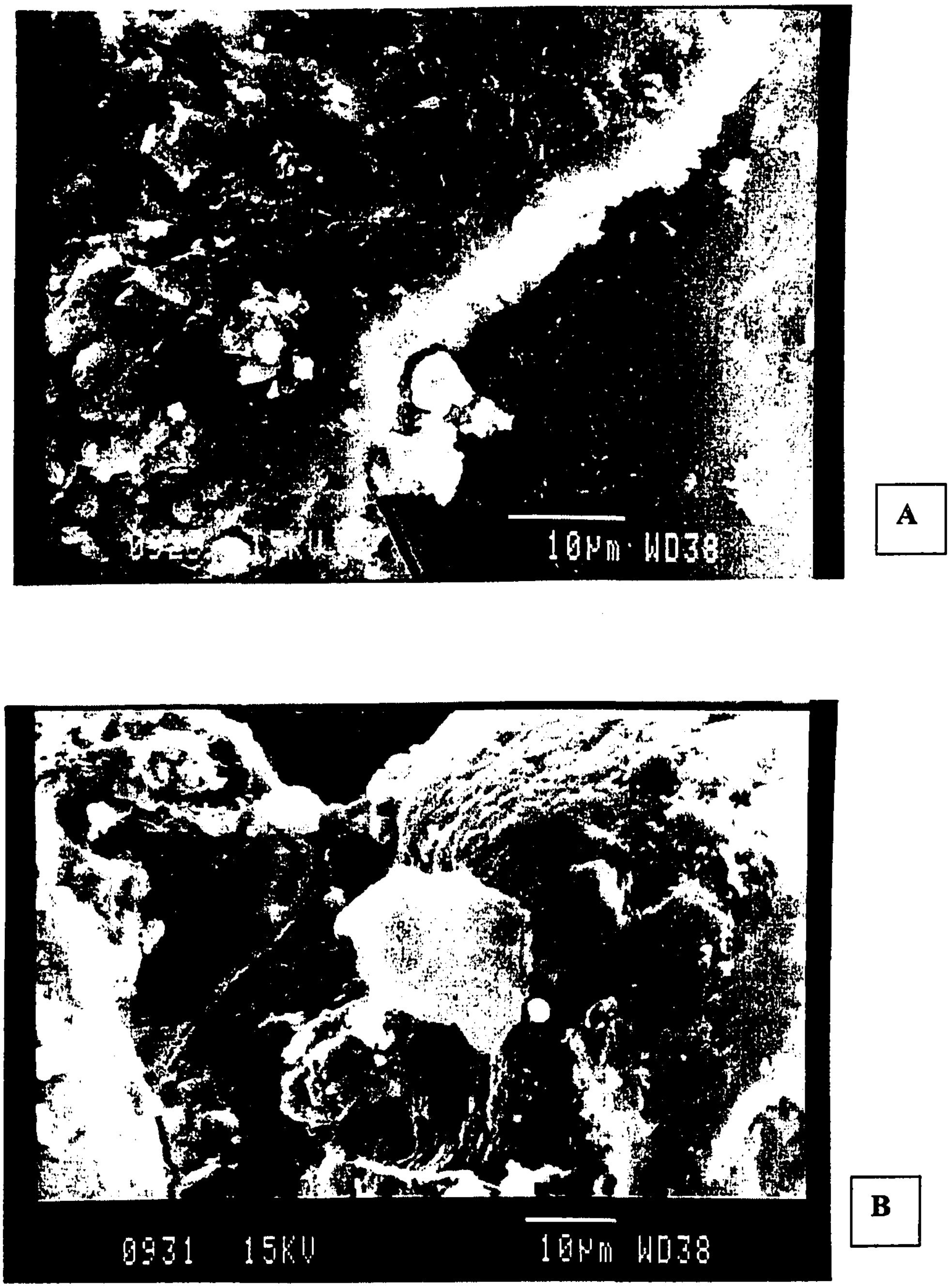

Fig. 19. SEM photographs of the Sapiria 2 well, at 105.8 m. (saturated zone) (A) Clays (left) are covering quartz (far right) with some calcite crystals at bottom center (1800 magnification). (B) Carbonate (center) with clays to the left and quartz to the right. Scale bar 10 µm.

Reproduced with permission of the copyright owner. Further reproduction prohibited without permission.

6. DISCUSSION

Objectives

The main goals of this study were to examine whether a repetitive sampling and analysis of ^{14}C and tritium together with other chemical and isotopic parameters could yield a better data set for groundwater age determination, as well as evaluating the factors that affect the initial ^{14}C value in this aquifer. The use of ^{14}C as a tracer for the source of the groundwater was also tested. It is most likely that in areas where groundwater has undergone minimal changes in its chemical composition, the groundwater flow-paths have also not altered significantly. Therefore, groundwater from wells in these areas can serve as the best example to compare differences in ^{14}C and tritium concentrations over the 25-year interval for better age determination. Moreover, even in the cases where significant differences in the chemistry were found, it could be due to dissolution of salt or seawater and brine infiltration and thus should not significantly affect the age determination process. In the case of a salt source, it would not affect the ^{14}C or tritium ages. In the case of a brine source, the effects on the main water body will depend on its characteristics. A very saline brine could significantly affect the chemistry and salinity, while having little effect on the groundwater ages. The effect on ^{14}C and tritium concentration is not expected to be significant if there is only a small contribution of brine, who's CO_2 is not anticipated to be very high. The flow path of the main water body could have remained unchanged, and therefore repetition of sampling may help even in the cases where salinity has increased. In the following discussion, we examine the chemical and isotopic composition of groundwater at different sections of the coastal aquifer to better understand the chemical and hydrological processes in this aquifer.

Reproduced with permission of the copyright owner. Further reproduction prohibited without permission.

The ^{14}C of most wells has not changed appreciably between the two sampling periods (Table 2). This is in contrast to the more discernable differences in the tritium content in most of the sampled wells (Table 2). The main reason for this is that bomb-spike tritium was much more intense than that of ^{14}C (Fig. 1). A similar observation was also reported, as mentioned previously, from a shallow aquifer in Canada (Fritz et al, 1991), where no changes at all were found in the ^{14}C values for the two sampling intervals.

Variations in the degree of openness of the coastal aquifer system

Results of ^{14}C analyses for the 1970s showed a distinction between the eastern and western sections of the aquifer with higher ^{14}C concentrations in the east relative to the west (Fig. 20). The differences in ^{14}C values cannot be interpreted simply as if they represent a difference in groundwater age (Bruce et al, 2001). Such a simplified age calculation would yield a difference of several thousand years between east and west, which is supported by neither the hydraulic ages nor the tritium content. The tritium concentrations do not show a significant difference between east and west (Fig. 21) and, therefore, no significant age difference is indicated. Another possible explanation of the lower ^{14}C values in the west could be due to the increased dissolution of old carbonate in this section of the aquifer. However, such an explanation would require the $\delta^{13}C$ values to be more positive in the west since more of the carbonate is of marine origin, which has $\delta^{13}C$ values close to zero. The results, however, show relatively uniform $\delta^{13}C$ values throughout the aquifer (Table 2).

A more comprehensive explanation is that the eastern part of the coastal aquifer behaves more like an open system than does the western part (Bruce et al, 2001). In such a case,

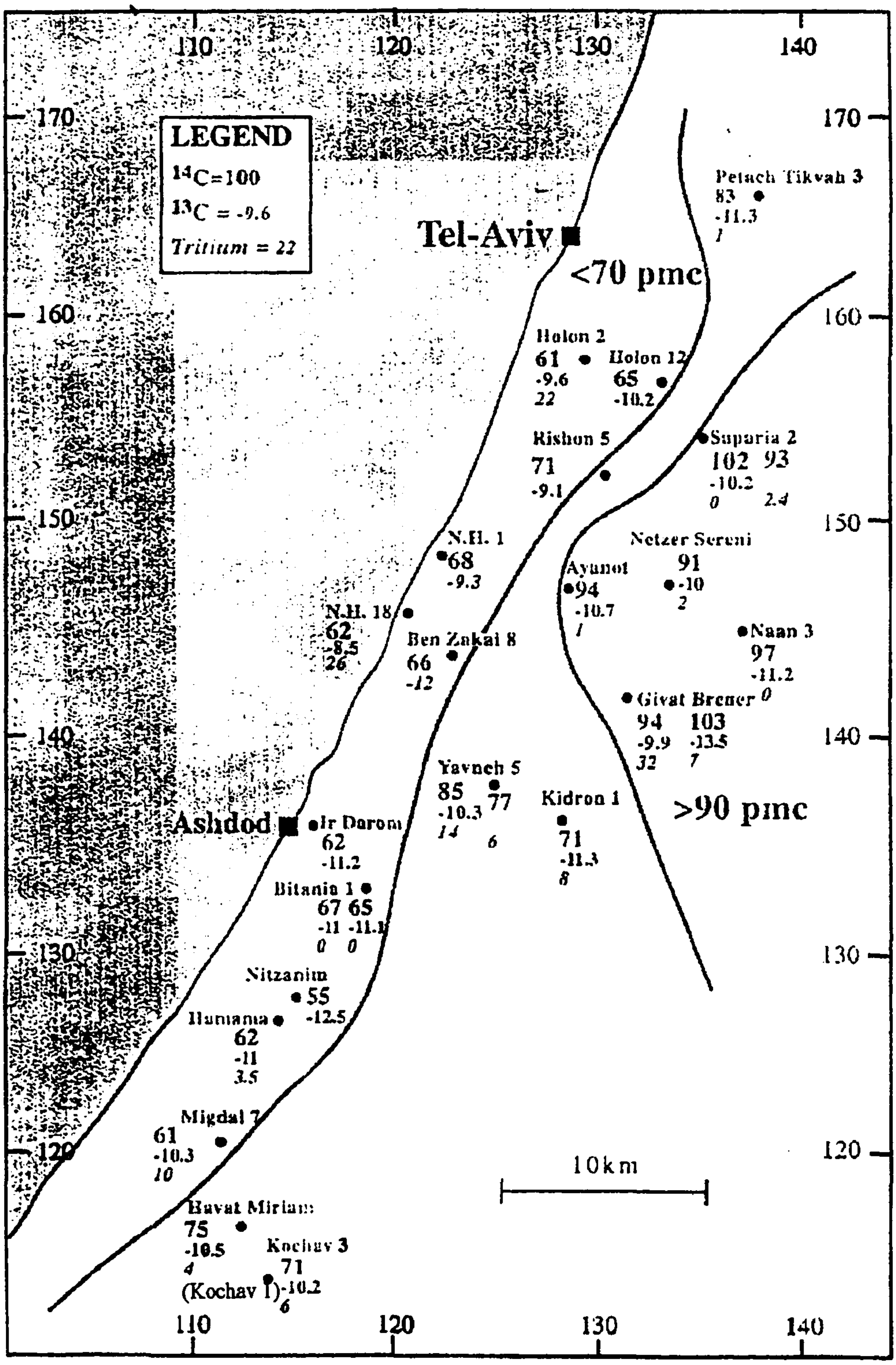

Fig. 20. Location map of wells sampled along the Coastal Aquifer of Israel during the 1970s (excluded are the northernmost wells and those from the Gaza Strip). The solid lines denotes concentration (>90 PMC in the east and <70 PMC in the west) (Bruce et al., 2001).

Reproduced with permission of the copyright owner. Further reproduction prohibited without permission.

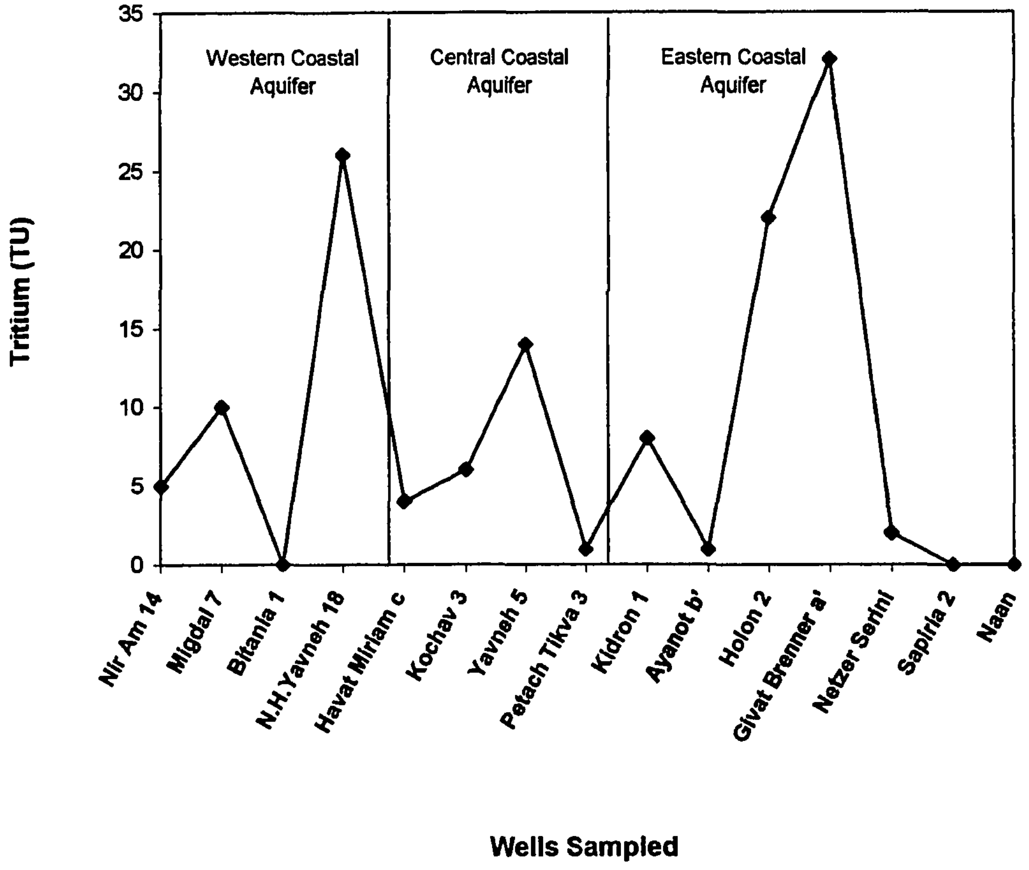

Fig. 21. Tritium values for wells sampled in the 1970s.

Reproduced with permission of the copyright owner. Further reproduction prohibited without permission.

the ^{14}C values in the eastern section remain close to the high values in the soil atmosphere while the $\delta^{13}C$ concentrations reach values of –15 ‰ and higher due to fractionation. On the other hand, the western section of the aquifer behaves as a closed system in which similar $\delta^{13}C$ values (around –12 ‰) are found due to dissolution of old carbonate, a process that is also responsible for lowering ^{14}C values. This explanation does not contradict the large variation in the tritium values without a significant difference between the eastern and western sections. These tritium values are determined by the specific recharge conditions at each sampling point, which may include, in some cases, mixing of several water bodies with different values. Such mixing could also be responsible for some of the variations in ^{14}C values, accounting for mixing between groundwater from different sub-aquifers and of different ages. The mixing could occur between groundwater recharge in the eastern part of the aquifer, traveling west in the lower sub-aquifers, with younger water infiltrating in the western part of the aquifer.

The variation in the degree of openness of the coastal aquifer system is supported by lithological properties, whereby the eastern section consists of a less-cemented sandstone than does the western section (Gvirtzman et al. 1984; Rosensaft et al. 1997). The existence of the marine clay layer in the west also contributes to the theory that a more closed system exists in the west relative to the east. It should be noted that the eastern section of the aquifer also contains only several permeable units while the western section has many permeable units.

This explanation shows that, despite the spatial differences in the initial ^{14}C and $\delta^{13}C$ concentrations, the groundwater in both areas of the aquifer is young (Bruce et al, 2001).

Reproduced with permission of the copyright owner. Further reproduction prohibited without permission.

The tritium values in most of the groundwater, which are significantly higher than zero, indicate that the transit time is less than 40 years. There are a few exceptions, such as the Bitania well, where no tritium was found, implying a longer transit time. The young ages imply that the initial ^{14}C values were influenced by nuclear tests, at least in the eastern part of the aquifer.

In many research studies, the unsaturated zone is considered an open system while the saturated zone is regarded as a closed system (e.g. Clark and Fritz 1997; Dorr et al. 1987;Wigley 1975). It can be argued, however, that the line between open and closed systems is not necessarily drawn between the unsaturated and saturated zones. A closed system may also begin within the unsaturated zone itself, depending on the type of sediments involved and the flow of the groundwater system. In some cases, the phreatic part of the aquifer is considered to be the open system, while the confined part the closed system. The present study is of an aquifer, which is basically phreatic, yet is partly an open system and partly a closed one.

Data analysis of both sampling periods

The data of the second sampling period in the 1990s are also consistent with this interpretation of an open and closed system for the coastal aquifer.

A relatively low concentration of tritium with high ^{14}C values was found in several locations, such as Saparia 1 and Ayanot b. Such phenomena could be observed in areas that are extensively irrigated (Huffen et al., 1972). In such a case, the tritium of the recycled irrigation water is old due to several cycles of pumping and irrigation of

Reproduced with permission of the copyright owner. Further reproduction prohibited without permission.

relatively older water. On the other hand, the case of ^{14}C is different since the penetrating irrigation water can equilibrate rapidly with the soil CO_2, whose concentration is very high, and therefore retain atmospheric values (Huffen et al., 1972).

Since the differences in ^{14}C values that were found between the two sampling periods cannot be interpreted simply as if they represent a difference in groundwater age, each case should be dealt with separately.

The extremely high PMC result for the Kfar Achim well (163 PMC, Table 2) in the first sampling period (1974) could possibly be explained if the sample was taken at the exact time of the bomb peak in the 1960s visible in both the CO_2 and tritium curves (Figs. 1 and 4). Since there is no tritium value for this sample, and this was a single result, one cannot rule out the possibility of analytical error. Moreover, the second sampling in the 1990s yielded a result of 85 PMC, similar to other wells within the same vicinity.

The unusually distinct rise in the ^{14}C concentration of the Holon 2 and Holon12 wells may be explained by the recharge of post-bomb peak water which took twenty years to reach this sampling point from its infiltration source and mix with the well water. The tritium value for the Holon 2 well in the 1970s was 22 TU, which would infer younger waters. This number decreased considerably in the 1990s to 7 and 5.5 TU, however, the tritium signal is nevertheless strong so the young component of the waters is still present in this well. Both the increase in concentration of ^{14}C along with the presence of tritium would presume either the infiltration of younger waters or an enhancement of pumping in this general area. In the Holon 12 well there is also a significant increase in salinity along

Reproduced with permission of the copyright owner. Further reproduction prohibited without permission.

with the increase in ^{14}C over the time interval. This increase in salinity could possibly be due to seawater intrusion. This intrusion is not expected to affect the ^{14}C significantly since the actual volume of seawater component is very small and thus the CO_2 contribution would also be minimal. The notable increases in ^{14}C may also be attributed to increased pumping in these wells during the 1990s, which may enhance the flow of younger waters into the system and allow less time for possible water rock interactions. A reduced amount of interaction in the aquifer's matrix is likely to be observed in the ^{14}C values but not in the tritium concentration. It should be noted that the SEM images of sediments from the both the Holon 2 well and the unsaturated and saturated zones of the Saparia 2 well clearly demonstrate the existence of carbonate in this system, as well as several generations of dissolution and precipitation (Figs. 15-19). XRD analysis confirms the presence of calcite, quartz and clay minerals in the wells sampled.

There was no significant change in the ^{14}C of the Migdal wells in the 20-year time span. There are, however, indications for infiltration of treated sewage for irrigation purposes in the Migdal 12 vicinity from the year 1980 (Zelinger; Mekorot Water Company, personal communication, 1998). This infiltration of treated sewage caused a significant increase in the salinity of the well (Table 1). In this case, the ^{14}C value demonstrates that the saline source has little contribution of water or CO_2, and the increase in salinity could be attributed to an increase in agricultural irrigation.

The groundwater in the Nir Am wells were determined to have low ^{14}C values (34 PMC in the 1970's and 49.6 PMC in the 1990's) with detectable tritium in both sampling periods. These lower ^{14}C values could not be explained by a slow recharge through a

Reproduced with permission of the copyright owner. Further reproduction prohibited without permission.

thick unsaturated zone because of the relatively high tritium. The tritium values, which are much higher than 0 T.U., indicate that there is a younger component to the water. Therefore, the recharge could not exclusively be of older (>40 years) rainwater. Rather, these low ^{14}C values can better be explained by the interaction of the water with old organic or inorganic carbon. The $\delta^{13}C$ value for the Nir Am 14 well in the 1970s was lower than any of the other wells (–17 ‰), implying oxidation of old organic matter that would contribute some amount of dead carbon to this source and thereby decrease the ^{14}C value. The oxidation of old organic matter has been shown to lower apparent ages significantly in other aquifers in the world (e.g. Boaretto et al., 1998). The elevated $\delta^{13}C$ detected at the Nir Am 15 well in the 1990s (-12.2 ‰) would be an indication for changes in flow conditions or pumping during this twenty year interval that would decrease the residence time and interaction with the organic matter.

Both the Tel Mond and Givat Haim wells are located in the northern section of the aquifer with thick unsaturated zones (approx. 50 m) that increase the transport time through the carbonate matrix. This may also increase the amount of carbonate dissolution, and thereby further lower the ^{14}C values (Table 2). The tritium value is very low in Tel Mond (0.2) in accordance with the relatively low ^{14}C values (50-51 PMC). A rough estimation of groundwater age in this well, using an initial value of 60-80 PMC, would yield an age minimum of several hundreds of years. The higher tritium value in the Givat Haim well (7.6 TU), together with the lower ^{14}C value (42 PMC) is less understood. This lower ^{14}C value of 42 PMC, which was of groundwater sampled in the 1970s, could possibly represent relatively old water, while the sample taken in the 1990s was of younger water containing tritium with a higher ^{14}C value (55 PMC). It is also

Reproduced with permission of the copyright owner. Further reproduction prohibited without permission.

possible that in this well there is a mixture of groundwater from two different sources: younger water (containing tritium and high ^{14}C) and older water (no tritium and lower ^{14}C).

Transit times and age estimation

The presence of tritium throughout most of the aquifer implies that the waters in this aquifer are relatively young, with a transit time of less than forty years. Mercado et. al. (1975) charts the transit time of water through the unsaturated zone of the coastal aquifer, taking into account the thickness of the unsaturated zone and the permeability of the sediments. According to his estimates, the fastest transit times of less than 10 years would be along the westernmost strip of the coast with the intervals increasing from 11 to 50 years in the middle section, and from 51 to 100 years along the eastern border of the aquifer. The majority of our wells, which are located along the westernmost strip and middle section of the aquifer fit into this model of transit times. Mercado et. al. (1975) noted transit times of greater than 100 years for the southeastern area of the aquifer bordering the eastern boundary of the Eocene. Two of the wells sampled (Kfar Achim and Chavat Miraim) extend slightly into the border of this southeastern area of the aquifer along the western side, however, they both have ^{14}C values above 75 PMC and high levels of detectable tritium. This indicates that Mercado's model should be modified, at least in this area of the aquifer. It also shows the advantage of using the radioisotope data to constrain the physical flow models.

As stated previously, one cannot rule out the possibility of the mixing of several bodies of water of different sources and ages. In such cases, it would be difficult to calculate an

Reproduced with permission of the copyright owner. Further reproduction prohibited without permission.

actual age of the groundwater. Rather, only an estimate of the age of the water sources may be possible to determine. According to Mercado (personal communication, 1998), there is such an instance of mixing in the central and western part of the aquifer between older groundwater recharging in the east and traveling to the west, and younger rainwater, which infiltrates downward (Fig. 6). This mixing could produce low ^{14}C results apparently indicating old groundwater of several hundred years or more with high tritium values indicating fairly young waters (less than 40 years). Only in a few places, in relatively isolated sub-aquifers, would these older ages make sense. Moreover, this mixing could be artificially initiated, because of pumping and/or mixing with water imported from the Judea Group Aquifer or from the Kinneret Lake (Fig. 5).

Tritium content and well screen depth

There appears to be a correlation, in some cases, between tritium content and well screen depth in the western section of the aquifer where several sub-aquifers (A, B, and C) exist. Additional wells were sampled along the coast in order to draw samples from the lower sub-aquifers (B and C) (Tables 3 and 4). Results of tritium from these wells show very low levels of detectable tritium (0.8 TU at the Herzalia a' well (Fig. 22), 0.7 TU at the 42/1 well, and 0.1 TU at the Lahat 3 well (Fig. 23). The Bitania well's perforation level located in sub-aquifer B_2 also had low tritium values of 0 TU in 1974 and 0.2 TU in 1993, respectively. This is in contrast to the higher tritium values found in samples taken from sub-aquifer A, such as 5.7 TU in N.H. Yavneh 18 and 7 and 5.5 TU in Holon 2. These tritium values imply older waters in the deeper sub-aquifers due to the increased transit times relative to those in sub-aquifer A (i.e. N.H. Yavneh 18 and 1, and Holon 2). This longer travel time could be partly due to the laterally long travel distance from east

Reproduced with permission of the copyright owner. Further reproduction prohibited without permission.

Fig. 22. Cross-section of the Herzalia a' well (modified after Tolmach, 1977).

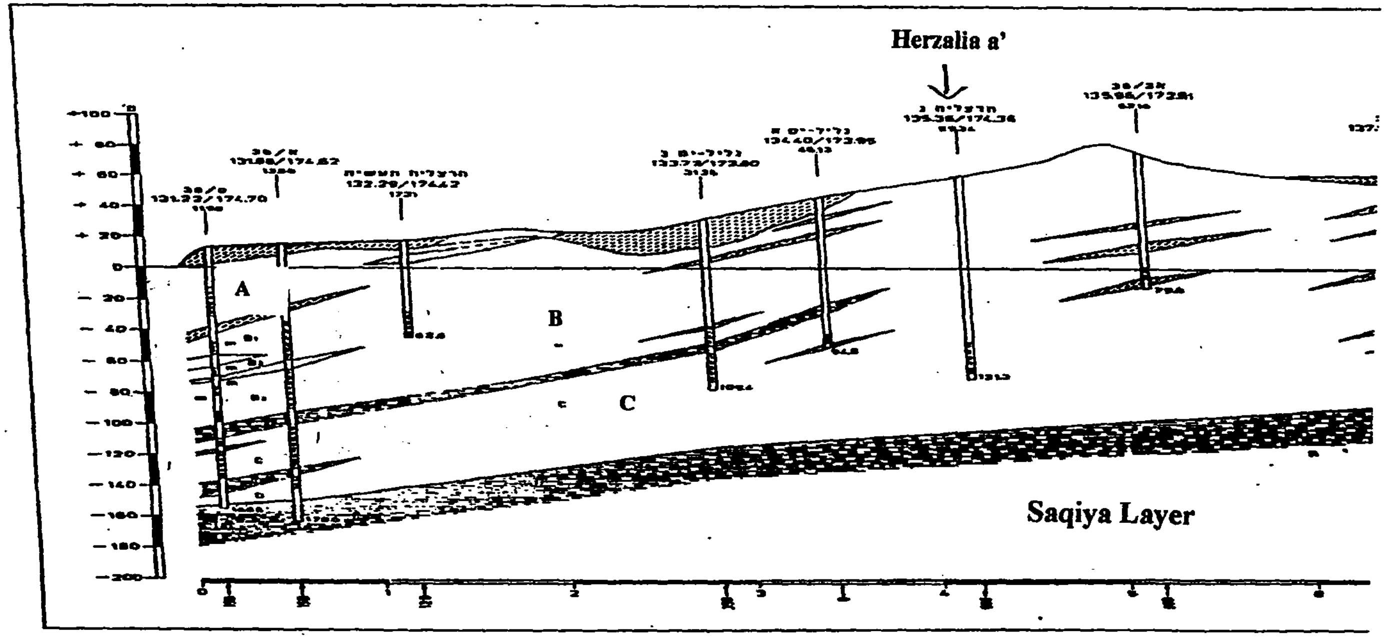

Reproduced with permission of the copyright owner. Further reproduction prohibited without permission.

Reproduced with permission of the copyright owner. Further reproduction prohibited without permission.

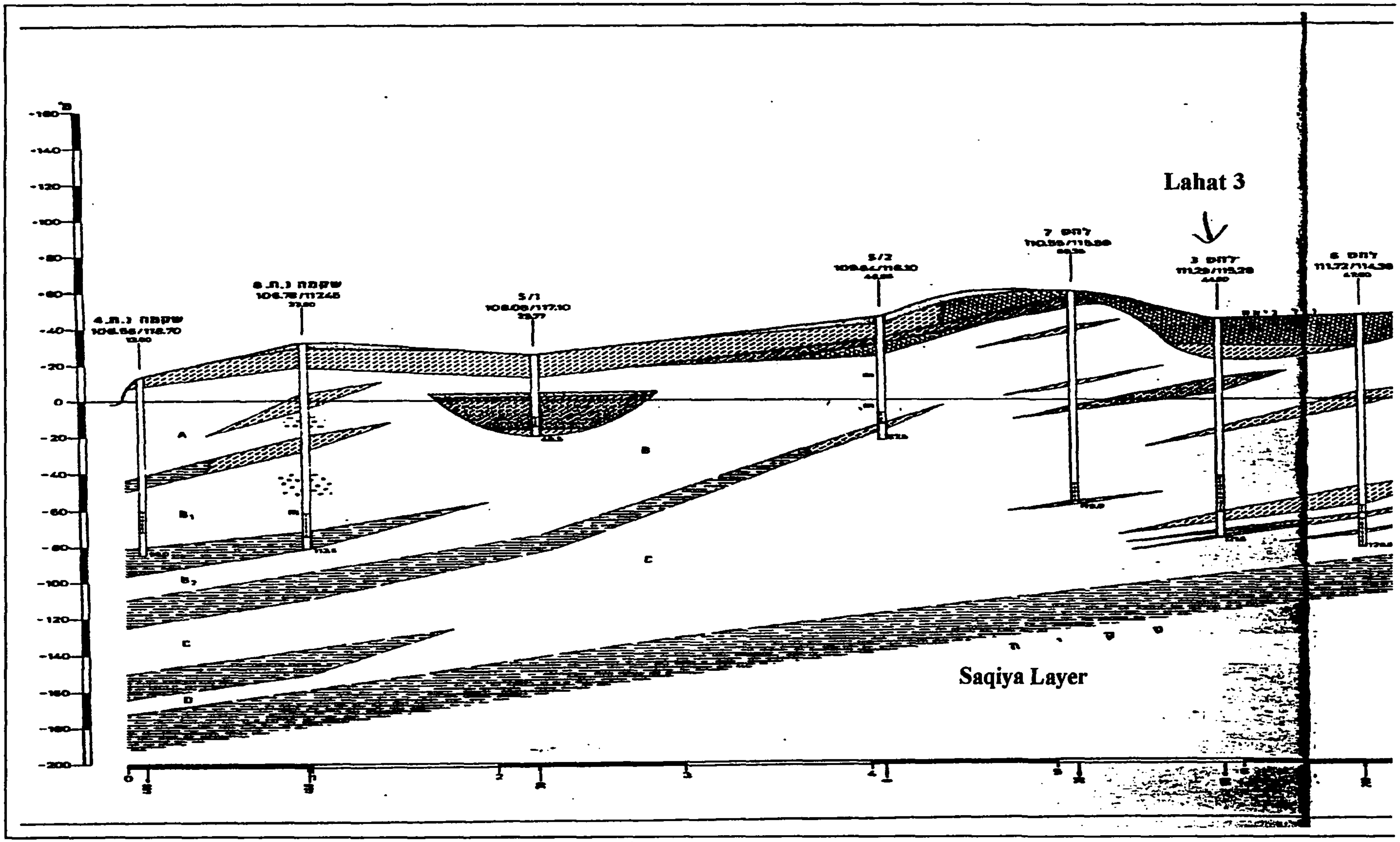

Fig. 23. Cross-section of the Lahat 3 well (modified after Tolmach, 1977).

to west and/or the longer vertical infiltration. It should be noted that both the Lahat 3 and Bitania wells are located in areas determined by Mercado et. al. (1975) to have transit times through the unsaturated zone of between 51 to 100 years. In the case of lower sub-aquifers with a confining clay layer above them, it is expected that most water will recharge in the eastern part of the aquifer and travel west, attaining a longer transit time.

Effects of infiltration and other potential saline sources

Most of the $\delta^{18}O$ values of samples taken in the 1990s are within the range of regional uncontaminated groundwater of -5.5 and –4.0 ‰. The remaining $\delta^{18}O$ values above –4 ‰ indicate effects of either Lake Kinneret or wastewater (Vengosh et al, 1999).

The effects of infiltration from the imported waters of Lake Kinneret (with a Cl value of approximately 220 mg/l and $\delta^{18}O$ value of –1 ‰) are evidently based on both Cl and $\delta^{18}O$ values in the Kochav 1, and Ayanot wells (Table 2). The Kochav 1 well shows a decrease in salinity over the time interval and a higher $\delta^{18}O$ value of -1.86. This well is located near a reservoir with waters imported from Lake Kinneret, and the decrease in salinity coincides with the Cl content of the Kinneret Lake waters (Fig. 14). No significant change was observed in the ^{14}C and tritium values since those of the Kinneret are close to atmospheric values (Stiller et al., 1998). Both the increase in salinity and the higher $\delta^{18}O$ value (-1.74) in the Ayanot well also indicate these anthropogenic influences of the Lake.

Na/Cl and SO_4/Cl ratios (Table 1) also indicate the effects of other potential saline sources such as wastewater and saline plumes. Vengosh et al (1999) determined the

Reproduced with permission of the copyright owner. Further reproduction prohibited without permission.

Na/Cl and SO_4/Cl ratios for the saline plume at the Beer Tuviya well to be 0.78 and 0.05. The ratios of the Kfar Achim well located in the same vicinity as the Beer Tuviya well appear to be within the range of those from the Beer Tuviya saline plume (Table 1). The Kidron 2 well has shown a marked increase in salinity over the twenty-year interval (Table 1). Its Na/Cl and SO_4/Cl ratios of 0.51 and 0.04 respectively, compare with those of a saline plume (0.5-0.8 Na/Cl, and 0.04 -0.06 SO_4/Cl) (Vengosh et al 1999). The $\delta^{18}O$ values of both the Kfar Achim and Kidron 2 wells, -4.13 ‰ and –4.04 ‰ respectively, are also in the range of a saline plume (–4.0 ‰ to –4.7 ‰) as determined by Vengosh et al (1999).

The chemical ionic ratios of the Naan well also fall within the range of a saline plume (Table 1). A trough was discovered by Rosenthal et al (1992) in the Naan area, in line with area faults that would facilitate saline water migration and possibly explain the increased salinity of the Naan well with the enhanced exploitation of the coastal aquifer. The higher $\delta^{18}O$ value at Naan of -3.80 would seem, however, to also indicate the effects of treated sewage effluents in the area, which are typically characterized by higher salinity's and $\delta^{18}O$ values of –3.45 ‰ to 0.92 ‰ (Vengosh et al, 1999). Similar ^{14}C values indicate that the flow pattern of the main water body has remained unchanged.

With regard to nitrate concentrations, the southernmost wells appear to have experienced a decrease in their nitrate levels, while most of those north of the Bitania 1 and Ir Darom wells have experienced a marked increase (Table 1). Wells such as Netzer Sereni and Tel Mond 8 have more than tripled their nitrate values between the twenty-year sampling intervals. The very distinct decrease in NO_3 from the Sapiria 1 to the Sapiria 2 wells

Reproduced with permission of the copyright owner. Further reproduction prohibited without permission.

cannot easily be explained and may be attributed to sampling error. In addition to agricultural development along the coastal aquifer, Kanfi et al. (1983) attributed the increase in nitrate concentrations to fertilizers, manure, sewage, and irrigation water, while changes in the hydrological regime can be ascribed to its decrease.

Reproduced with permission of the copyright owner. Further reproduction prohibited without permission.

7. REPETITION AS A METHOD FOR IMPROVING AGE DETERMINATION

As stated previously, the determination of groundwater ages by radioactive isotopes is problematic in many cases. It is, therefore, suggested that repetition of analysis will improve the credibility of this method of age determination by both tritium and ^{14}C analysis. This method requires sampling of groundwater from the same location at least twice with a large difference in time between the two sampling periods using tritium and ^{14}C values. The Givat Brenner and Yavneh 18 wells are used here as examples to illustrate this point. Because of the sharp rise and fall of the rain tritium in 1962-68, the tritium value of 32 T.U., obtained in the Givat Brenner well in 1974 could indicate either an age of 1-2 years or of 12-14 years (Fig. 24). Similarly, the value in 1997 (7 T.U.) indicates an age of either 12- 24 or 38-40 years (Fig. 24). Combining the values from both sampling periods, assuming that the flow regime has not changed significantly, it seems that the groundwater age is in the range of 12-14 years old. The ^{14}C value for this well in 1974 was 94 PMC. The ^{14}C value in the troposphere in 1962 (12 years earlier) was 120-140 PMC (Levin et al. 1980). The Q factor for this area is, therefore, 0.72 (94/130). Using this value to correct the dilution factor, it is possible to calculate an estimated age of groundwater in the coastal aquifer.

The tritium value of 26 T.U. obtained at the Yavneh 18 well in 1974 could indicate either an age of 12 years or 15 years (Fig. 25). Likewise, the value in 1998 of 5.7 T.U. could indicate either an age of less than 12 years or 37 years (Fig. 25). By linking the values from both the 1974 and 1998 sampling periods, again assuming that the flow regime has

Reproduced with permission of the copyright owner. Further reproduction prohibited without permission.

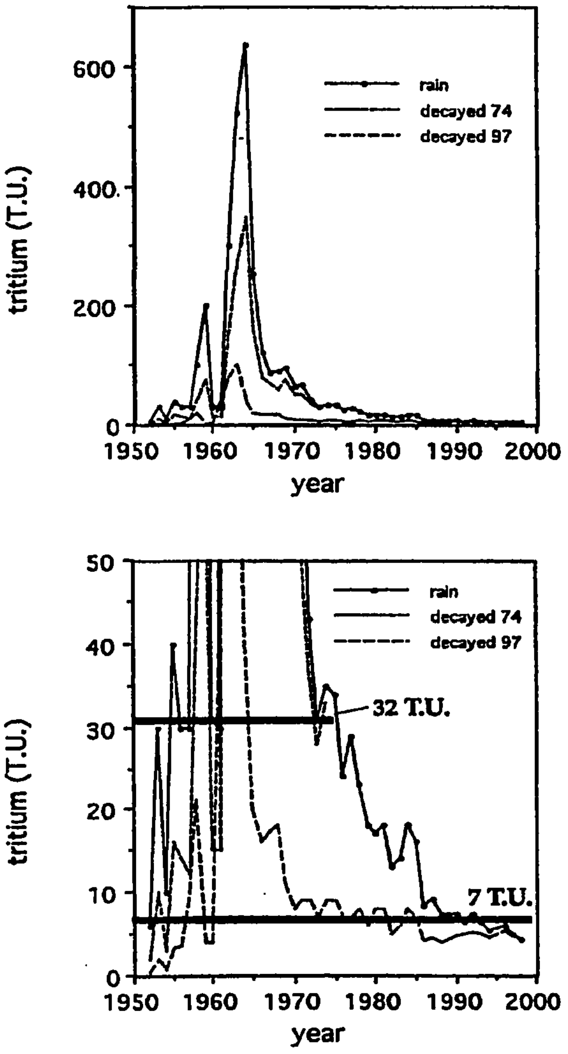

Fig. 24. Tritium concentrations in rain and their expected decayed values in groundwater for both 1974 and 1997, when groundwater samples were collected (modified after Yechieli et al. 1994). Note that the lower graph is an enlargement of the upper graph. Also shown are the values found in well Givat Brenner in 1974 and 1997 (denoted by the solid lines).

Reproduced with permission of the copyright owner. Further reproduction prohibited without permission.

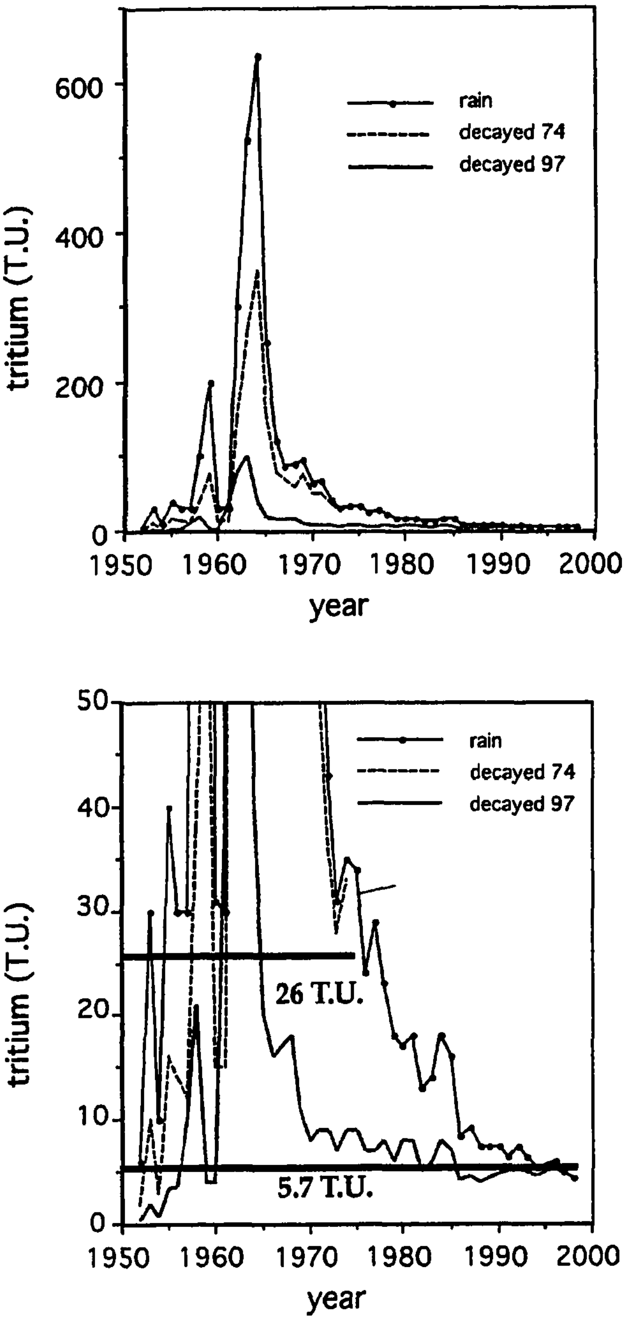

Fig. 25. Tritium concentrations in rain and their expected decayed values in groundwater for both 1974 and 1998, when groundwater samples were collected (modified after Yechieli et al., 1994). Note that the lower graph is an enlargement of the upper graph. Also shown are the values in well N.H. Yavneh 18 in 1974 and 1998 (denoted by the solid lines).

Reproduced with permission of the copyright owner. Further reproduction prohibited without permission.

not changed significantly, it would appear that the groundwater is approximately 12 years old. This is similar to the age approximated for the Givat Brenner well. The ^{14}C value for the Yavneh 18 well in 1974 was 62 PMC. Using a ^{14}C value in the troposphere for 1962 to be approximately 130 PMC (Levin et al., 1980; Clark and Fritz, 1997), the Q factor for this area is, therefore, 0.48 (62/130). Ages of groundwater in the aquifer using this Q factor can now be calculated utilizing the Wigley equation (Wigley, 1975) and adjusting for A_0 relative to its range in the troposphere for the respective time period. The following equation can be given for an adjusted ^{14}C age:

$$A = QA_0 2^{-t/T} \quad \text{(Wigley, 1975)}$$

Where A is the measured ^{14}C activity, Q is the dilution factor, A_0 is the activity at time zero, t is the age and T is the half-life.

A factor that should also be considered when determining Q is the mixing of organic sources from several different years in the soil, which would cause the ^{14}C of the soil atmosphere to differ from that of the atmosphere. Depending on the ^{14}C levels in the atmosphere, the soil ^{14}C could be higher or lower than that of the atmosphere.

An example for determining groundwater age would be with Well 23/0 sampled by Nativ and Weisbrod (1994), which is located in close proximity to the Yavneh 18 well. ^{14}C samples with A_0 taken to be approximately 100 PMC were found to be 36.1 PMC at sub-aquifer B_1 and 18.3 PMC at sub-aquifer C. Using our method, better ages determinations could be made for the groundwater located in the lower sub-aquifers of Nativ and Weisbrod (1994).

Reproduced with permission of the copyright owner. Further reproduction prohibited without permission.

Well	Sub-aquifer	A (PMC)	Q	A_0 (PMC)	T (Years)	t (Years)
23/0						
	B_1	36.1	0.48	100	5730	2400
	C	18.3	0.48	100	5730	8000

The $\delta^{13}C$ values determined by Nativ and Weisbrod (1994) for these sub-aquifers of –6.9 for B_1 and –4.2 for C are very positive. This may indicate increased water-rock interactions for this well, which should also be examined, while the numbers here are given as an example.

It should be emphasized, that this calculation might include effects besides dissolution of carbonate with dead carbon. Possible changes in the hydrological regime, and mixing of groundwater of different ages transforms this coastal aquifer into a more complex model, which obviates a simple calculation.

Reproduced with permission of the copyright owner. Further reproduction prohibited without permission.

8. CONCLUSIONS

Groundwater in the Coastal Aquifer of Israel is a mixture of waters derived from a combination of sources. As indicated by detectable tritium one source would be from precipitation in the post-bomb era contributed by a shallow-flow system, as well as deeper sub-aquifers containing older waters in addition to artificial recharge sources. The coastal aquifer has undergone numerous changes to its system in flow path and chemistry over the two sampling periods due to increased pumping and replenishment with imported waters. Multiple samplings and analysis of Cl showing increases and/or decreases in Cl concentrations also confirm an anthropogenic input of Kinneret Lake waters into the coastal aquifer.

The spatial variation in the ^{14}C values between the eastern and western parts of the coastal aquifer may be explained by open and closed systems in the same aquifer. Aquifer conditions indicate a variation in the degree of openness of the system dependent on the amount of carbonate in the aquifer, which would serve to explain the spatial differences in the ^{14}C concentrations.

Groundwater in the whole aquifer appears to be young. The ^{14}C values determined appear to be a factor of both water-rock interactions and the bomb-effect rather than a function of age. Presence of tritium values, with a few exceptions, indicates a transit time of less than forty years.

Reproduced with permission of the copyright owner. Further reproduction prohibited without permission.

Sample repetition over an extended period of time assists in more accurately determining groundwater ages. By combining tritium values from both sampling periods a clearer picture of where the sampled water is located on the tritium bomb spike curve can be determined, thereby allowing a calculation of the dilution factor. However, mixing of groundwater of different ages and changes in the management of this coastal aquifer complicate any simple calculation using ^{14}C to estimate groundwater age. Nevertheless, ^{14}C can still be useful along with tritium and chemical analyses for age estimation or as a tracer in determining possible sources of water and solutes for coastal aquifers and shallow groundwater systems.

Reproduced with permission of the copyright owner. Further reproduction prohibited without permission.

9. FUTURE RESEARCH

Attempts to describe the behavior of ^{14}C in the unsaturated zone have been made by various researchers. Previous models used to estimate the distribution of ^{14}C between CO_2, DIC, and matrix solids in the unsaturated zone have not been able to quantify the retardation of $^{14}CO_2$ movement. Striegl and Armstrong (1990) used laboratory measurements of carbon dioxide retention and carbon exchange on unsaturated Quaternary sediments to more accurately describe the retardation of $^{14}CO_2$ transport. Experimental results found the CO_2 losses in the unsaturated zone in wet conditions to be 8 to 17 times greater than losses predicted by calcite equilibria (Striegl and Armstrong, 1990). These results indicate a sink for ^{14}C that is not accounted for in the carbonate equilibrium control models. This difference can alter the carbon isotope composition of soil CO_2 as well as dissolved inorganic carbon of interstitial waters in the unsaturated zone (Striegl and Armstrong, 1990). This should be taken into account when doing $^{14}CO_2$ modeling of movement in the unsaturated zone or determining ^{14}C ages of infiltrating water.

Davidson et al. (1995) compared the method of vacuum distillation vs. centrifugation and compression methods for extracting ^{14}C from pore water in unsaturated rock. Advantages cited for the use of distillation over the other two methods were:

1. It is possible to recover a greater amount of interstitial water from sediments that will not typically yield water by centrifugation or compression.
2. The mass needed for ^{14}C analysis can be extracted in one sampling.
3. The water and carbon extracted are isolated together, reducing the risk of contamination.

Reproduced with permission of the copyright owner. Further reproduction prohibited without permission.

4. The distillation method is more cost-efficient.

Due to incomplete recovery of carbon during distillation, fractionation occurs making the use of stable isotope applications unsuitable. However, its effect on ^{14}C applications was not significant (maximum fractionation in this study was *ca.* 4%) (Davidson et al., 1995). Mass balance calculations show "that there may be a significant reservoir of carbon absorbed to mineral surfaces, that is only partially removed by this method" (Davidson et al., 1995). However, it was found that incorporation of this adsorbed carbon into the recovered sample did not significantly change the ^{14}C activity.

Future research would thereby include sampling of both sediments and pore water from the unsaturated zone for the purpose of both determining the best experimental procedure for the pore-water extraction, as well as the use of this water to better approximate the distribution of ^{14}C between CO_2, DIC, and matrix solids in the unsaturated zone.

Another area of future research would be to examine the use of possible organic tracers for the purpose of more accurate age determination. One example of this type of tracer would be chlorofluorocarbons (CFCs). The CFC method has been successfully utilized in the U.S.A. (Dunkle et al., 1993; Szabo et al., 1996), but never in Israel. The utilization of CFCs as an organic tracer is based on the knowledge of the changes in concentration of CFC in the atmosphere over the past 40 years. Therefore, its path can be traced in infiltrating water and groundwater.

Reproduced with permission of the copyright owner. Further reproduction prohibited without permission.

The helium-tritium method is another dating method utilized, along with tritium sampling, to further assist in gathering more accurate groundwater ages. By measuring tritium with its daughter product, helium, ages can be determined through calculations, which do not rely on knowledge of the initial tritium concentration. Studies by Schlosser et al. (1989), and Szabo et al. (1996) have been done on the application of the helium-tritium method for shallow groundwater. This technique may also assist in determining water sources in areas where mixing of water of different ages can occur, as well as yielding more accurate dates of younger water, i.e. water which has reached groundwater level in the past 40 years.

Reproduced with permission of the copyright owner. Further reproduction prohibited without permission.

APPENDIX 1

Detailed listing of well logs in alphabetical order as taken from the hydrogeological archives of the Geological Survey of Israel (translated from the original Hebrew).

Reproduced with permission of the copyright owner. Further reproduction prohibited without permission.

Ayanot b'

Location: 12798/14696
Well depth: 51.1m
Height above sea level: N/A
Depth to water relative to ground level: N/A
Drill date: N/A

Well Log

Depth (meters)	Description
0.7	Brown sandy loam
1.05	Same as above
1.6	Brownish-red sandy loam
3.35	Reddish-brown sandy loam
4	Brown sandy loam
7.2	Dark brown sandy loam
9.1	Same as above
10.5	Brown sand, light in color with a light loamy cement
15.8	Very gray calcareous sandstone
19.95	Concretions of gray calcareous sandstone, a bit porous.
20.75	Concretions of gray calcareous sandstone, with a bit of fragmented fauna.
22.5	Concretional brownish-gray calcareous sandstone, fine grained.
27	Concretional calcareous sandstone, brown and porous.
33.8	Brown sand with a light loamy cement
35	Brown sand, light in color, fine grained.
37.7	Brown sand, fine grained.
38.1	Brown sand, a bit loamy and closely compacted calcareous sandstone.
39	Brown sand

Reproduced with permission of the copyright owner. Further reproduction prohibited without permission.

41.8	Brown sand, a bit loamy and closely compacted calcareous sandstone.
44.2	Brown loamy sand
49	Drilling cuttings of gray concretional calcareous sandstone
50.3	Same as above but fine
50.8	Concretions of gray calcareous sandstone, porous.
51.1	Same as above in drilling cuttings with fauna

Reproduced with permission of the copyright owner. Further reproduction prohibited without permission.

Bitania 1

Location: 11966/13172
Well depth: 98m
Height above sea level: 22.4m
Depth to water relative to ground level: 16m
Drill date: 1950

Well Log

Depth (meters)	Description
0-12	Dark brown silty loam
12-23	Light brown loam
23-30	Concretional calcareous sandstone, weathered
30-42	Same as above
42.40	Compacted calcareous sandstone, gray
44	Gray silty loam, rich in chalk stains
44-50	Brown silty clay
55.5	Turbid calcareous sandstone, and light brown silt.
56	Calcareous sandstone conglomerates, turbid in color with sandstone concretions of the same color and smooth fractures.
58.7	Seashell breccia, a little porous
60	Plate-like concretions of calcareous sandstone
66.5	Chocolate brown clay, with small pebbles
68.5	Concretional balls of calcareous sandstone
75.30	Silty, clayey loam rich in lime stains
88.2	Mostly coarse calcareous sandstone as well as calcareous sandstone concretions.
89	Very sandy loam, light brown in color
93.7	Calcareous sandstone, coarse and porous
98	Clayey loam, greenish gray

Reproduced with permission of the copyright owner. Further reproduction prohibited without permission.

Givat Chaim b'

Location: 14389/20060
Well depth: 94m
Height above sea level: 24.07m
Depth to water relative to ground level: 15.5m
Drill date: 1952

Well Log

Depth (meters)	Description
1	Turbid sand
3	Orange loamy sand
6	Orange sandy loam
8	Gray-brown loam
12.5	Red loam
29	Yellowish sand
39.5	Brown loam
43.5	Gray-brown loam
47	Rock pieces
52-66.4	Sand, light in color, contains mica crystals
68	Concretions of calcareous sandstone rich in shell imprints
70.5	Yellowish loamy sand
72.7	Rounded concretions of calcareous sandstone
74.4	Concretions of calcareous sandstone rich in shell imprints
76.5	Very small concretions of calcareous sandstone
77.3	Whitish, compacted calcareous sandstone
79.7	Silty sand, yellowish light in color

Reproduced with permission of the copyright owner. Further reproduction prohibited without permission.

81.5	Concretional calcareous sandstone, contains shell imprints
84	Calcareous sandstone sufficiently porous
84.5	Yellow silty sand
89.5	Concretions of calcareous sandstone, light in color
90.5	Fragments of calcareous sandstone
94	Dark gray silt with gray calcareous sandstone rich in shell formations

Reproduced with permission of the copyright owner. Further reproduction prohibited without permission.

Havat Miriam c'

Location: 11591/11562
Well depth: 94.5m
Height above sea level: 76m
Depth to water relative to ground level: N/A
Drill date: N/A

Well Log

Depth (meters)	**Description**
6	Dark brown silt, a little sandy
12	Brown silt, a little sandy
17	Sandy silt, brown
23	White concretions of calcareous sandstone, fine grained
27	Sand, light in color, fine grained with a small amount of drill cuttings of calcareous sandstone.
29	White, porous concretions of calcareous sandstone
39.6	Same as above
40.5	Brown silty sand
52	White, porous concretions of calcareous sandstone
61	Dense concretions of calcareous sandstone
66.7	Dense concretions of calcareous sandstone, gray
71	Small flint pebbles
72.5	Calcareous sandstone, sub-conglomerate, porous
84.5	Light sand, and concretions of calcareous sandstone
85	Same as above
86.5	Dense concretions of calcareous sandstone, white
88.5	White concretions of calcareous sandstone, porous, coarse grained
90.5	Dark gray concretions of calcareous sandstone, porous, coarse grained

Reproduced with permission of the copyright owner. Further reproduction prohibited without permission.

93	White concretions of calcareous sandstone, porous, coarse grained
93.5	Dense, white sandy limestone
94.3	Marly clay, gray, limonitic
94.5	Calcareous sandstone, gray, dense

Reproduced with permission of the copyright owner. Further reproduction prohibited without permission.

Holon 2

Location: 12855/15823
Well depth: 52.1m
Height above sea level: 25.2m
Depth to water relative to ground level: 18.2m
Drill date: 1946

Well Log

Depth (meters)	Description
12.5	Yellowish-brown sand
15	Black silt
20	Brown silt
24.1	Black silt
25.1	Black loam
33.4	Turbid fragments of calcareous sandstone
44.3	Concretional calcareous sandstone and sandy loam, yellowish-brown in color
48.3	Concretional calcareous sandstone
49.6	Porous calcareous sandstone in coarse grained seashell fragments
50.4	Same as above
50.9	Seashell breccia
51.3	Same as above but much finer with small sandstone pebbles
51.45	Calcareous sandstone rich in shells a portion of which are calcified
51.55	Same as above but much more porous and black
51.9	Same as above but lighter in color
52.1	Same as above but with portions of black and calcareous sandstone, plate-like, yellowish.

Reproduced with permission of the copyright owner. Further reproduction prohibited without permission.

Holon 12

Location: 13210/15718
Well depth: 101m
Height above sea level: 30m
Depth to water relative to ground level: 22m
Drill date: 1953

Well Log

Depth (meters)	Description
2.5	Black silty-loam
3.5	Same as above
5.5	Same as above
6	Brown loam
6.2	Same as above
6.6	Turbid yellow sand
7.6	Brown loam
7.7	Black, silty, clayey loam
9.7	Same as above
12.5	Same as above but black
13.8	Yellowish sand
15.47	Yellowish-brown sand
18.4	Brown, silty, clayey loam
20	Yellowish-brown sand
22.5	Brown loam
26.8	Same as above
30.8	Yellowish sand
31.5	Same as above but more light in color

Reproduced with permission of the copyright owner. Further reproduction prohibited without permission.

31.8	Calcareous sandstone, somewhat concretional, sufficiently dense
32.2	Same as above but more concretional
33.75	Same as above with sand
39.8	Same as above without sand
45.2	Yellow brown sand
46.9	Turbid, brown silty loam
47.9	Yellowish sand
48.07	Concretions of calcareous sandstone as above
48.5	Same as above
49	Calcareous sandstone sufficiently porous, contains coarse grained shell fragments
50	Porous calcareous sandstone sufficiently friable, rich in coarse grained shell fragments
54	Concretions of weathered calcareous sandstone and sand
55.3	A large amount of calcareous sandstone
56	Rounded (ball-like) concretions of calcareous sandstone
69.3	Sand and small rounded concretions
70.3	Dense concretional calcareous sandstone
73.3	Same as above
74.7	Calcareous sandstone rich in seashell fragments
75	Concretional calcareous sandstone
75.2	Same as above with flattened pebbles
75.8	Porous calcareous sandstone rich in coarse grained shell fragments
76.3	Dense, yellowish calcareous sandstone
76.6	Yellow sand
78	Small concretions of calcareous sandstone

Reproduced with permission of the copyright owner. Further reproduction prohibited without permission.

78.2	Same as above
79.1	Calcareous sandstone rich in coarse grained shell fragments
79.4	Conglomerates, pebbles and calcareous sandstone
79.6	Calcareous sandstone, sufficiently dense, contains seaweed molds
79.8	Calcareous sandstone rich in seashell forms
80.6	Dense calcareous sandstone
81.1	Yellow silt, and fragments of calcareous sandstone
81.6	Same as above
84.25	Concretions of whitish calcareous sandstone
84.65	White sand
86	Calcareous sandstone rich in shells and pebbles
87.3	Pebbles and calcareous sandstone
89	Same as above
91.8	Same as above
92.5	Concretional calcareous sandstone with seashell fragments
93.4	Concretions of whitish calcareous sandstone
94	Yellowish-green loam
94.3	Compacted calcareous sandstone, gray
94.4	Same as above with gray loam
94.9	Whitish sand
95.5	Concretions of calcareous sandstone and pebbles
96.4	Gray loam (Neogene- Quaternary)
98.7	Same as above with white sand and brown clay (Neogene- Quaternary)
101	Clayey, silty loam, greenish-gray

Reproduced with permission of the copyright owner. Further reproduction prohibited without permission.

Kidron 2

Location: 12903/13838
Well depth: 64.3m
Height above sea level: 40m
Depth to water relative to ground level: 23.65m
Drill date: 1952

Well Log

Depth (meters)	Description
5	Silty clay, alluvial, brown
10.5	Flat, flint pebbles
15	Brown silty loam
17	Pebbles and brown silty loam
18.5	Calcareous sandstone, sufficiently porous, contains coarse-grained seashell fragments.
21	Same as above, plate-like
23.5	Same as above
34	Concretional calcareous sandstone, compacted
39.5	Sand, fragments of calcareous sandstone, and pebbles
42.5	Conglomerates, pebbles, and calcareous sandstone
45	Same as above, and concretional calcareous sandstone
49	Concretional calcareous sandstone rich in mica crystals
54	Concretional calcareous sandstone, compacted
58.5	Same as above
63	Calcareous sandstone, sufficiently coarse, rich in calcified shell formations
64.3	Concretional calcareous sandstone, compacted

Reproduced with permission of the copyright owner. Further reproduction prohibited without permission.

Kochav 1

Location: 11649/11175
Well depth: 123m
Height above sea level: 90.41m
Depth to water relative to ground level: 88.5m
Drill date: 1960

Well Log

Depth (meters)	Description
0-5	Brown sandy loam, medium to fine grained, contains remnants of vegetation, concretions of white calcareous sandstone, weathered, fine grained. The loam is continental in origin.
5-7	Yellow- brown sand, medium grained with small concretions of loam and very small amount of calcareous sandstone, whitish as in the previous.
7-9	Brown sand, medium to fine grain, a bit clayey, contains pieces of grayish calcareous sandstone, medium to fine grained.
9-10	Grayish-yellowish calcareous sandstone, medium to fine grained, rich in heavy minerals, contains very small pebbles.
10-14	Yellowish calcareous sandstone, medium grained, contains a small amount of broken seashell fragments, rich in heavy minerals, porous.
14-17	Brown loam, contains remnants of vegetation, contains blocks of calcareous sandstone, whitish, weathered.
17-18	Calcareous sandstone, medium to fine grained, yellowish, contains small pebbles.
18-23	Yellow sand, medium to fine grained, contains a small amount of broken seashell fragments and heavy minerals.
23-24.5	Whitish-grayish calcareous sandstone, medium to fine grained, contains a small amount of broken seashell fragments, porous. Contains a small amount of loam in channels
24.5-30	Whitish-grayish calcareous sandstone, medium to fine grained, contains a small amount of broken seashell fragments, contains many open spaces.
30-35	Whitish-grayish calcareous sandstone, medium to fine grained, contains pebbles up to 3 mm in size, porous, concretional, This calcareous sandstone is found inside sand of the same composition and grain size.
35-42	Whitish-grayish calcareous sandstone, fine grained, porous, concretional, inside yellowish sand, fine to medium grained that contains a small amount of broken seashell fragments.
42-49	Brown loam, with very small amounts of calcified grains
49-56	Yellowish sand, fine to medium grained, contains concretions of white calcareous sandstone, fine grained.
56-59	Yellowish sand, fine to medium grained.
59-61	Yellow to brown sand, fine to medium grained, with very small pebbles.
61-64	Yellowish sand, fine grained to medium grained, small amounts of gypsum grains, and heavy minerals.

Reproduced with permission of the copyright owner. Further reproduction prohibited without permission.

64-69	Grayish-yellowish calcareous sandstone, medium to fine grained, contains very small pebbles, rich in heavy minerals. The stone is built from concretions, a bit porous. It is found inside sand of the same composition and same grain size.
69-74	Same as above
74-82	1. Grayish-yellowish calcareous sandstone, medium to fine grained, lacking in heavy minerals, concretional, porous. 2. There are also fragments of brown calcareous sandstone, dense, hard and cemented. Both types of the above-mentioned calcareous sandstone appear inside sand, fine to medium grained, yellowish in color and contain a small amount of broken seashell fragments.
82-91.5	Yellowish-brown calcareous sandstone, fine to medium grained, appears in concretions, porous, a small amount of heavy minerals. This is found together with white-grayish calcareous sandstone, fine, hard grains.
91.5-93	Calcareous sandstone, hard and cemented, grayish-brown, fine to medium grained, also contains rounded river pebbles.
93-95	Grayish-brown calcareous sandstone, fine to medium grained, appears with rounded pebbles and fragments of silicified pebbles.
95-97.2	White-grayish calcareous sandstone, fine grained, hard and cemented tightly appears with sand, fine, coarse and medium grained and with very small pebbles.
97.2-99	White-grayish calcareous sandstone, grain size ranges from fine to coarse (up to 1 mm). It is found inside sand of the same composition and grain sizes. There are also rounded pebbles within the sand fragmented pebbles of quartz and flint.
99-100.5	Beige colored sand, fine to medium grained and small amounts of coarse grains. Contains very small pebbles.
100.5-105.5	Light beige sand, fine grained to silty.
105.5-108	Calcareous sandstone, fine to medium grained, white-yellowish in color. Cemented tightly, with sand medium to coarse grained.
108-112	Calcareous sandstone, fine to medium grained, white-yellowish, cemented, concretions appear in sand of grain size fine to coarse, also contains pieces of rock in the sand.
112-113.5	Calcareous sandstone, fine grained, white-grayish, contains heavy minerals of the same grain size and slightly larger. Hardened and cemented tightly.
113.5-115.4	Calcareous sandstone, fine grained, white-grayish, contains lamina of heavy minerals, tightly consolidated, and hardened.
115.4-119.5	Grayish calcareous sandstone, fine grained, a small amount of gypsum, rich in heavy minerals, a little porous, hardened.
119.5-121.5	Very coarse sandy limestone rich in fauna fragments (mostly gastropods), light brown in color. Small pieces of flint and quartz, medium porous.
121.5-122.5	Brown-grayish loam, rich in calcite grains and fauna, Elphidium, fragments of sea urchin thorns, ammonia, seashells and more. Many brown bodies, cloven, up to half a mm in size.
122.5-123	Gray clay contains silt rich in micro-fauna and sea urchins thorns, Elphidium, etc. shreds of mica. A portion of the fauna has undergone pyritization. (Neogene)

Reproduced with permission of the copyright owner. Further reproduction prohibited without permission.

Kochav 3

Location: 11667/11280
Well depth: 145m
Height above sea level: 109.5m
Depth to water relative to ground level: 102.4m
Drill date: N/A

Well Log

Depth (meters)	Description
0-80	Sand, calcareous sandstone and loam
130	Calcareous sandstone and sand
140	Calcareous sandstone and silt
145	Gray clay- Saqiye

Reproduced with permission of the copyright owner. Further reproduction prohibited without permission.

Migdal 7

Location: 11271/11856
Well depth: 109.75m
Height above sea level: 51m
Depth to water relative to ground level: 44.8m
Drill date: 1953

Well Log

Depth (meters)	Description
4	Gray loam
6.5	Turbid brown loam
10	Brown loam
15	Concretions of calcareous sandstone
22	Same as above with sand
23.5	Turbid brown loam
25	Concretional calcareous sandstone, more or less porous
30	Sand and fragments of calcareous sandstone.
31	Brown clayey loam
42.5	Concretions of calcareous sandstone and sand
43	Turbid brown loam
45	Concretions of calcareous sandstone and sand
45.5	Loam, turbid in color
47	Sand and concretions of calcareous sandstone
50	Calcareous sandstone, more or less porous, appears weathered.
56	Concretions of calcareous sandstone
56.5	Brown loam
63	Concretional calcareous sandstone, more or less porous, contains very coarse-grained seashell fragments.

Reproduced with permission of the copyright owner. Further reproduction prohibited without permission.

72.7	Same as above with sand
73.3	Dense calcareous sandstone
76.8	Concretional calcareous sandstone, more or less porous, and friable
81.5	Same as above
95	Same as above with sand
104.3	Crystalline concretions of calcareous sandstone with sand
105.5	White, dense calcareous sandstone with sand.
106.2	Gray silty clay with foraminifers.
108.75	Gray, dense calcareous sandstone with loam

Reproduced with permission of the copyright owner. Further reproduction prohibited without permission.

Migdal 12

Location: 11326/11773
Well depth: 103m
Height above sea level: 46.48m
Depth to water relative to ground level: 45.2m
Drill date: 1961

Well Log

Depth (meters)	Description
0-6.5	Dark brown clayey loam with concretions
8	Brown loam
11	Brown to reddish sandy loam
13.5	Dark brown clayey loam with chalky concretions
16.3	Beige colored concretional calcareous sandstone, medium to coarse grained, friable, chalky and weathered, with light brown sand.
25.4	Brownish loamy clay
27	Brown loam with few weathered broken fragments of thin seashells
29	Light brown sand, somewhat loamy, with concretions of weathered, friable, chalky calcareous sandstone.
31	Dark brown clayey loam with some pieces of whitish weathered calcareous sandstone.
35	Same as interval 27-29m.
40	Brownish, hard and compact clay
40.5	Dark brown loamy clay
45.5	Brown sandy loam
49.3	Brown reddish sandy loam
54.8	Brown loamy sand, coarse grained, contains a small amount of broken, coarse grained seashell fragments
69.4	Beige colored coarse-grained sand, contains small amount of calcified broken seashell fragments, as well as preserved fauna, with concretional calcareous sandstone of the same composition.
80.8	Same as above but lighter in color and less sandstone.

Reproduced with permission of the copyright owner. Further reproduction prohibited without permission.

86	Sandstone and sand as in section 54.8-69.4. The grain size is very coarse and there are many seashell fragments.
87.65	Whitish calcareous sandstone, very coarse grained, calcified, porous. Composed mainly of eroded seashell particles of 1-4 millimeter in size (fine seashell breccia).
90.65	Breccia- same as above but coarser and better cemented.
95.4	Calcareous sandstone, beige in color, medium to coarse grained, calcified, porous, very rich in calcified seashell fragments and contains a small amount of micro fauna and sand.
103	Gray to beige concretional calcareous sandstone, medium grained, very rich with micro fauna, also contains fine seashell fragments, mica, and very small pebbles with sand of the same composition.

Reproduced with permission of the copyright owner. Further reproduction prohibited without permission.

Naan

Location: 13696/14530
Well depth: 80.3 m
Height above sea level: N/A
Depth to water relative to ground level: 53.5 m
Drill date: N/A

Well Log

Depth (meters)	Description
1.5	Brown soil
3	Sandy brown soil
5	Hamra (reddish to brownish clayey sand with a variable amount of clay)
10	Medium grained sand mixed with a small amount of Hamra
20	Fine grained sand to silt mixed with a small amount of Hamra
39	Medium grained sand, a little reddish
46	Sand, white to yellowish in color, medium grained, mixed with coarse-grained white sand.
50	Reddish silt, mixed with approximately 15% clay
53	Medium to fine grained sand, yellowish, clean
58	Medium to coarse-grained sand, yellowish to light brown, mixed with fragments of limestone, contains gray clay crystals.
62	White, fine-grained sand contains large, rounded pebbles of limestone and flint, unconsolidated.
67	Medium grained sand, yellowish brown
68	White sand, coarse grained, rounded, and contains rounded pebbles of lime and flint.
71.9	Concretions of calcareous sandstone, coarse grained and porous appears in plates
74	Conglomerate, coarse grained, contains concretions of calcareous sandstone and shells, hard and porous, rich in calcite.
78	Dense concretions of calcareous sandstone, medium grained
79.5	Dense gray chalk with iron stains
80.3	Bituminous chalk

Reproduced with permission of the copyright owner. Further reproduction prohibited without permission.

Netzer Serini

Location: 13212/14806
Well depth: 92.4m
Height above sea level: N/A
Depth to water relative to ground level: N/A
Drill date: 1959

Well Log

Depth (meters)	Description
40.25-46	Light brown sand with fragments of pebbles.
50	Same as above
52	Light brown sand
52.7	Light brown sandy loam
54	Pieces of rock and sand
57	Light sand
60	Same as above
63	Same as above
65	Same as above
65.15	Gray clayey loam
68	Light sand
71	Same as above
74.5	Same as above
75.75	Concretions of calcareous sandstone with sand, contains shells and pebbles.
76	Concretions of calcareous sandstone, contains shells and pebbles.
77.3	Fine sand, a little silty
80.6	Same as above

Reproduced with permission of the copyright owner. Further reproduction prohibited without permission.

82	Same as above
87.5	Yellow sand
88	Calcareous sandstone rich in mica crystals. Contains broken fragments of calcified seashells.
90	Calcified concretions of calcareous sandstone.
91.25	Same as above
92.4	Gray clay

Reproduced with permission of the copyright owner. Further reproduction prohibited without permission.

Nir Am 14

Location: 10849/10269
Well depth: 143m
Height above sea level: 110m
Depth to water relative to ground level: 107m
Drill date: 1961

Well Log

Depth (meters)	Description
0-1.2	Brown clayey loam
6	Brown loam
7.5	Brown loam and a small amount of weathered calcareous sandstone
10.5	Brown loamy sand
15	Yellowish-beige sand and pieces of light beige calcareous sandstone
17.5	Red loamy sand
20.5	1. Chalky, silty sand, light beige 2. Chalky, silty calcareous sandstone, light beige Both appear to be of continental origin
24	Red-brown loamy sand
29.5	Yellowish sand and small concretions, medium grained, sub-angular
32	Brown loamy sand
35.5	Sand and small concretions of calcareous sandstone, yellowish (0.5 cm.) with larger grains the majority rounded.
37	Brown loam
43	Fine grained sand, angular, very light yellowish, and concretions
49	Silty sand a little bit loamy, light brown and pieces of calcareous sandstone medium to fine grained, appears very weathered. Silty chalk, light beige.
55	Fine sand, crème colored
59	Same as above
65	Fine to medium sand, angular to rounded, crème colored
70.5	Sand in different sizes, mostly medium to silty grained, yellowish and a bit brown.

Reproduced with permission of the copyright owner. Further reproduction prohibited without permission.

75	Sand and concretions of calcareous sandstone (of the same size), the majority medium grained, but there are also fractions of fine and coarse grained in crème color.
82	Silty sand, a bit loamy, light brown
87	White sand, the majority medium grained, rounded and sub-angular, and small concretions of calcareous sandstone (up to 0.5 cm.).
92	Crème-white sand, the majority medium grained, rounded and sub-angular
97.8	Concretions of calcareous sandstone (majority), and sand medium to coarse, rounded, contains broken fragments of fine seashells, contains many sea urchin (Echinoderm) thorns, and nice Elphidium.
102	Different sized grains of calcareous sandstone, contains broken fragments of seashells the majority from chalky fragments of shells
103.5	Silty sand, very chalky and loamy, contains mica, light khaki in color
108	Sand and sandstone of different size grains, very silty, chalky, friable, contains micro chalky shell fragments, crème colored.
111.5	Sandstone, chalky and silty as above
113	Same as above
116	Calcareous sandstone, crème, the majority medium grained, a little silty with a small amount of algae.
120	Same as above
121.35	Calcareous sandstone as above, with a lot of algea, flint pebbles (up to 1.5 cm.)
122.1	Flint pebbles, 2mm to 0.5 cm in size
124	Large flint pebbles
125.4	Calcareous sandstone, medium grained, crème- white with algae, and nice Elphidium.
128	White sand, medium grained, a bit silty
131.3	Sandy loam, chalky, khaki colored
132	Calcareous sandstone, very fine grained, contains foraminifers
134.7	Calcareous sandstone as above
139.2	Calcareous sandstone, dense, with mica
142.5	Calcareous stone, yellow organic algae, contains macro-fauna and micro-fauna
143	Gray silt, contains macro and micro-fauna

Reproduced with permission of the copyright owner. Further reproduction prohibited without permission.

Nir Am 15

Location: 10929/10366
Well depth: 132.7m
Height above sea level: 103.12m
Depth to water relative to ground level: 98.73m
Drill date: 1967

Well Log

Depth (meters)	Description
0-5.5	Light brown sandy loam with pebbles of calcareous sandstone (0.5 m.)
5.5-10	Light orange to white calcareous sandstone
10-13	Fine grained sand, orange in color
13-17.5	Whitish calcareous sandstone, cemented very tightly
17.5-19	Fine grained sand, orange
19-25	Whitish calcareous sandstone
25-27	Medium grained sand, orange
27-47	Whitish calcareous sandstone
47-54	Medium grained sand, orange
54-63	Whitish calcareous sandstone
63-64	Coarse grained sand with brown, calcareous clay
64-67	Same as above with pebbles of calcareous sandstone
67-70	Calcareous sandstone with a small amount of calcareous clay
70-71.5	Light brown silt
71.5-79	Whitish calcareous sandstone
79-89.5	Whitish chalky sandstone, soft
89.5-90.5	Grayish, chalky sandstone, soft

Reproduced with permission of the copyright owner. Further reproduction prohibited without permission.

90.5-109.7	Yellowish to whitish calcareous sandstone
109.7-112.7	White chalky silt
112.7-118	White silt-stone
118-120	Gray to yellowish marl
120-121.7	Calcareous sandstone, medium grained, gray to yellow
121.7-124.7	Sandy limestone, contains fauna, yellow
124.7-127	Grayish limestone, contains fauna
127-129	Gray limestone, contains fauna
129-132.7	Gray chalky silt-stone

Reproduced with permission of the copyright owner. Further reproduction prohibited without permission.

Nitzanim

Location: 11630/12610
Well depth: 87m
Height above sea level: 38m
Depth to water relative to ground level: 33.7m
Drill date: 1955

Well Log

Depth (meters)	Description
3	Red, sandy loam
7	Fragments of calcareous sandstone and turbid sand
9	Red-brown loam
10	Concretions of calcareous sandstone and loamy sand.
14.2	Concretions of turbid calcareous sandstone
22	Same as above
23	Brown sandy loam
43	Concretions of calcareous sandstone and turbid sand
47	Gray clay
52	Brown, clayey sand
56.8	Concretions of calcareous sandstone
57	Red loam
61.5	Concretions of calcareous sandstone and turbid sand
62.5	Concretions of calcareous sandstone
71.5	Concretional calcareous sandstone
87	Very porous calcareous sandstone, crystalline, rich in coarse-grained calcified seashell fragments and formations.

Reproduced with permission of the copyright owner. Further reproduction prohibited without permission.

Petach Tikva 3

Location: 13745/16666
Well depth: 39.75m
Height above sea level: N/A
Depth to water relative to ground level: 18m
Drill date: 1951

Well Log

Depth (meters)	Description
3	Dark sand
4.75	Hamra sand
5.6	Yellow sand
6.2	Hamra sand
7.75	Yellow sand
8.9	Hamra
9.4	Yellowish sand
11.25	Hamra sand
13	Yellow sand
14.25	Red hamra
16	Yellow sand
17.25	Sand and hamra
21	Thin white sand
28	Coarse, light sand
30	Light sand with wadi rocks
35	Coarse, light sand
36	Crystallized rocks and plates
39.75	Small pieces of rock which have a nice finger-like appearance

Reproduced with permission of the copyright owner. Further reproduction prohibited without permission.

Rishon 5

Location: 12970/15230
Well depth: 134m
Height above sea level: 54.99m
Depth to water relative to ground level: 49.7m
Drill date: 1960

Well Log

Depth (meters)	Description
0-7.5	Fine yellowish chalky sand
9	Dark brown clayey loam
12	Brownish-black clayey loam
15.5	Dark brown clayey loam
27.3	Fine yellowish chalky sand
32	Brown loam
34.5	Silty sand- beige to reddish in color.
38	Fine yellowish chalky sand
40	Concretional calcareous sandstone and sand
49.8	Medium to coarse grained calcareous sandstone, yellowish, porous
55.9	Dark brown clayey loam
64-69	Sand and small concretions of beige colored calcareous sandstone.
71.7	Medium to coarse grained calcareous sandstone
77	Brown loamy sand
87	Weathered sections of calcareous sandstone with silty sand
91	Continental deposits of sand and calcareous sandstone
95	Continental deposits of calcareous sandstone

Reproduced with permission of the copyright owner. Further reproduction prohibited without permission.

100-109	Concretional calcareous sandstone
110.5	Sandy loam light brown in color
113	Breccia shells and calcified sand
115.5-120	Continental calcareous sandstone
123	Concretional calcareous sandstone, porous
125	Coastal calcareous sandstone
128.8	Calcareous sandstone, yellowish, porous
130	Marine calcareous sandstone, yellowish, porous
133	Calcareous sandstone, yellowish, porous with sand, marine
134	Dark brown loamy clay

Reproduced with permission of the copyright owner. Further reproduction prohibited without permission.

Sapiria 2

Location: 13486/15436
Well depth: 110m
Height above sea level: 53.2m
Depth to water relative to ground level: 40.3m
Drill date: 1950

Well Log

Depth (meters)	Description
0	Dark brown loam
3	Orange sandy loam
10	Yellowish brown sand with a bit of loam
15	Yellowish sand
23	Whitish, friable calcareous sandstone and yellowish sand.
27	Yellowish sand
32	Yellowish sand with friable calcareous sandstone.
37	Brown, yellow sand
41	Yellow sand with fragments of calcareous sandstone.
50	Orange loamy sand
69.5	Yellow sand
73	Orange yellow sandy loam
80.5	Sandy loam yellowish orange
85	Sandy loam yellowish orange with pebbles and mica crystals
95.3	Concretions, which have a pillar-like appearance, of white calcareous sandstone with mica crystals, pebbles and sand.
95.8	Whitish, compacted calcareous sandstone
105	Rounded plate-like concretions of compacted calcareous sandstone
105.8	Greenish gray loam with small pieces of sufficiently coarse sand
110	Same as above

Reproduced with permission of the copyright owner. Further reproduction prohibited without permission.

Tel Mond 13

Location: 14266/18364
Well depth: 72m
Height above sea level: N/A
Depth to water relative to ground level: 33.5m
Drill date: N/A

Well Log

Depth (meters)	Description
0-23	Fine to medium grained brown sand and pieces of rounded rock
32	Light brown sand, fine to medium grained
40	White sand, thin to medium grained, contains mica scales
48	Light brown sand, fine to medium grained, contains mica scales
51	Light gray calcareous sandstone, medium grained, contains mica scales, and sand light in color, coarse grained with pieces of mica.
60	Gray calcareous sandstone, fine grained and closely compacted. Parts contain calcified seashells and pebbles.
72	Gray calcareous sandstone, fine grained, compacted

Reproduced with permission of the copyright owner. Further reproduction prohibited without permission.

Tel Mond 8

Location: 14102/18386
Well depth: 95m
Height above sea level: 47.78m
Depth to water relative to ground level: 31.26m
Drill date: 1955

Well Log

Depth (meters)	Description
7	Brown loam
14	Yellowish sand
20	Gray-brown loam
27	Red loamy sand
29	Reddish loam
43	Red sandy loam
50	Yellowish sand
60	Yellow sandy loam
72	Yellow sand
79	Porous calcareous sandstone rich in pebbles, and sandstone containing pebbles and mica crystals.
85.3	Same as above
87	Whitish calcareous sandstone, compacted
90-95	Same as above, a bit concretional

Reproduced with permission of the copyright owner. Further reproduction prohibited without permission.

Yavneh 5

Location: 12520/13760
Well depth: 101m
Height above sea level: 48.3m
Depth to water relative to ground level: 39.5m
Drill date: 1941

Well Log

Depth (meters)	Description
3.25	Dark brown sand with lime stains, sand light in color with broken fragments of calcareous sandstone.
4.4	Yellow sand with broken fragments of calcareous sandstone
9.4	Solid calcareous sandstone
14.4	Same as above
16.85	Same as above
20.95	Ocher sand with broken fragments of coarse grained calcareous sandstone
22.85	Red-brown sand, consolidated
27.85	Sand with small pieces of calcareous sandstone, red-brown sand (Hamra) with lime stains
31.3	Hamra with lime stains, coarse grained calcareous sandstone, porous
36.3	Concretional calcareous sandstone
41.3	Same as above
41.85	Same as above
46.85	Yellow sand, broken fragments of porous calcareous sandstone
47.45	Same as above
48.6	Yellow sand, less broken fragments of porous calcareous sandstone
53.6	Solid calcareous sandstone
54.3	Solid concretional calcareous sandstone
59.2	Yellow sand with less broken fragments of calcareous sandstone

Reproduced with permission of the copyright owner. Further reproduction prohibited without permission.

60.4	Porous calcareous sandstone
61.7	Yellow sand
66.2	Calcareous sandstone
71.2	Calcareous sandstone and sand
76.2	Dense continental calcareous sandstone
77.4	Concretional calcareous sandstone
82.4	Same as above
83.5	Same as above
85.6	Same as above
90.6	Conglomerates of calcareous sandstone with small flint pebbles
98.8	Concretional, plate-like calcareous sandstone
101	Concretional calcareous sandstone

Reproduced with permission of the copyright owner. Further reproduction prohibited without permission.

Lahat 3

Location: 1132/11528
Well depth: 121.6m
Height above sea level: 44m
Depth to water relative to ground level: 38m
Drill date: 1952

Well Log (no sample available)

Reproduced with permission of the copyright owner. Further reproduction prohibited without permission.

Yad Mordecai 2

Location: 10725/11029
Well depth: 105.2m
Height above sea level: 25m
Depth to water relative to ground level: 14.6m
Drill date: 1951

Well Log

Depth (meters)	Description
0-0.5	Loam and chalk
0.5-18	Calcareous sandstone, porous
18-30	Concretions of calcareous sandstone
30-39	Concretions of calcareous sandstone, porous
39-45.5	Sand and concretions of calcareous sandstone
45.5-50	Concretions of loamy sand
50-59	Concretions of calcareous sandstone with broken seashell fragments.
59-61	Sand
61-68.5	Sand and concretions of calcareous sandstone
69	Very fine concretions of calcareous sandstone
69-75	Sand and concretions of calcareous sandstone
75-77	Sandy loam, brown with a small amount of marl
77-80.5	Coarse sand and concretions of calcareous sandstone
80.5-82	Calcareous sandstone rich in broken seashell fragments
83	Concretions of calcareous sandstone
87.7-90.5	Clayey loam, brown sand
90.5-96	Silty sand, brown-black, with chalk concretions
96-99.5	Chalky marl, limonitic
99.5-105.2	White, chalky marl

Reproduced with permission of the copyright owner. Further reproduction prohibited without permission.

Yad Mordecai 6

Location: 10707/11094
Well depth: 70.3
Height above sea level: 23.8m
Depth to water relative to ground level: 15.3m
Drill date: 1951

Well Log

Depth (meters)	Description
0-5	Brown clay
8	Weathered calcareous sandstone
8-30	Calcareous sandstone
31.7	Concretional calcareous sandstone, in pieces
36.2	Brown sandy clay
37.2	Calcareous sandstone
37.2-51	Solid sandy clay, brown
51-54	Calcareous sandstone
54-58.5	Same as above
58.5-61	Calcareous sandstone of definite sea origin
61-64	Calcareous sandstone
65	Calcareous sandstone with seashells
65.5	Same as above
68.3	Calcareous sandstone of sea origin
70	Coarse sand

Reproduced with permission of the copyright owner. Further reproduction prohibited without permission.

Beit Yehoshua 9

Location: 13743/18500
Well depth: 86m
Height above sea level: 21.89m
Depth to water relative to ground level: 19m
Drill date: 1969

Well Log

Depth (meters)	Description
1.0	Gray sand
6.0	Reddish loamy sand and sand
12.0	Reddish sand, loamy
17.0	Reddish loamy sand with grayish stains
19.5	Brown-orange loamy sand
24.0	Silty sand, light brown
41.0	Yellowish sand
45.0	Concretional calcareous sandstone
47.5	Calcareous sandstone with pebbles and seashells (beachrock)
49.0	Calcareous sandstone and sand with rounded algea
52.5	Reddish-gray loamy sand
53.5	Calcareous sandstone rich in algea and sand
58.0	Calcareous sandstone as above with many seashells (beachrock)
61.5	Calcareous sandstone as above with pebbles (beachrock)
68.0	Calcareous sandstone with a small amount of pebbles
79.0	Calcareous sandstone with an abundance of seashells (beachrock)
80.5	Calcareous sandstone
86.0	Calcareous sandstone with seashells (beachrock)

Reproduced with permission of the copyright owner. Further reproduction prohibited without permission.

42/1

Location: 13660/18638
Well depth: 141.8m
Height above sea level: 14.94m
Depth to water relative to ground level: N/A
Drill date: 1958

Well Log

Depth (meters)	Description
2.00	Reddish-brown loam
5.50	Concretions of calcareous sandstone
10.20	Coarse grained fragments of seashells, calcareous sandstone
19.60	Brown sandy loam
33.70	Seashell fragments of fine grained calcareous sandstone
45.00	Same as above
52.50	Gray silt
61.90	Seashell fragments of concretional calcareous sandstone,
66.60	Same as above
71.30	Same as above
80.70	Same as above
85.40	Same as above
90.10	Same as above
94.80	Same as above
99.50	Same as above
104.20	Concretional calcareous sandstone, dense, fine grained, and concretions of calcareous sandstone, dense, fine grained.
113.00	Same as above
113.60	Dark gray silt

Reproduced with permission of the copyright owner. Further reproduction prohibited without permission.

118.30	Coarse grained fragments of seashells, calcareous sandstone
123.00	Fragments and coarse grained shells of calcareous sandstone
127.70	Dark gray silt, and coarse grained shells of calcareous sandstone
132.40	Same as above
137.10	Same as above
141.80	Brown loam mixed with dark gray silt, and coarse grained shells of calcareous sandstone

Reproduced with permission of the copyright owner. Further reproduction prohibited without permission.

Herzalia a'

Location: 13536/17436
Well depth: 131.35m
Height above sea level: 59.1m
Depth to water relative to ground level: 54m
Drill date: 1937

Well Log

Depth (meters)	Description
5.00	Yellow and brown sand with iron and loam and with pieces of rounded sandstone
10.00	Yellow sand with calcareous sandstone
12.50	Light sandstone, weathered with a calcareous cement
83.00	Yellow sand with rounded foraminifers
86.00	Red-brown iron-sand
95.25	Grayish sandstone, compacted, with calcareous grains small in size and few in number.
104.50	Yellow sand with small sandstone concretions
105.00	Calcareous sandstone with seashell fragments with foraminifer etc. (of sea origin)
110.25	Calcareous sandstone with many shell fragments that have calcified
126.00	Concretions of sandstone (Kurkar)
131.25	Gray sandstone

Reproduced with permission of the copyright owner. Further reproduction prohibited without permission.

Bnei Dror c'

Location: 14071/18513
Well depth: 82.40m
Height above sea level: 28m
Depth to water relative to ground level: 11.60m
Drill date: 1952

Well Log

Depth (meters)	Description
3.2	Red sandy loam
5.8	Red clayey loam
10.4	Brown loamy sand
13.8	Orange loamy sand
25	Same as above but more clayey
34	Red clay
43.2	Orange loamy sand
46.4	Brown loam
59.2	Same as above
61.8	Sand with rock pieces
63.7	Sand with concretions of calcareous sandstone rich in shells
65.1	Sand with rock pieces
66.9	Concretional calcareous sandstone
69	Same as above with seashell fragments
70-82.40	Gray clay

Reproduced with permission of the copyright owner. Further reproduction prohibited without permission.

Reproduced with permission of the copyright owner. Further reproduction prohibited without permission.

APPENDIX 2

Table 7: Results of trace ions in mg/l from samples taken in 1997 and 1998.

Well	Sc	P	Mo	B	Zn	Pb	Cd	Co	Ni	Ba	SiO2	Mn	Fe	Cr	Al	V	Be	Cu	Ag	Ti	Sr	Li
Nir Am 15	4.76	0	0.003	0.37	0.021	-0.01	0.0024	-0.001	-0.015	0.091	14.2	-0.001	-0.002	0.002	0.02	0.005	-0.0007	0.002	0	0.007	0.814	0.039
Migdal 12	5.09	-0.1	0.008	-0.8	0.002	0	-0.0019	0.003	0.002	0.108	23.8	-0.0001	0	-0.002	0	0.047	0.0014	0.001	0.002	0.003	1.83	0.036
Nitzanim	5.18	-0.1	0.003	0.91	0.014	-0.03	0.0009	0	0.002	0.123	22	0.0001	0.002	-0.001	-0.01	0.038	0.0008	0	0.002	0.004	1.43	0.026
Ir Darom 1	5.08	0	-0.01	-0.49	0.007	-0.01	-0.0036	-0.002	-0.002	0.143	13.1	-0.0009	-0.013	0.01	-0.01	-0.006	-0.0106	-0.002	-0.004	0.003	0.975	0.144
Kochav 1	4.55	-0.3	0.01	0.31	0.014	0.02	0.0035	0	-0.01	0.045	18.7	-0.0001	-0.005	0.004	0.03	0.018	-0.0005	0.036	-0.002	0.005	0.73	0.042
N.H. Yavneh 18	4.75	0.2	0.006	0.06	0.026	0.03	0.0004	0.003	-0.008	0.135	14.1	0.0001	-0.004	0.018	-0.01	0.003	0	-0.001	0	0.017	1.43	0.013
N.H. Yavneh 1	4.85	0.2	0.004	0.06	0.02	-0.01	0.0041	0	-0.003	0.161	14.2	-0.0001	-0.006	0.022	-0.02	-0.001	-0.0001	-0.001	0	0.015	2.1	0.011
Kfar Achim 4	4.75	0.1	-0.003	-0.22	0.027	0.01	-0.0007	0	0.003	0.231	34.3	-0.0005	-0.015	0.003	0.01	0.001	-0.0094	-0.001	-0.003	0.006	1.89	0.226
Ayanot b'	5	0	-0.002	0.03	0.021	-0.01	0.0011	0	0.005	0.1	20.7	0.0013	-0.009	-0.001	0.02	0.018	0.0009	0.002	0.002	0.006	0.437	-0.002
Holon 2	4.92	0.1	0.002	0.04	0.032	0.01	0.0032	0	-0.005	0.05	15.3	0	-0.003	0.009	-0.02	-0.001	-0.0002	0.004	0.001	0.015	0.4	0.009
Kidron 2	4.66	0	0.003	-0.18	0.03	-0.03	-0.0022	0.003	0.006	0.208	20.4	0.001	0.01	0.002	0.01	-0.001	-0.0089	0.006	-0.003	0.008	1.79	0.221
Rishon 5	5.01	-0.3	-0.008	-1.38	0.021	-0.01	-0.0019	0.001	0.004	0.045	19.2	0.0001	-0.002	0.004	-0.01	0.046	0.0007	0	0	0.003	0.327	0.021
Givat Brener a	4.82	-0.02	-0.008	-0.41	0.064	0	-0.0009	0	0.018	0.195	16.5	-0.0008	-0.015	-0.001	0.01	-0.009	-0.0095	-0.001	-0.002	0.006	1.24	0.191
Holon 12	5.17	0	0.004	0.07	0.075	-0.02	-0.001	0.002	0.007	0.085	14.1	0.0131	0.09	-0.001	0.06	0.018	0.0006	0.01	-0.001	0.004	0.785	0.001
Netzer Serini	4.92	-0.2	0.009	-1.27	0.041	0.02	0	0	0.003	0.128	21.3	0.0008	-0.001	0.004	0	0.048	0.0014	0.002	0.001	0.007	0.578	0.025
Naan	4.63	-0.1	-0.003	0.8	0.031	-0.03	-0.0001	0.002	0.01	0.119	18.9	0.437	0.54	-0.009	0.03	0.014	0.0015	0.005	0.002	0.016	4.54	0.009
Tel Mond 13	4.81	0	0.003	0.05	0.062	-0.01	-0.0007	0.006	0.006	0.076	26.2	0.0011	-0.007	0.001	0.01	0.016	0.0009	0.01	-0.002	0.004	0.326	-0.001
Givat Haim o'	4.18	-0.1	0.019	0.14	0.01	0.02	0.0001	0.007	0.011	0.092	23.7	0.0707	0.028	-0.001	0.05	0.01	0.0021	0.003	0.002	0.005	0.42	-0.002

APPENDIX 3

XRD peak intensity graphs for the Nitzanim, Kfar Achim 4, and Naan wells.

Reproduced with permission of the copyright owner. Further reproduction prohibited without permission.

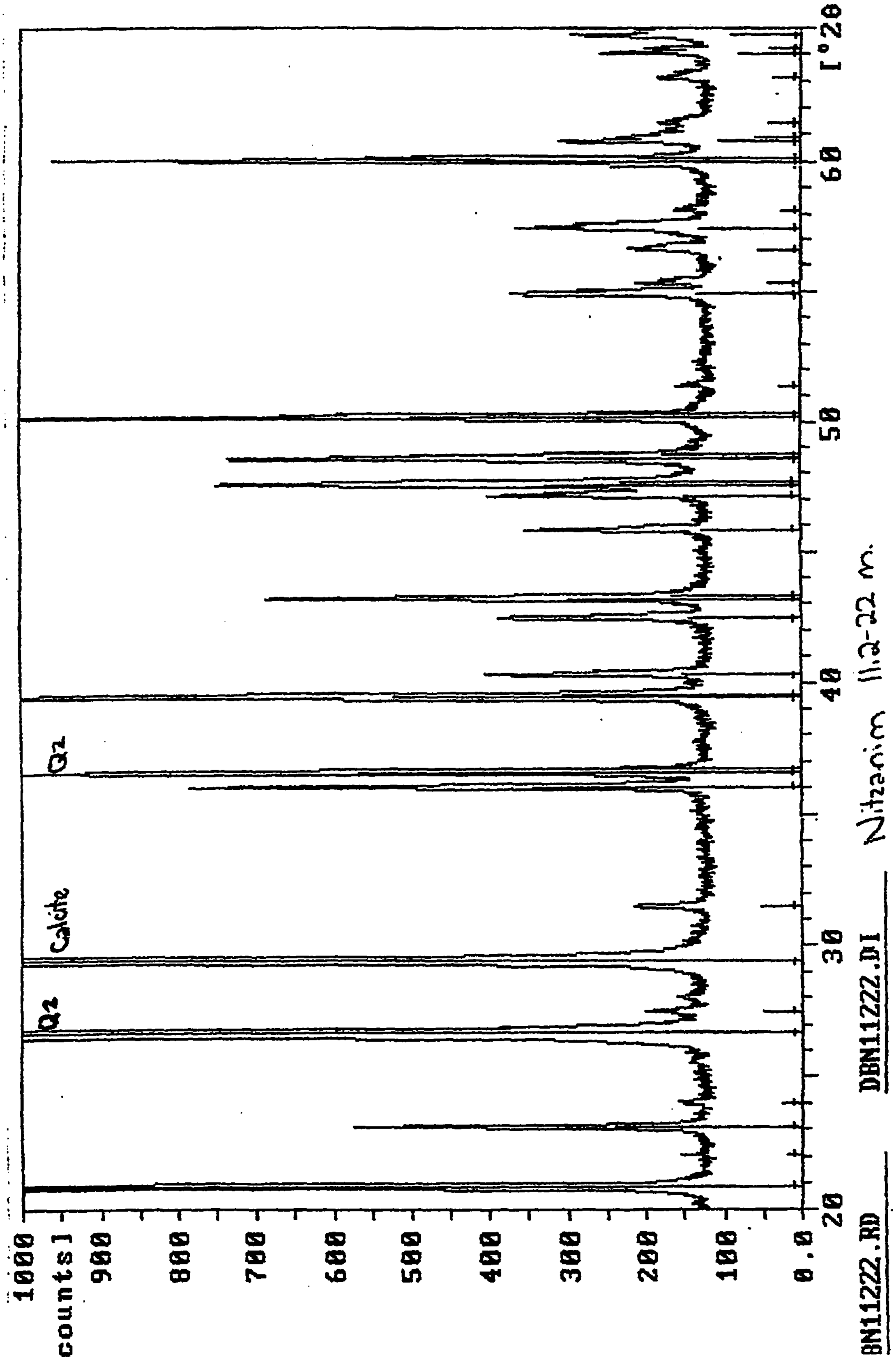

Reproduced with permission of the copyright owner. Further reproduction prohibited without permission.

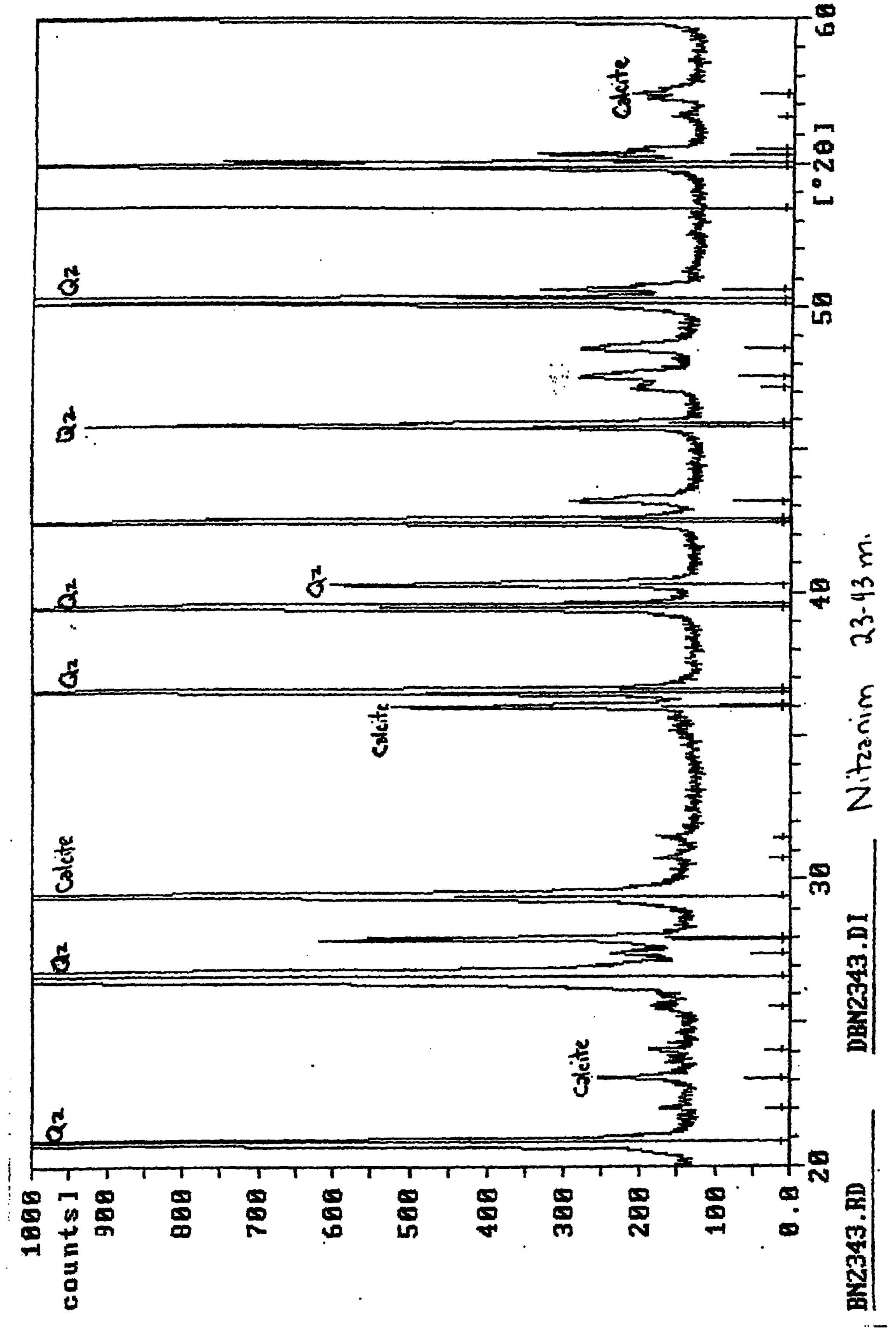

Reproduced with permission of the copyright owner. Further reproduction prohibited without permission.

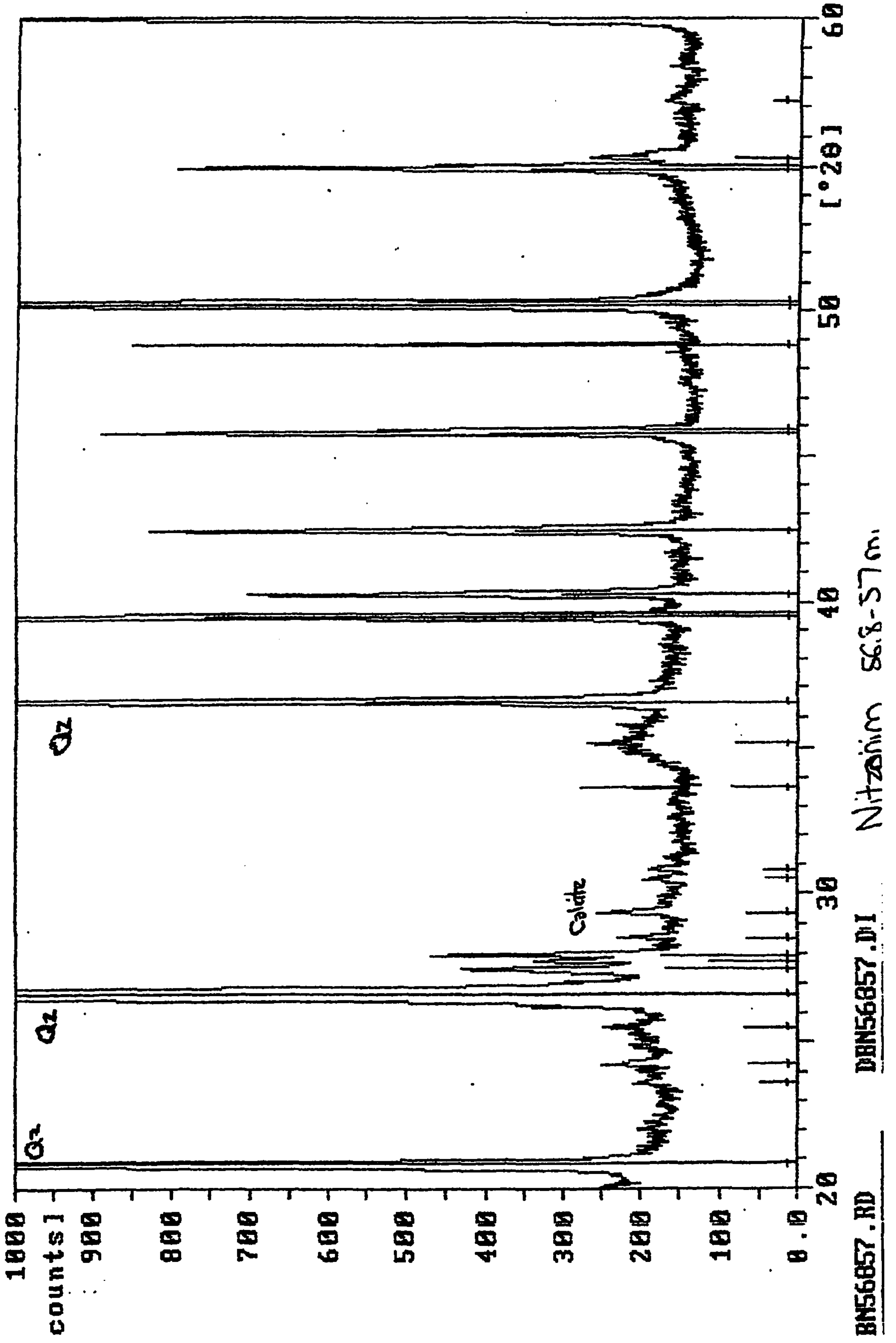

Reproduced with permission of the copyright owner. Further reproduction prohibited without permission.

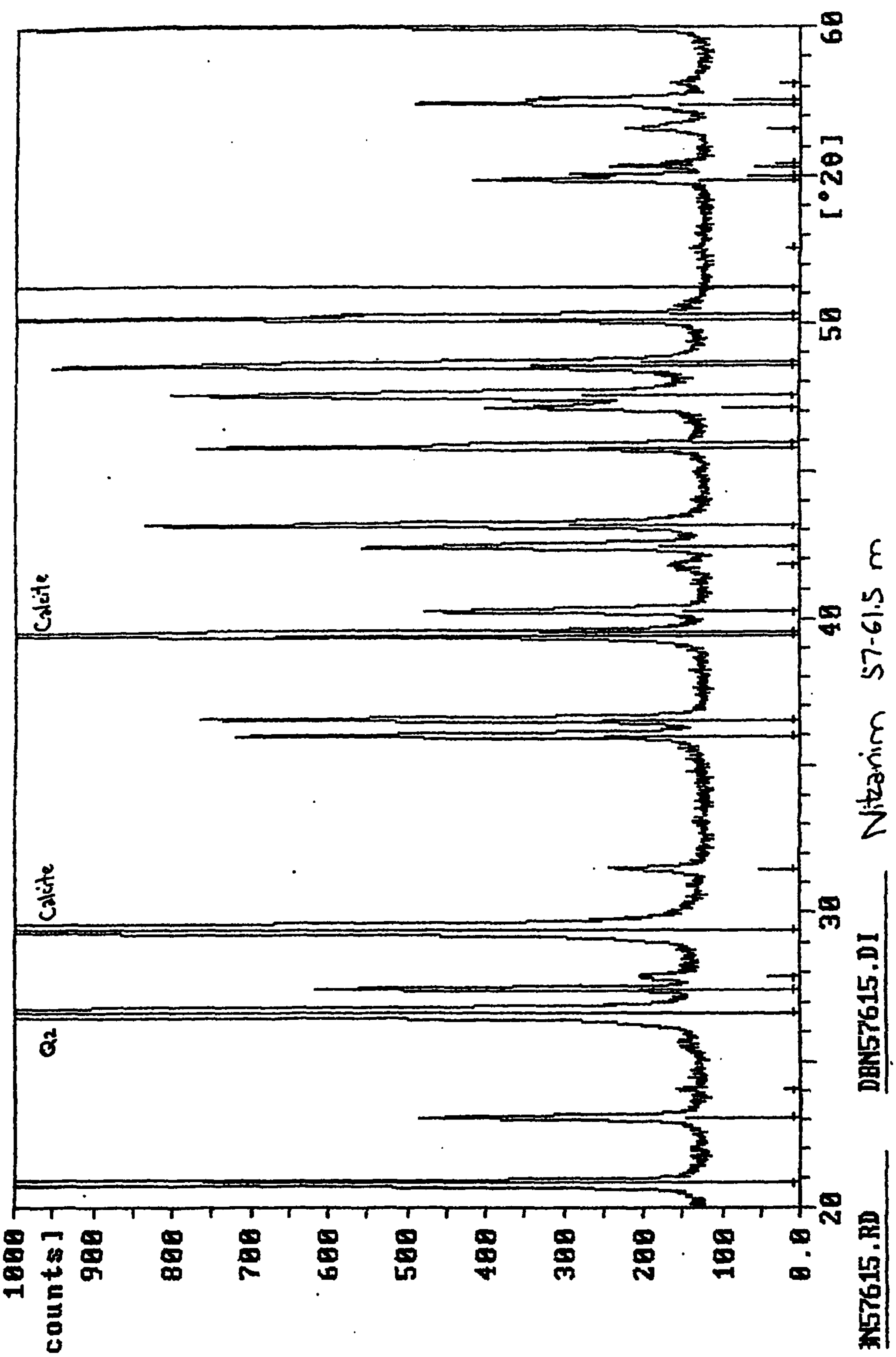

Reproduced with permission of the copyright owner. Further reproduction prohibited without permission.

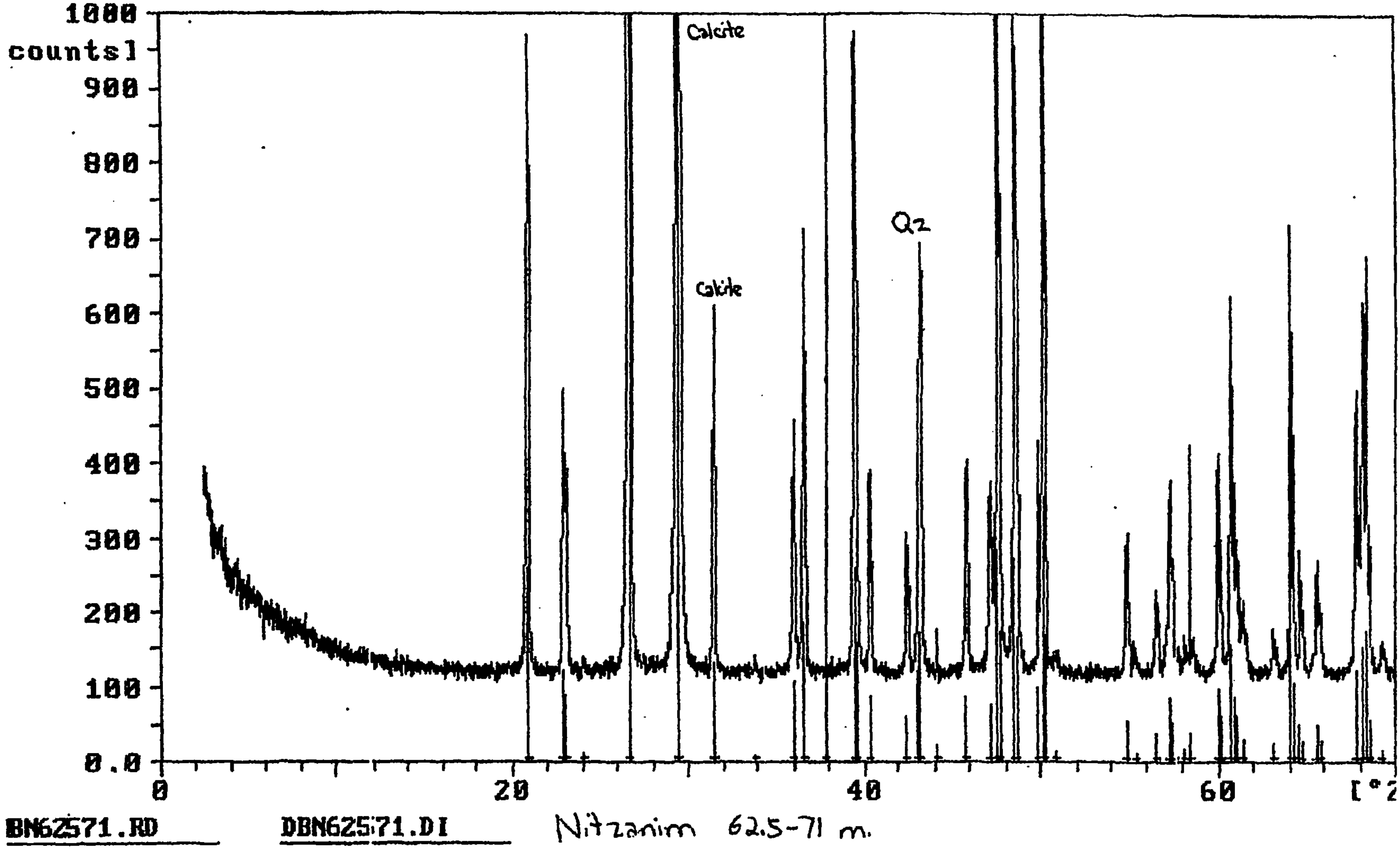

Nitzanim 62.5-71 m.

Reproduced with permission of the copyright owner. Further reproduction prohibited without permission.

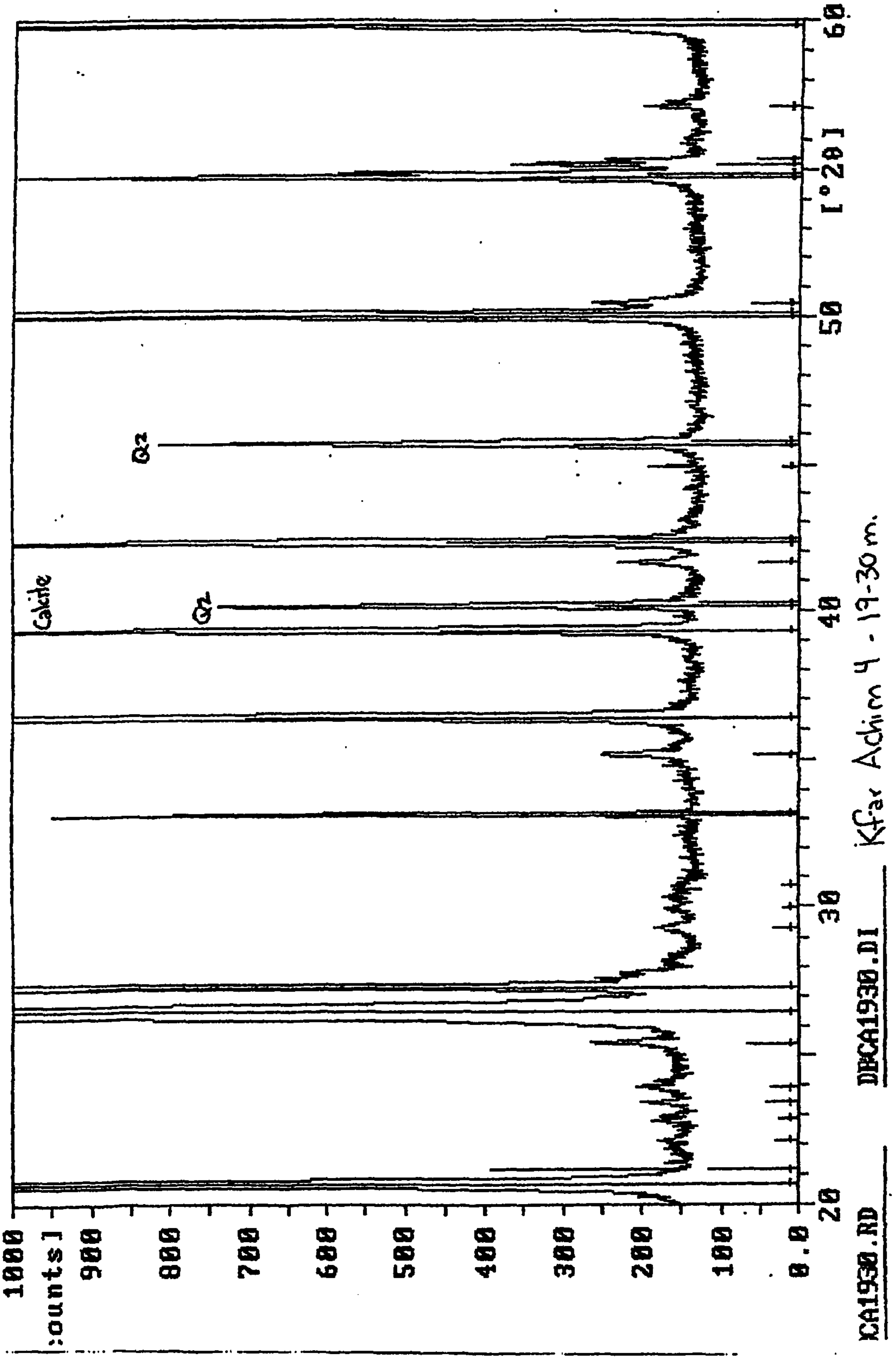

Kfar Achim 4 - 19-30 m.

Reproduced with permission of the copyright owner. Further reproduction prohibited without permission.

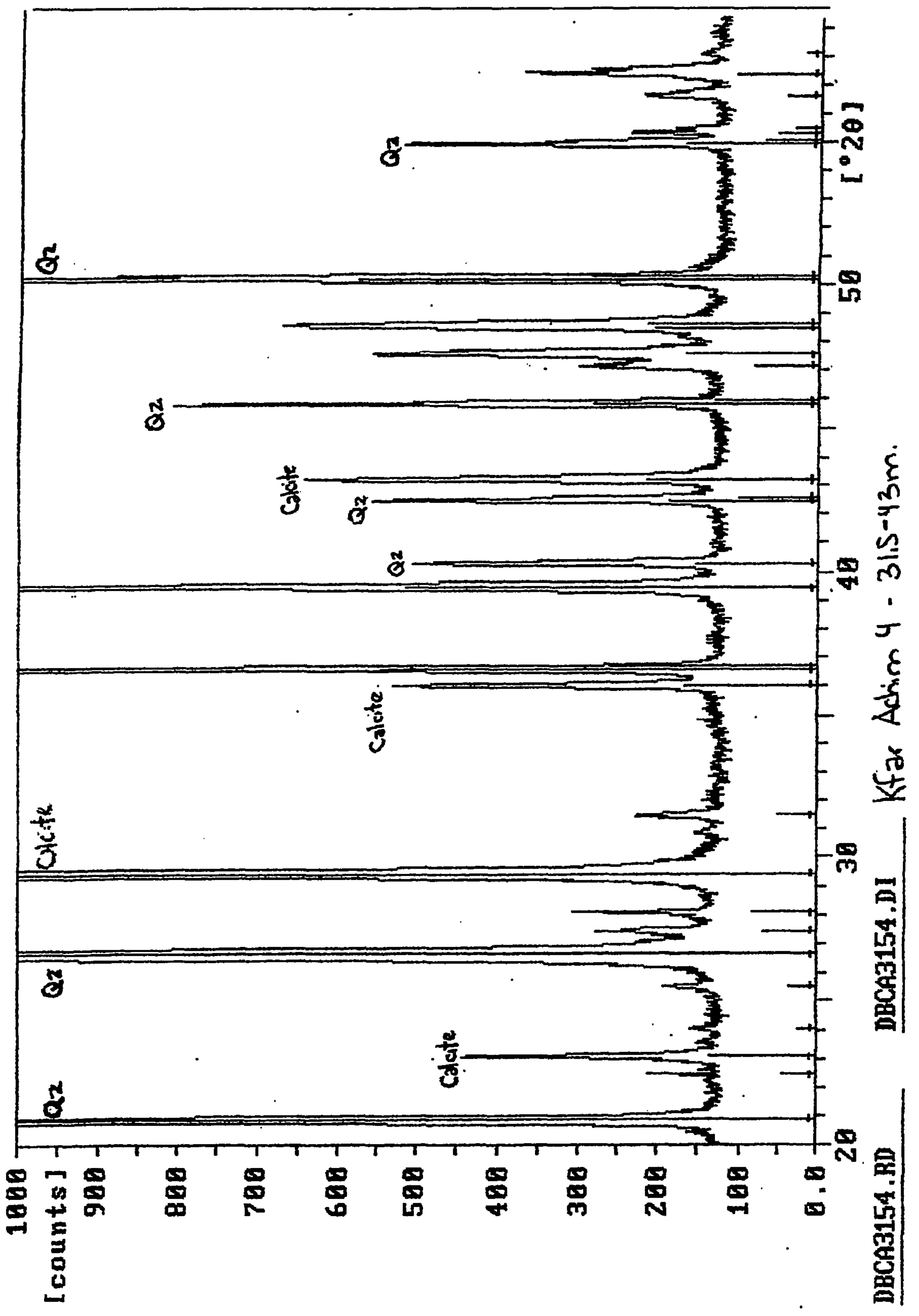

Reproduced with permission of the copyright owner. Further reproduction prohibited without permission.

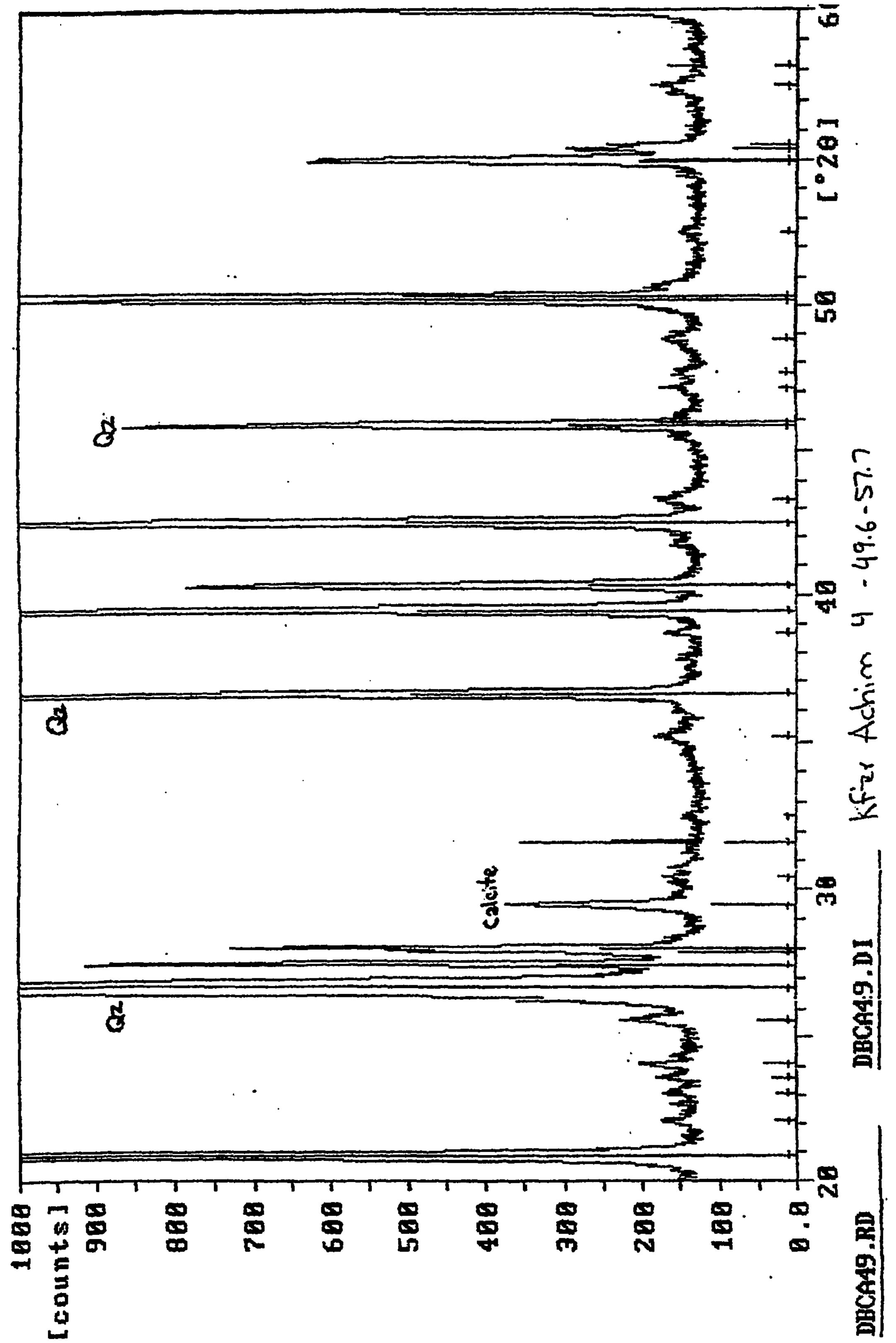

Reproduced with permission of the copyright owner. Further reproduction prohibited without permission.

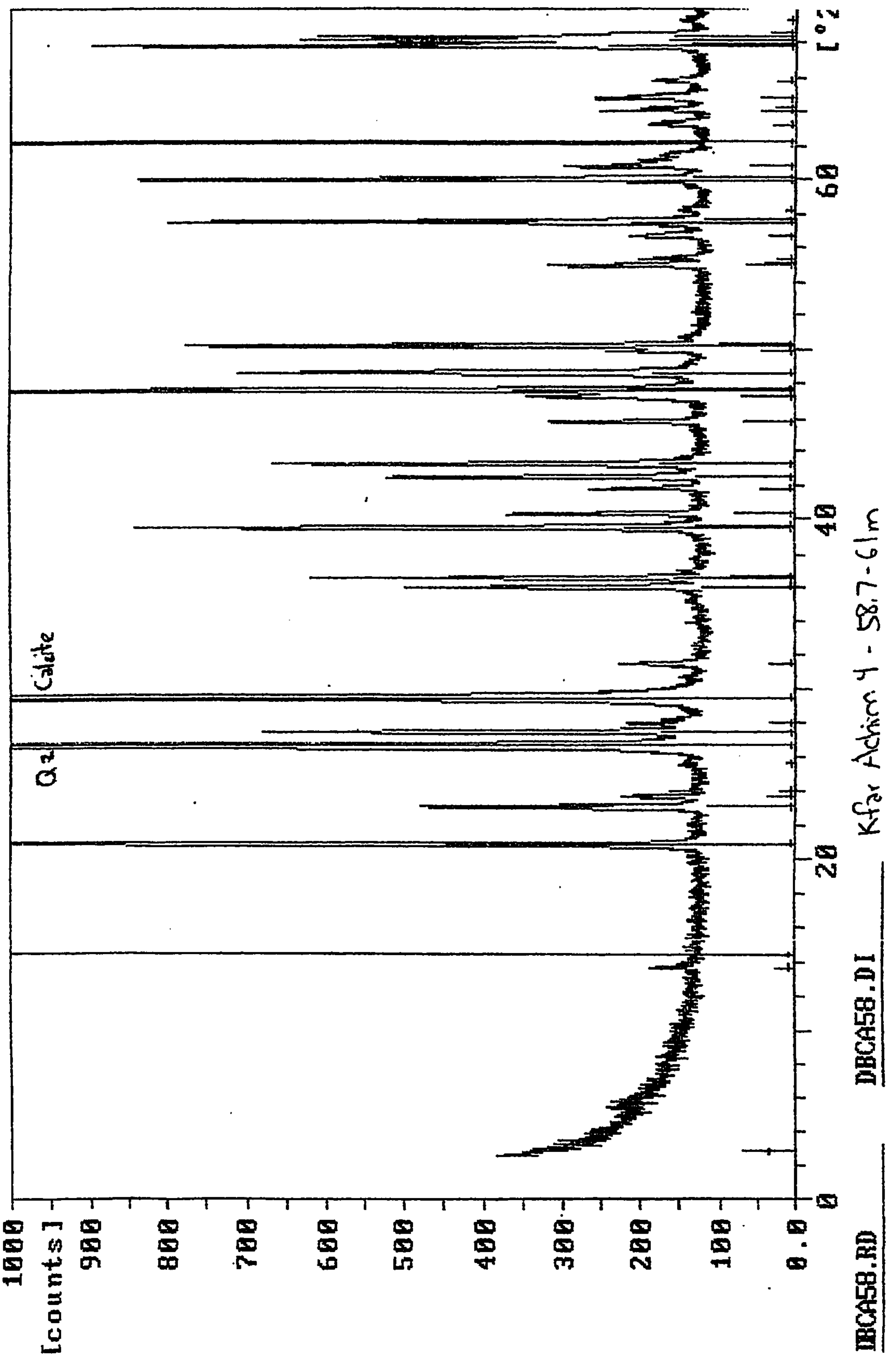

Reproduced with permission of the copyright owner. Further reproduction prohibited without permission.

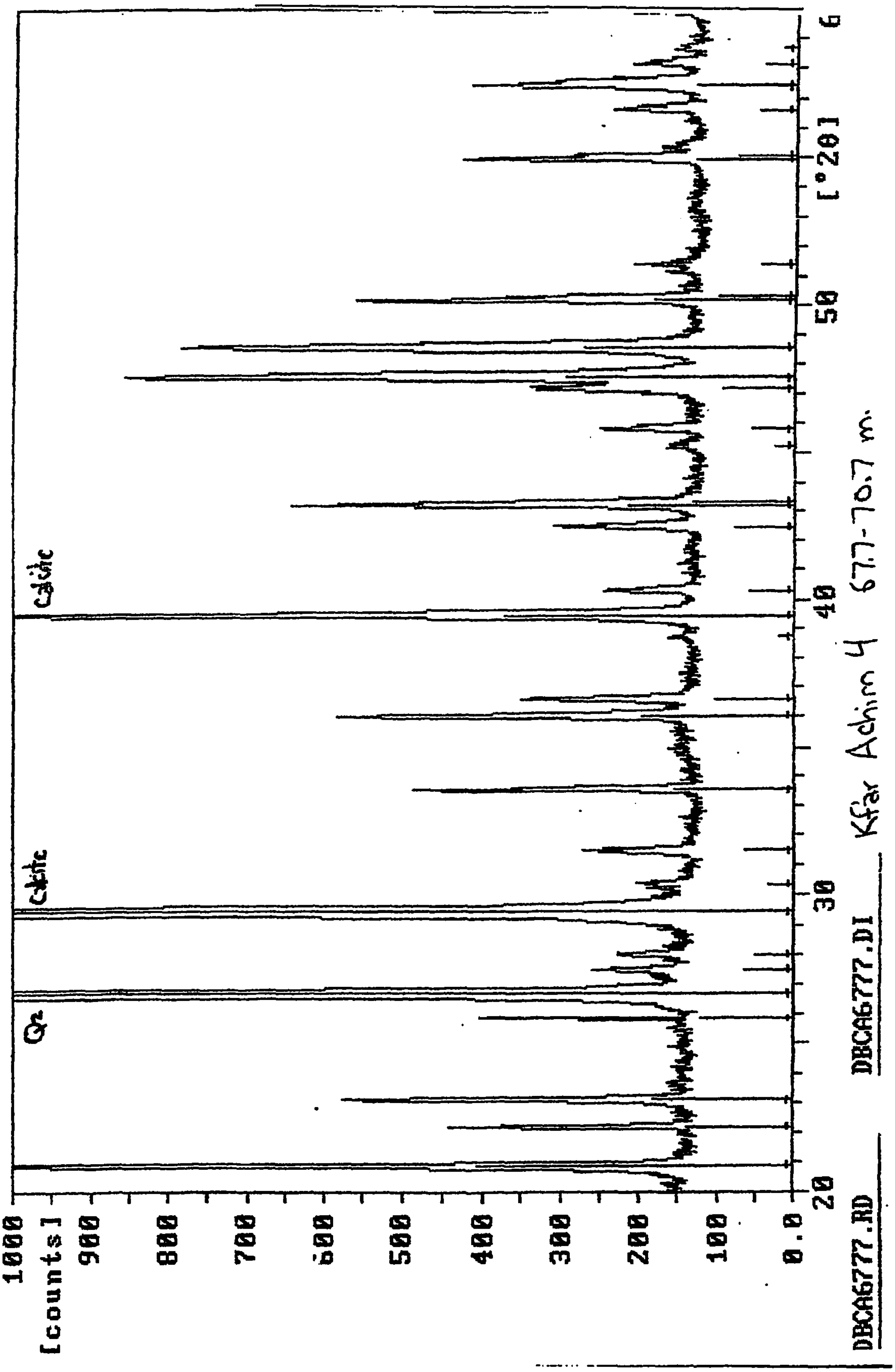

Reproduced with permission of the copyright owner. Further reproduction prohibited without permission.

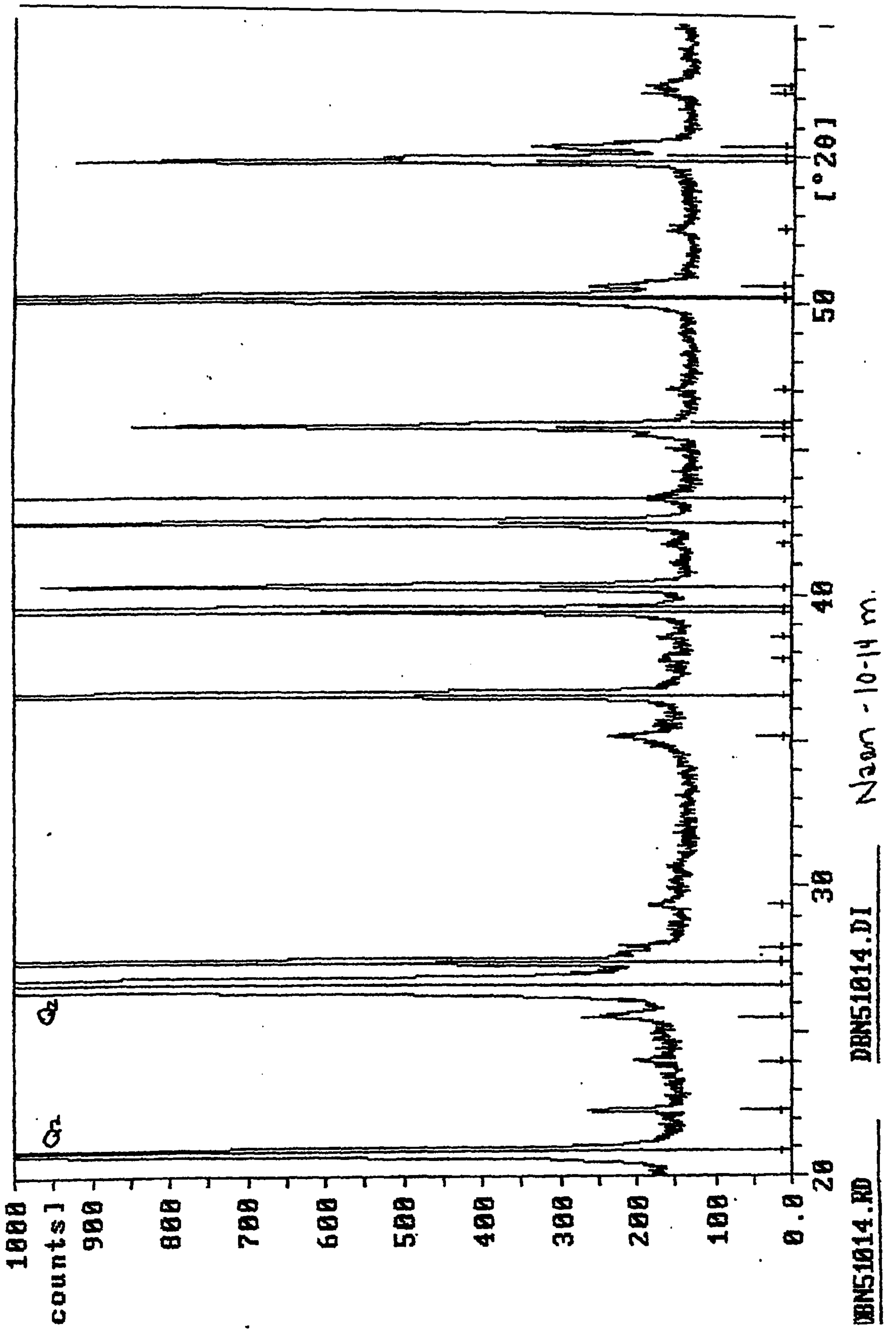

Naan - 10-14 m.

Reproduced with permission of the copyright owner. Further reproduction prohibited without permission.

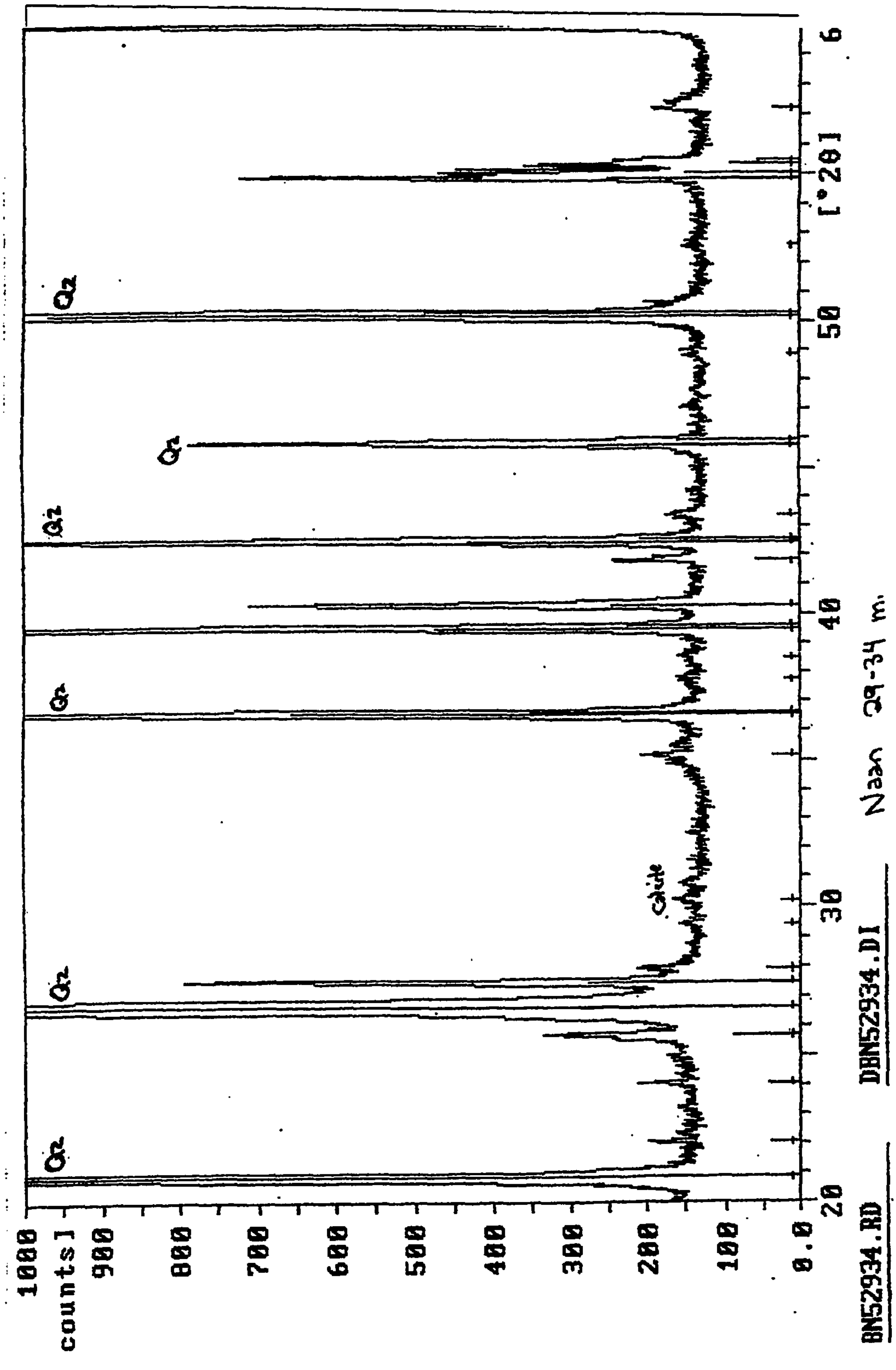

Reproduced with permission of the copyright owner. Further reproduction prohibited without permission.

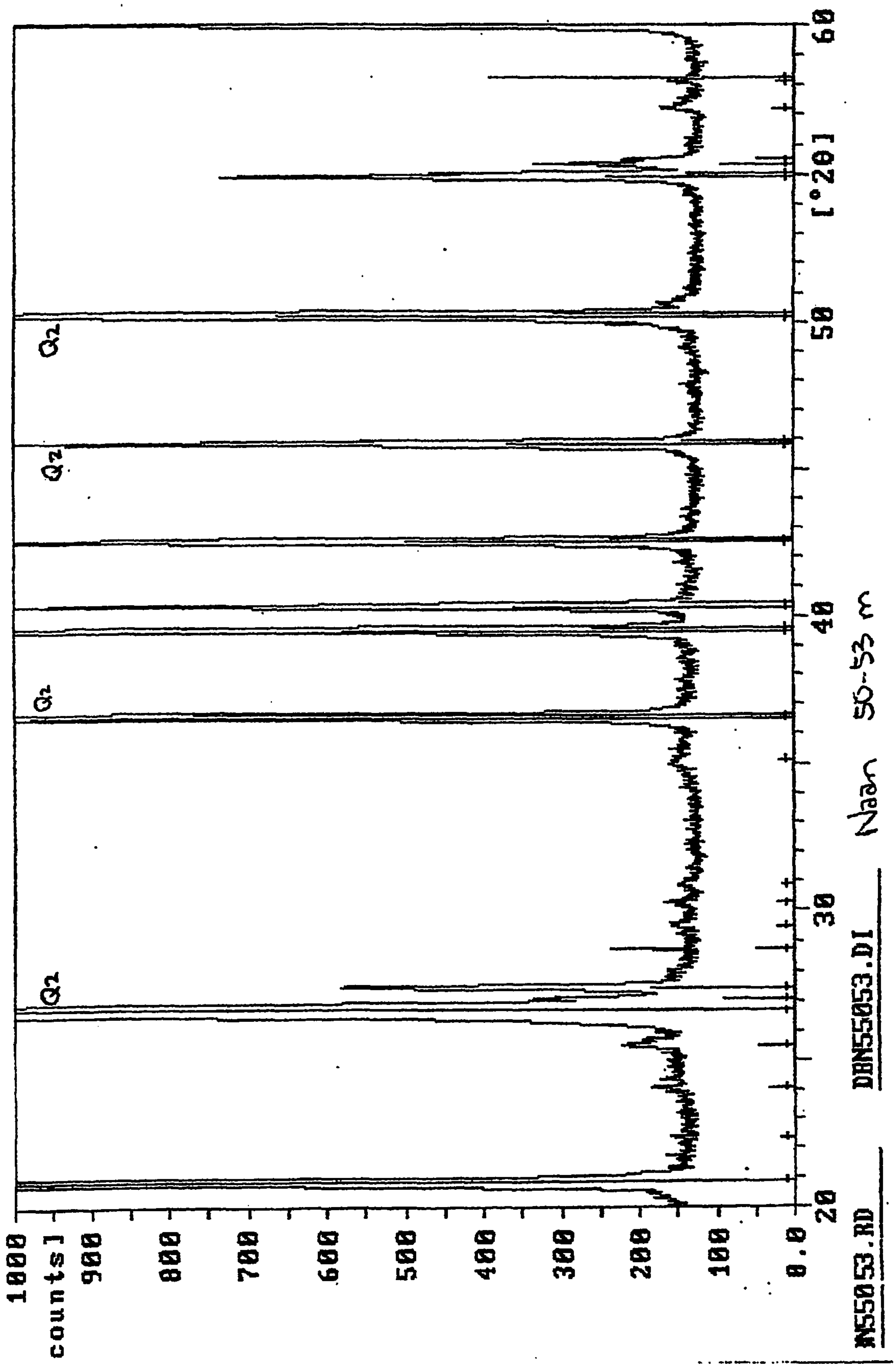

Reproduced with permission of the copyright owner. Further reproduction prohibited without permission.

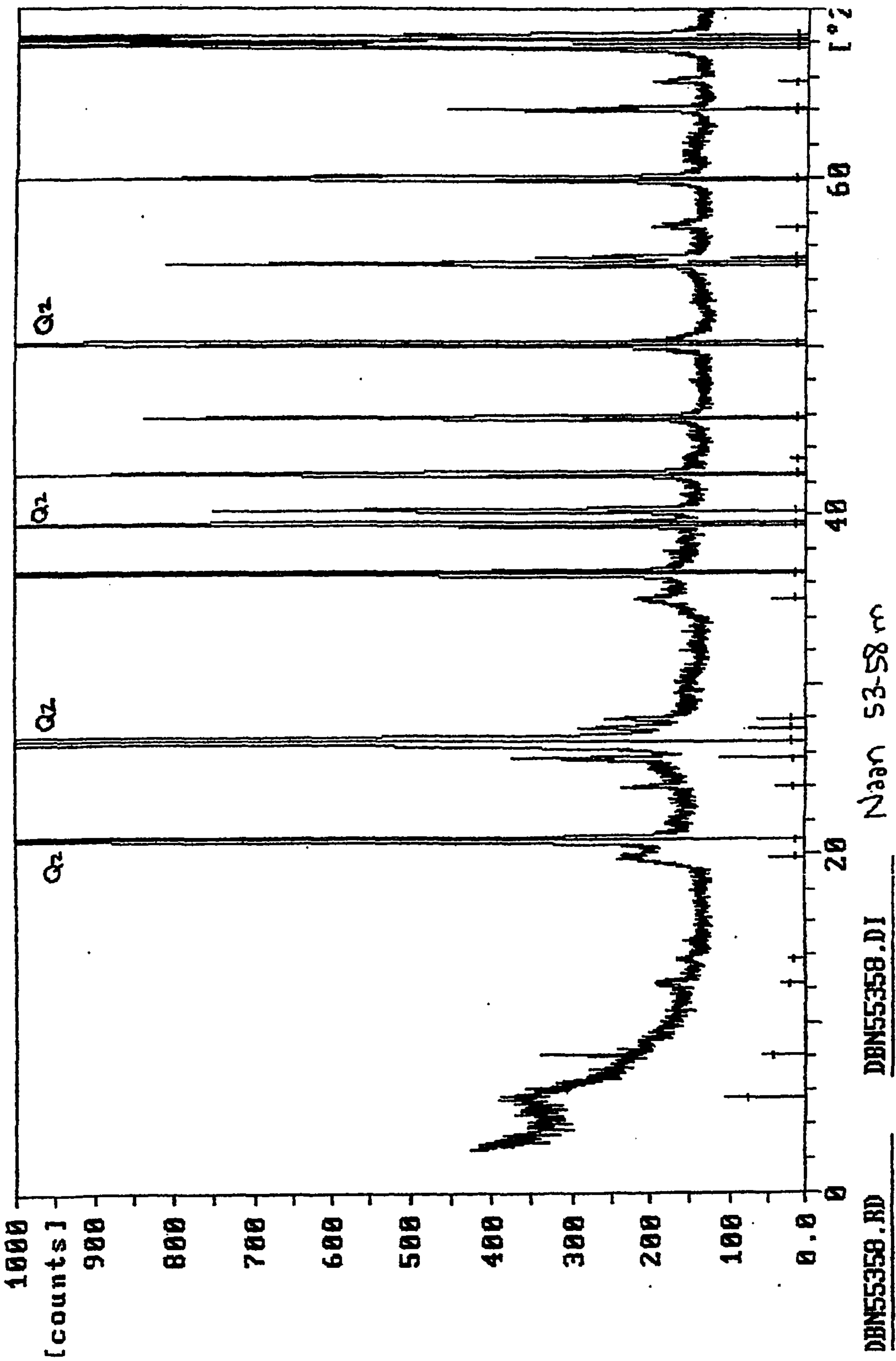

Reproduced with permission of the copyright owner. Further reproduction prohibited without permission.

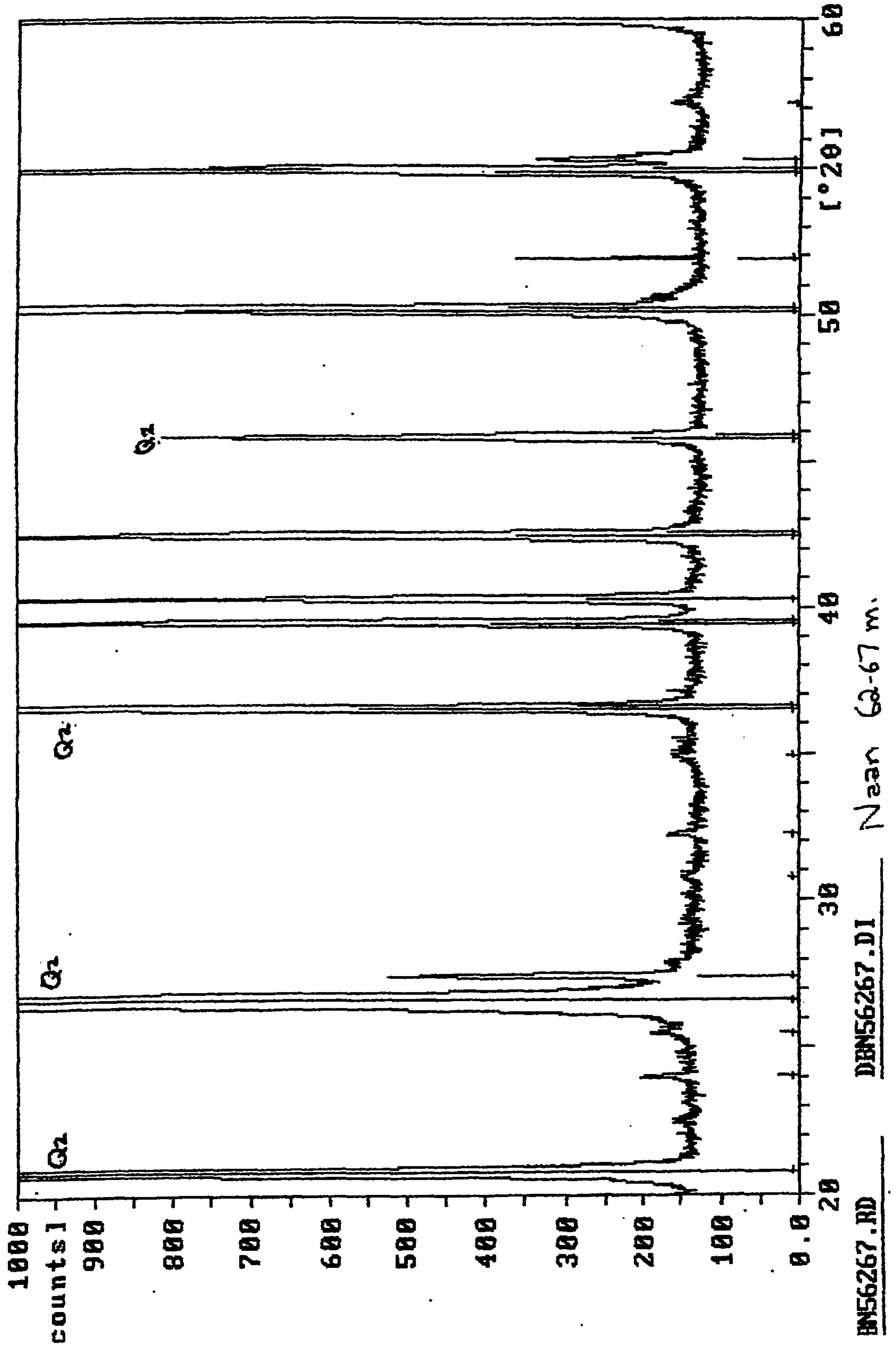

Reproduced with permission of the copyright owner. Further reproduction prohibited without permission.

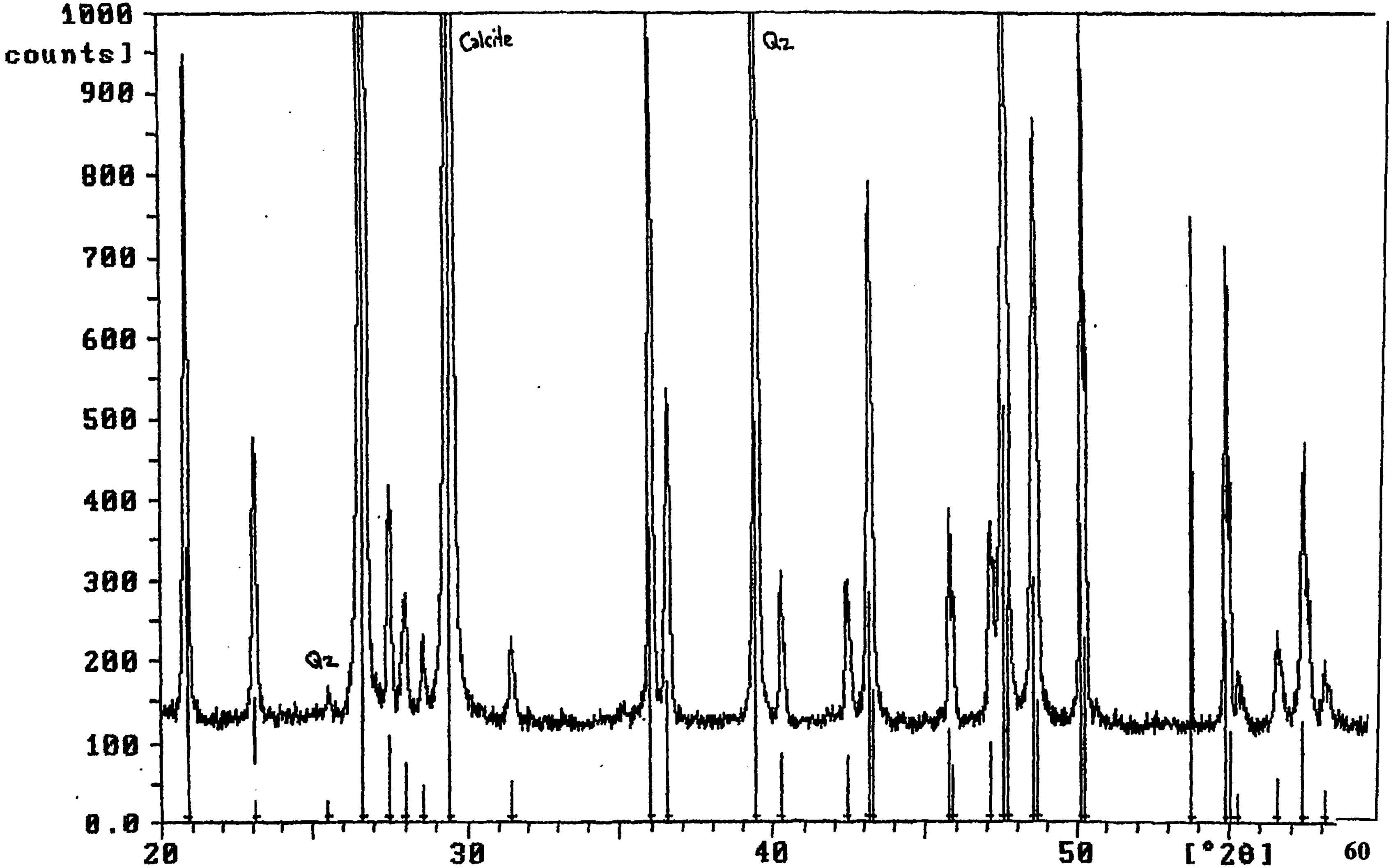

BN56871.RD DBN56871.DI Naan 68-71 m.

Reproduced with permission of the copyright owner. Further reproduction prohibited without permission.

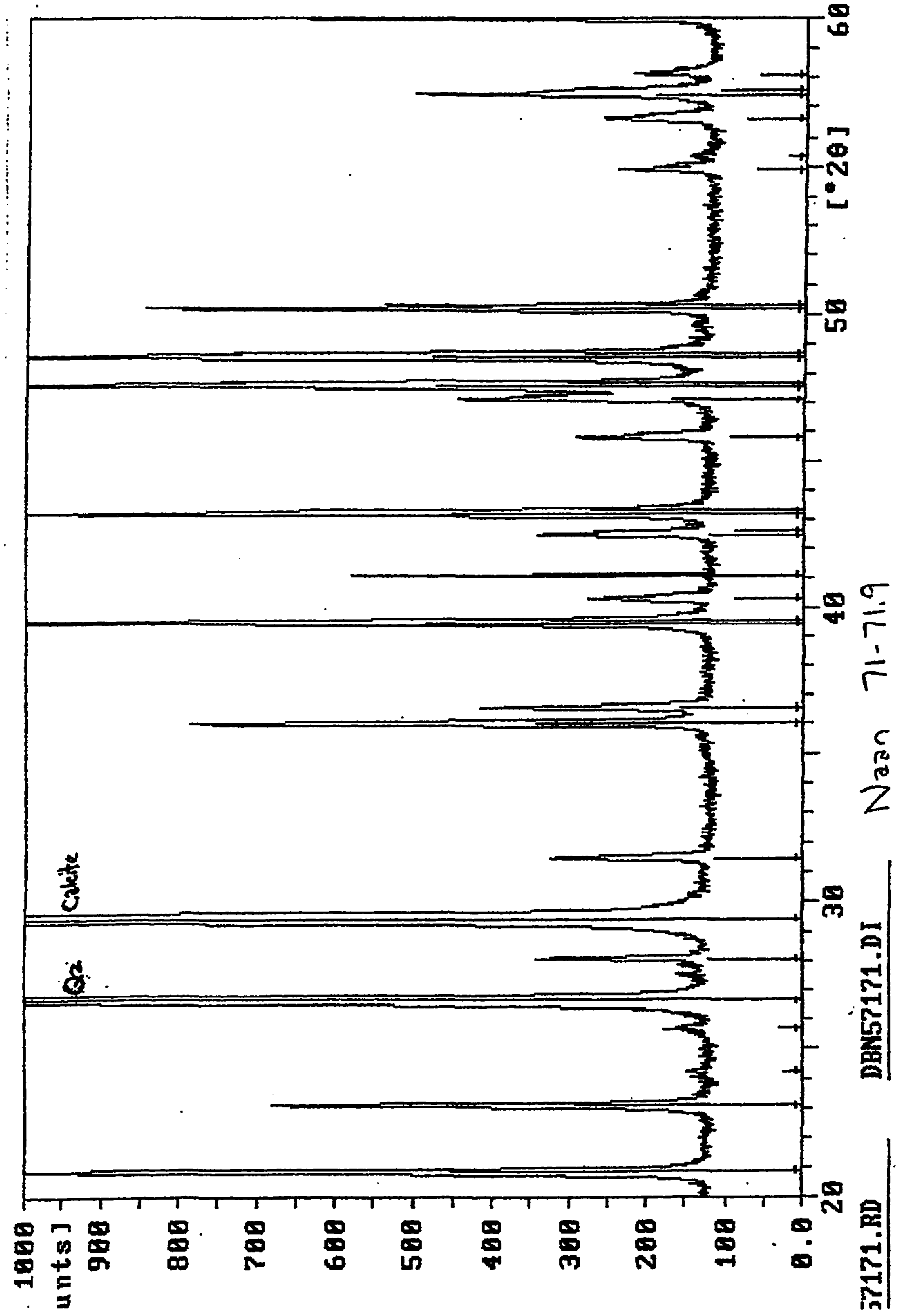

Reproduced with permission of the copyright owner. Further reproduction prohibited without permission.

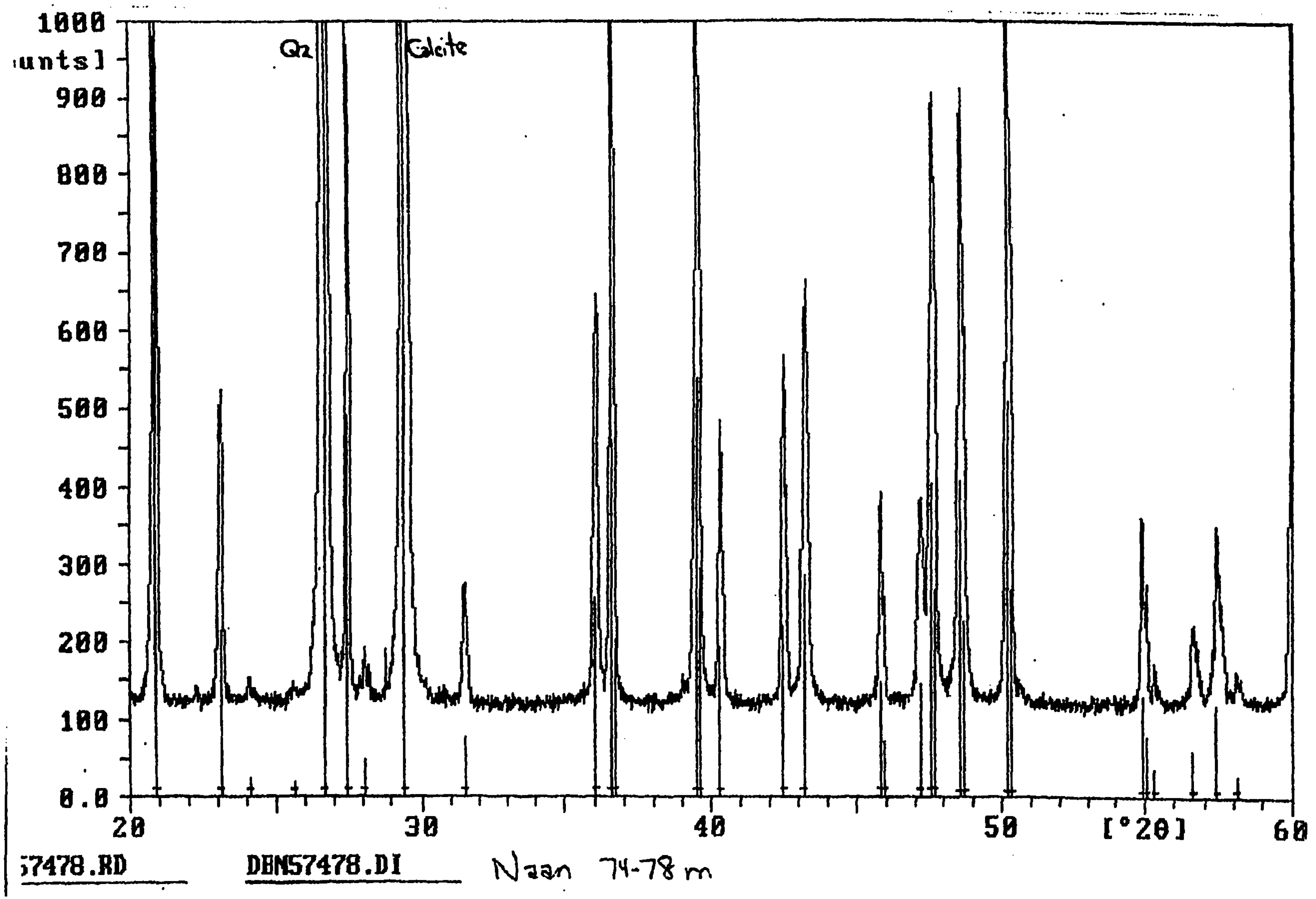

Naan 74-78 m

Reproduced with permission of the copyright owner. Further reproduction prohibited without permission.

BIBLIOGRAPHY

Acker, A. 1999 Selected geological cross-sections and subsurface maps in the coastal aquifer of Israel. Geological Survey Report GSI/18/99.

Avnimelech, M., 1962 Late Quaternary Sediments of the coastal plain of Israel: *Research Council Israel Bull.*, Vol. 2, pp. 51-57.

Boaretto, E., Thorling, A., Sveinbjornsdottir, A.E., Yechieli, Y. and Heinemeier, J. 1998 Study of the effect of fossil organic carbon on ^{14}C in groundwater from Hvinningdal, Denmark. *Radiocarbon,* Vol. 40:2, pp. 915-920.

Bruce, D., Friedman, G.M., Kaufman, A., Yechieli, Y., 2001 Spatial Variations of radiocarbon in the Coastal Aquifer of Israel- Indicators of open and closed systems, *Radiocarbon,* Vol. 43:2 B, pp. 783-791.

Buchbinder, L.G. and Friedman, G.M. 1980 Vadose, phreatic, and marine diagenesis of Pleistocene-Holocene carbonates in a borehole: Mediterranean coast of Israel. *Journal of Sedimentary Petrology.* Vol. 50:2, pp. 395-408.

Carmi, I., Gat, J.R., 1973 Tritium in precipitation and freshwater sources in Israel. *Isr. J. Earth Sci.* Vol. 22, pp. 71-92.

Clark, I. D. and Fritz, P. 1997 Environmental Isotopes in Hydrogeology. Lewis Publishers: New York, pp.112-189, 200-231.

Davidson, G.R., Hardin, E.L., and Bassett, R.L 1995 Extraction of ^{14}C from pore water in unsaturated rock using vacuum distillation. *Radiocarbon.* Vol. 37:3, pp. 861-874.

Dorr, H., Sonntag, C., and Regenberg, W. 1987 Field study on the initial ^{14}C content as a limiting factor in ^{14}C groundwater dating. *IAEA-SM-299/38*, pp. 73-86.

Dunkle, S.A., Plummer, L.N., Rusenberg, E., Phillips, P.J., Denver, J.M., Hamilton, P.A., Michel, R.L., and Coplen, T.B. 1993 Chlorofluorocarbons (CCl_3F and CCl_2F_2) as dating tools and hydraulic tracers in shallow groundwater of the Delmarva Peninsula, Atlantic Coastal Plain, United States. Water Resources Res. Vol. 29, pp. 3838-3860.

Emery K.O., and Neev, D., 1960 Mediterranean beaches of Israel. *Israel Geol. Survey Bull.* 26, pp. 1-13.

Faure, G.1991 Principles and Applications of Inorganic Geochemistry. Macmillian Publishing Co.: New York. pp. 117-118.

Fontes, J.C., and Garnier, J.M. 1979 Determination of the initial ^{14}C activity of the total dissolved carbon: A review of the existing models and a new approach. *Water Resources Research* Vol 15:2, pp.399-413.

Reproduced with permission of the copyright owner. Further reproduction prohibited without permission.

Fritz, S., Drimmie, R., and Fritz, P. 1991 Characterizing shallow aquifers using tritium and ^{14}C: periodic sampling based on tritium half-life. *Applied Geochemistry* Vol. 6, pp. 17-33.

Gavish, E. and Friedman, G.M. 1969 Progressive diagenesis in Quaternary to late Tertiary carbonate sediments: sequence and time scale. *Journal of Sedimentary Petrology*. Vol. 39:3, pp. 980-1006.

Gavish, E. and Friedman, G.M. 1973 Quantitative analysis of calcite and Mg-calcite by X-ray diffraction: effect of grinding on peak height and peak area. *Sedimentology* Vol. 20, pp. 437-444.

Geyh, M. A.1972 On the determination of the dilution factor of groundwater. *Proc. 8th Int. Conf. Radiocarbon Dating.* New Zealand, pp. 369-380.

Geyh, M. A. and Kunzl, R. 1981 Methane in groundwater and its effect on ^{14}C groundwater dating. *Journal of Hydrology.* Vol. 52, pp. 355-358.

Geyh, M. A. and Wirth, K. 1980 ^{14}C ages of confined groundwater from the Gwandu Aquifer, Sokoto Basin, northern Nigeria. *Journal of Hydrology* Vol. 48, pp. 281-288.

Golts, S., and Kolton, Y. 1994 The influence of tectonics in salinization in the Coastal Aquifer. In: *Israel Geological Society Annual Meeting.* Israel Geological Society. Jerusalem, Israel. p. 36.

Gvirtzman, G., Shachnai, E., Bakler, N. and Ilani, S. 1984 Stratigraphy of the Kurkar Group (Quarternary) of the Coastal Plain of Israel. Curr. Res. Geo. Surv. Isr., pp. 70-82.

Huffen, T.H., Buddemeier, R.W. and Lau, L.S. 1972 Tritium and radiocarbon in Hawaiian natural water – Part 1, Technical report No 53, Water Resources Research Center, University of Hawaii, 54 pp.

Ingerson, E. and Pearson, F.J. 1964 Estimation of age and rate of motion of groundwater by the ^{14}C method. In: Recent Researches in the Fields of Hydrosphere, Atmosphere and Nuclear Geochemistry. Maruzen:Tokyo, pp. 263.

Issar, A., 1961 The Plio-Pleistocene geology of the Ashdod area. *Bull. Res. Counc. Israel,* Vol. 10G, pp. 173-182.

Issar, A. 1968 Geology of the central coastal plain of Israel. *Israel Journal of Earth-Sciences* Vol. 17, pp. 16-29.

Issar, A., 1980 Stratigraphy and paleoclimates of the Pleistocene of central and northern Israel. *Palaeogeography, Palaeoclimatology, Palaeoecology,* Vol. 29, pp. 261-280.

Reproduced with permission of the copyright owner. Further reproduction prohibited without permission.

Itzhaki, Y., 1961 Pleistocene shorelines in the Coastal Plain of Israel, Contributions to the study of the Pleistocene in the Coastal Plain of Israel. *Geo. Surv. Israel Bull.* No.32, pp. 1-9.

Izbicki, J.A., Michel, R.L., and Martin, P. 1992 ^{3}H and ^{14}C as tracers of ground-water recharge, in Irrigation and Drainage: Saving a Threatened Resource; In Search of Solutions: Proceedings of the Irrigation and Drainage Session at Water Forum 1992 (Baltimore, MD, U.S.A.), edited by Engman, T. American Society of Civil Engineers: New York, pp. 122-127.

Kanfi, Y., Ronen, D., and Magaritz, M. 1983 Nitrate trends in the Coastal Plain Aquifer of Israel. *Journal of Hydrology.* Vol. 66, pp. 331-341.

Kaufman, A. 1976 (?) Carbon isotopes in waters of the Israeli Coastal Aquifer. Dept. Isotope Research, Weizmann Institute of Science. Rechovot, Israel (unpublished work).

Kroitoro, L., Carmi, I., and Mazor, E.1989 Groundwater ^{14}C activity as affected by initial water- rock interactions in the Judean Mountains, Israel. *Chemical Geology.* Vol. 79, pp. 259-274.

Leaney, F.W. and Allison, G.B 1986 Carbon-14 and stable isotope data for an area in the Murray Basin: its use in estimating recharge. *Journal of Hydrology* Vol. 88, pp. 129-145.

Levin, I., Munnich, K.O., and W. Weiss 1980 The effect of anthropogenic CO_2 and ^{14}C sources on the distribution of ^{14}C in the atmosphere.*Radiocarbon* Vol. 22: 2, pp. 379-391.

Mercado, A., Avron, M. and Kahanovitch, Y. 1975 Groundwater salinity in the coastal plain – chloride inventory and assessment of future salinity trends. Tahal Report 01/75/88 (in Hebrew).

Mercado, A. 1985 The use of hydrogeochemical patterns in carbonate, sand, and sandstone aquifers to identify intrusion and flushing of saline water. *Groundwater* Vol. 23, pp. 635-644.

Mook, W.G. 1976 The dissolution-exchange model for dating groundwater with ^{14}C. In: *Interpretation of Environmental Isotope and Hydro-chemical Data in Groundwater Hydrology.* IAEA, Vienna, pp. 163-189.

Mook, W.G. 1980 Carbon-14 in hydrogeological studies. In Fritz, P. and Fontes, J.Ch., eds., *Handbook of Environmental Isotope Geochemistry,* Vol. 1, *The Terrestrial Environment.* New York, Elsevier Scientific Publishers, pp. 49-74.

Nativ, R. and Weisbrod, N. 1994 Hydraulic connections among subaquifers of the Coastal Plain Aquifer, Israel. *Groundwater* Vol. 32:6, pp. 997-1007.

Reproduced with permission of the copyright owner. Further reproduction prohibited without permission.

Pearson, F.J. and Hanshaw, B.B. 1970 Sources of dissolved carbonate species in groundwater and their effects on carbon 14 dating. *Isotope Hydrology*. IAEA, Vienna, pp. 271-286.

Pearson, F.J., Jr., and Swarzenki, W.V. 1974 ^{14}C evidence for the origin of arid region groundwater, Northeastern Province, Kenya. In: *Isotope Techniques in Groundwater Hydrology,* 2. IAEA, Vienna, pp. 95-108.

Picard, L., 1937 Inferences on the problem of the Pleistocene climate of Palestine and Syria drawn from flora, fauna, and stratigraphy. *Cambridge, Proc. Preh. Soc.*, No. 5, pp. 58-70.

Picard, L. and Avnimelech, M., 1937 On the geology of the central coastal plain. *Bull. Geology Dept.*, Hebrew Univ., 1, 45p.

Picard, L., 1943 The structure and evolution of Palestine: Geol. Dept., Hebrew Univ., Jerusalem, Bull. Nos. 2-4, pp. 1-134.

Rosenthal, E., Vinokurov, A., Ronen, D., Margaritz, M., and Moshkovitz, S. 1992 Anthropogenically induced salinization of groundwater: A case study from the Coastal Plain aquifer of Israel. *Journal of Contaminant Hydrology* Vol. 11, pp.149-171.

Rosensaft, M., Ecker, A., Levitte, D., Ilani, S., Shimron, A., Rosenfeld, A., Sneh, A., and Bein, A. 1997 The three-dimensional configuration and lithological composition of the coastal aquifer and the unsaturated zone, Israel. Geological Survey of Israel Report GSI/15/95.

Salmons, W., and Mook, W.G. 1976 Isotope geochemistry of carbonate dissolution and reprecipitation in soils. *Soil Science.* Vol. 122, pp. 15-24.

Schlosser, P., Stute, M., Sonntag, C., and Munnich, K.O. 1989 Tritogenic ^{3}He in shallow groundwater. *Earth and Planetary Science Letters.* Vol. 94, pp.245-254.

Stiller, M., Kaufman, A., Carmi, I., Mintz, G. 1998 Calibration of lacustrine sediment ages using the relationship between ^{14}C levels in lake waters and in the atmosphere: The case of Lake Kinneret *Radiocarbon-Proceedings of the 17th International ^{14}C Conference* (edited by I. Carmi and E. Boaretto) Vol 43:2, pp.1-10.

Striegl, R.G., and Armstrong, D.E. 1990 Carbon dioxide retention and carbon exchange on unsaturated Quaternary sediments. *Geochimica et Cosmochimica Acta.* Vol. 54, pp. 2277-2283.

Szabo, Z., Rice, D.E., Plummer, L.N., Busenberg, E., Drenkard, S., and Schlosser, P. 1996 Age dating of shallow groundwater with chlorofluorocarbons, tritium/helium-3, and flow path analyses, southern New Jersey coastal plain. *Water Resources Research* Vol. 32, pp.1023-1038.

Reproduced with permission of the copyright owner. Further reproduction prohibited without permission.

Taylor, C.B. 1994 Hydrology of the Poverty Bay flats aquifer, New Zealand: recharge mechanisms, evolution of the isotopic composition of dissolved inorganic carbon, and ground-water ages. *Journal of Hydrology.* Vol. 158, pp. 151-185.

Taylor, C.B. and Fox, V.J. 1996 An isotopic study of dissolved inorganic carbon in the catchment of the Waimakariri River and deep ground water of the North Canterbury Plains, New Zealand. *Journal of Hydrogeology* Vol. 186, pp.161-190.

Tolmach, Y. 1977 Hydrological Atlas of Israel-Geological sections in the Coastal Plain area, Volumes 1-6. Israel Hydrological Service, Jerusalem.

Vengosh, A., Starinsky, A., Kolodny, Y., and Chivas, A.R. 1991 Boron isotope geochemistry as a tracer for the evolution of brines and associated hot springs from the Dead Sea, Israel. *Geochimica et Cosmochimica Acta.* Vol. 55, pp. 1689-1695.

Vengosh, A. and E. Rosenthal 1994 Saline groundwater in Israel- its bearing on the water crisis in the country. *Journal of Hydrology.* Vol. 156, pp. 389-430.

Vengosh, A., Spivack, A., Artzi, Y., and Ayalon, A. 1999 Geochemical and boron, strontium, and oxygen isotopic constraints on the origin of the salinity in groundwater from the Mediterranean coast of Israel. *Water Resources Research.* Vol. 35: 6, pp. 1877-1894.

Vogel, J.C., and Ehalt, D.1963 The use of carbon isotopes in groundwater studies. In: *Radioisotopes in Hydrology.* IAEA, Vienna, pp. 383-396.

Wigley, T.M.L. 1975 Carbon 14 dating of groundwater from closed and open systems. *Water Resources Research.*Vol. 11:2, pp. 324-328.

Yechieli, Y., Ronen, D. Kaufman, A. and Carmi, I. 1994 New tritium data in waters of the Dead Sea area. *Isr. J. Earth Sciences.* Vol. 43, pp. 213-220.

Yechieli, Y., Ronen, D., and Vengosh, A. 1996 Preliminary ^{14}C study of groundwater at the fresh-saline water interface of the Mediterranean Coastal Plain Aquifer of Israel. *SWIM,* Malmo. pp. 84-90.

Yechieli, Y., Ronen, D., and Vengosh, A. 1997 Isotopic measurements and groundwater dating at the fresh-saline water interface region of the Mediterranean Coastal Plain Aquifer of Israel. Geological Survey of Israel Report GSI/28/96.

Yechieli, Y., Sivan, O., Lazar, B., Vengosh, D., Ronen, D., and Herut, B. 2001 ^{14}C in seawater intruding into the Israeli Mediterranean coastal aquifer. *Radiocarbon* Vol. 43(2B), pp. 773-781.

Reproduced with permission of the copyright owner. Further reproduction prohibited without permission.